THE UNIVERSITY OF CHICAGO

SHARED DEVELOPMENTAL AND REGULATORY FEATURES OF FINS AND LIMBS

A DISSERTATION SUBMITTED TO

THE FACULTY OF THE DIVISION OF THE BIOLOGICAL SCIENCES

AND THE PRITZKER SCHOOL OF MEDICINE

IN CANDIDACY FOR THE DEGREE OF

DOCTOR OF PHILOSOPHY

DEPARTMENT OF ORGANISMAL BIOLOGY AND ANATOMY

BY

JOYCE PIERETTI

CHICAGO, ILLINOIS

AUGUST 2016

To my parents, Ana and Bethwell Pieretti

Siempre para adelante; nunca para atrás ni para coger impulso

TABLE OF CONTENTS

LIST OF TABLES

LIST OF FIGURES

ACKNOWLEDGEMENTS

I would like to acknowledge my collaborators José Luis Gómez-Skarmeta, Jeff Klomp, Joaquín Letelier, Elisa de la Calle-Mustienes, Ignacio Maeso, Juan Ramón Martinez Morales, and Igor Schneider for making much of the work presented in this dissertation possible. Thank you also to Tetsuya Nakamura for his friendship, constructive feedback, and generally making the Shubin lab a bustling place of collaboration and constant experiments.

I would like to thank my advisor, Neil Shubin, for constantly being a positive influence in my research and always demonstrating that science is more than working at the bench. If I had not joined his lab, I may not have caught the same bug of science communication and outreach. I can only hope to bottle some of his vivacity to later share with others interested in science. To my committee members, Victoria Prince, Urs Schmidt-Ott, and Ilya Ruvinsky, thank you for your excellent support, patience, and feedback throughout the course of my research.

I would like to express my gratitude to (current and former) members of the Shubin lab: Noritaka Adachi, Justin Lemberg, Darcy Ross, and Andrew Gehrke. Thank you for creating an inquisitive, positive, and supportive lab atmosphere. A sincere thanks also go to John Westlund for his attentive aid in fish care and excellent figure design.

Thank you to my friends and members of the Biological Sciences Division, especially those involved with the Multicultural Graduate Community. Thank you Allison Johnson, Brian Gallagher, Daniela Palmer, and Victoria Flores for your special friendships and support even during gloomy winters, both literally and metaphorically.

Finally, sincere thanks go to my family, especially my parents, Ana and Bethwell Pieretti, for always encouraging and supporting me in my academic and personal pursuits. A special thank you to my partner, Collin Soderberg-Chase for his steadfast love and support.

ABSTRACT

Of the many unique chronicles of development and paleontology, none are so compelling as the transition from fins to limbs. What causes effected the development of our ancestors in the transition from an exclusively aquatic to primarily terrestrial lifestyle? Researchers have sought to answer this question by probing the developmental and genetic processes that build both fins and limbs, revealing extensive parallels in the networks which pattern these structures. This thesis is a contribution to that body of knowledge through my exploration of common developmental programs in paired and median fins as well as shared regulatory features of limb and fin patterning. In Chapter I, I discuss the challenge of assessing homology at various levels, introduce hypotheses on the origin of paired appendages, and overview the shared gene networks between fins and limbs. In Chapter II, I characterize gene expression in paddlefish and skate fins and submit that a common developmental module featuring 5' *Hox* genes is present in both paired and median fins. In analyzing the phenotype of *hoxa13* zebrafish (*Danio rerio*) mutants, I found that dorsal and pectoral fin dermal elements were severely truncated, indicating that *hoxa13* is necessary for proper dorsal and pectoral fin development. This work lends experimental support to the hypothesis that this developmental module originated in the midline and was later co-opted in development of paired fins. In Chapter III, I used mouse and zebrafish transgenics to assess the functional conservation of the ZRS, a limb-specific *Sonic hedgehog* (*Shh*) enhancer, from multiple donor organisms and conclude that this element likely originated in the ancestor of gnathostomes. I also analyzed the pectoral fin phenotype of a ZRS medaka mutant with a reduced number of proximal radials. This result suggests a role for *Shh* in specifying the number of endoskeletal elements in fins. I end in Chapter IV by proposing that future avenues of research must fully characterize the developmental regulatory networks that

define the identity of a body part, providing insight on both the evolutionary origin of such parts and the deep homology of networks. I argue that from using modern genetic and epigenomic techniques to characterize these networks, there will emerge broader commonalities in the evolution of generative processes.

Two appendices accompany this dissertation.

CHAPTER I

INTRODUCTION

1.1 Author contributions

Sections of this chapter were published as part of: Pieretti, J., Gehrke, A.R., Schneider, I., Adachi, N., Nakamura, T., and Shubin, N.H. 2015. Organogenesis in deep time: A problem in genomics, development, and paleontology. Proc. Natl. Acad. Sci. U. S. A. *112*, 4871–4876. Figure 1.1 was previously published as part of said publication.

1.2 Homology and evolutionary-developmental biology

As comparative anatomy and embryology flourished during the 19th century, one of the most striking observations made was the remarkable similarity that underlay obviously different structures across species. Owen conceptualized his observations of the vertebrate limb and put forth the idea of homology as "the same organ in different animals under every variety of form or function," (Owen, 1848). Generations of scientists since have sought to understand how the genes that control embryonic development influence the diversity of organismal form and function. This interest is at the crux of evolutionary developmental (evo-devo) biology, where research focuses on decoding the evolutionary relationships of the genetic and developmental processes that build distinctive morphological traits. Over time, the morphological homology of Owen's time has been reworked and modified, reflecting the modern challenges of the homology concept (Wagner, 1989, 2007; Hall, 1994; Abouheif et al., 1997; Shubin et al., 2009).

As a field, evo-devo unifies embryological, anatomical, phylogenetic, and genetic evidence to put forth hypotheses to test and explain the ancestry of parts and the divergence of characters. But with the discovery that a common developmental toolkit is shared across virtually

all metazoans (Carroll, 2008), defining and identifying homology across different levels of biological organization has been challenging (Muller, 2003). Definitive studies have characterized toolkit genes such as *Pax6* in eye formation (Gehring, 2004), *Nkx2.5/tinman* in heart formation (Olson, 2006), and *dlx* in many types of outgrowths (Panganiban et al., 1997; Panganiban and Rubenstein, 2002), illustrating the deep conservation of these genes across Bilateria. However, determining the evolutionary relationship between these analogous molecular features is complex because these relationships may reflect either convergence or true homology (e.g. a shared character in a pair of organisms due to common ancestry) among taxa. Conversely, differences in molecular features such as *cis*-regulatory elements can be due developmental systems drift (True and Haag, 2001; Gordon and Ruvinsky, 2012) or because the features are not homologous to one another.

Hypotheses of homology can be made at various levels of biological organization, such as that of genes, regulatory networks, and organs or cell types (Hillis, 1994; Abouheif et al., 1997; McCune and Schimenti, 2012; Liebeskind et al., 2016). Like homology, convergence too spans different levels of organization. Studies of convergent phenotypic features such as cryptic pigmentation have been shown to be the result of underlying mutations in different genes, different mutations in the same gene, and the same mutation in the same gene among different species (reviewed in Manceau et al., 2010). Given the complexity of scenarios for homology, homoplasy, and parallel evolution, a holistic experimental approach is necessary to examine the influence of the genotype on the phenotype. This methodology is best exemplified in studies of the origin and novelty of the vertebrate appendage.

1.3 Hypotheses on the Origin of Paired Appendages

The origin of paired fins is one of the critical events in the history of vertebrates. Two hypotheses, dating back to the 19th century, have been generated to explain this transition: (i) the gill-arch hypothesis, in which the posterior-most gill arch is considered to be a precursor to the pectoral girdle and paired fins (Figure 1.1, A) (Gegenbaur, 1878), and (ii) the fin-fold hypothesis, which posits that paired fins are derived from lateral longitudinal folds that appear early in development and evolution, resembling the embryonic median fin fold (Figure 1.1, B) (Thacher, 1877; Mivart, 1879; Balfour, 1881). Both hypotheses were originally proposed from observations of comparative embryology and anatomy of extant sharks, amphioxus (*Branchiostoma*) and paddlefish (*Polyodon*). Evidence accumulated over the past 120 years has helped evaluate these two hypotheses and by assessing new fossil, developmental, and molecular data from a variety of species, another scenario for the origin of paired fins can be examined.

The general structure of extant vertebrate paired fins consists of a shoulder girdle connected to a series of radials that articulate with a distal dermal skeleton. According to the gill-arch hypothesis, the shoulder girdle and fin skeleton gradually evolved from the gill endoskeleton and constituent gill rays (Figure 1.1, A). Currently, two pieces of evidence from chondrichthyan biology are used as support for this hypothesis. Morphological evidence shows that gill structures and pectoral girdles of sharks exhibit similar shape and position within the body (Gegenbaur, 1878). Another line of evidence comes from chondrichthyan embryology—namely, skates (*Leucoraja erinacea*). A recent study showed that the fibroblast growth factor-sonic hedgehog-retinoic acid (FGF-SHH-RA) signaling axis, key to fin development and patterning, is also deployed in skate gills (Figure 1.1, C) (Gillis et al., 2009; Gillis and Hall, 2016). However, *Shh*, *Fgf*, and RA pattern other tissues during development,

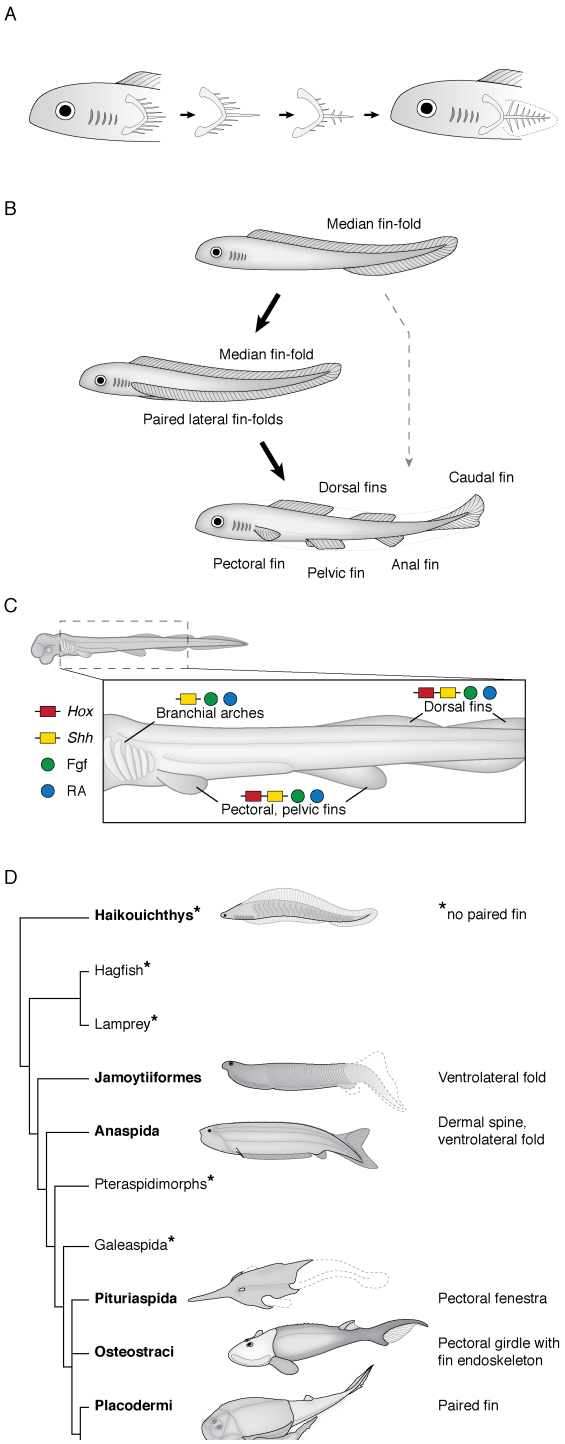

Figure 1.1 - Origin of vertebrate paired fins. Scheme of **(A)** the gill-arch hypothesis and **(B)** the fin-fold hypothesis, which supposes redeployment of the median fin developmental program through paired lateral fin folds or an unknown process leading to pectoral and pelvic fins. **(C)** Shared genetic features of gill arches, paired, and median fins in a generalized gnathostome embryo. **(D)** A phylogenetic tree of early vertebrates, modified from (Sansom, 2010). Taxa with associated illustrations are shown in bold. All vertebrates listed are agnathans except Placodermi and crown gnathostomes.

including median fins (Freitas et al., 2006; Dahn et al., 2007), implying that whatever similarities exist between gill arches and fins may not reflect transformations of arches into appendages, but the co-option of gill signaling networks by fins. Morphological observations of Paleozoic fossils further weaken the gill-arch hypothesis, showing that primitive sharks have an osteichthyan-like gill structure. This finding suggests that modern chondrichthyan gills represent a derived condition (Pradel et al., 2014). Another shortcoming of this hypothesis is the absence of fossils that show transitional gill-like fin structures. Thus, more evidence from both fossil and developmental work is needed to provide robust support of the gill-arch hypothesis.

Founders of the fin-fold hypothesis proposed that lateral fin folds are an iteration of median fin folds of ancestral agnathans, which were then specialized into two separate paired appendages, the pectoral and pelvic fins (Figure 1.1, B) (Thacher, 1877; Mivart, 1879; Balfour, 1881). Central to this hypothesis was the similar anatomical configuration of median and paired fins (Thacher, 1877; Mivart, 1879; Balfour, 1881). Thacher (1877) writes:

> As the dorsal and anal fins were specializations of the median folds of *Amphioxus*, so the paired fins were specializations of the two lateral folds which are supplementary to the median in completing the circuit of the body. These lateral folds, then […] as in the median fins, there were formed chondroid and finally cartilaginous rods. (p. 298)

While no evidence of an extant organism with a lateral fin fold has been found, the presence of a transient ectodermal thickening along each side of the body in chondrichthyan embryos seems to support the existence of an ancestral lateral fin fold (Balfour, 1881). In addition, it has been shown that the flank region has the competency to produce extra limbs, which could be a developmental remnant of a lateral fold (Cohn et al., 1995; Yonei-Tamura et al., 2008). Finally, as mentioned before, similar signaling cues pattern median and paired appendages (Figure 1.1, C) (Freitas et al., 2006; Dahn et al., 2007; Davis et al., 2007). Together, these findings support

the recruitment of median fin developmental programs to the paired fins, yet the precise mechanism of this process remains elusive (Figure 1.1, B).

Initially, fossil data appeared to support the fin-fold hypothesis because extinct agnathans, such as jamoytiids and anaspids, possess ventrolateral fin folds (Figure 1.1 B, D). However, lateral folds found in these stem gnathostomes are unevenly distributed in the phylogenetic tree and are interpreted as having convergently evolved (Figure 1.1, D) (Coates, 2003; Janvier, 2007; Sansom, 2010). Furthermore, these lateral folds differ substantially from paired appendages in lacking bony pectoral or pelvic girdles (Janvier, 1996, 2007; Coates, 2003). Contemporary observations have also failed to detect lateral fin folds in catshark (*Scyliorhinus canicula*) embryos (Tanaka et al., 2002).

A reevaluation of gnathostome fossils provides an alternative scenario for the origin of paired fins. Placoderms, the sister group to the crown gnathostomes, possess pectoral and pelvic fins supported by girdles comparable to those of modern fishes. Their closest relatives, osteostracans and pituriaspids, have pectoral fins morphologically similar to those of primitive placoderms and lack lateral fin folds or pelvic fins (Figure 1.1, D) (Janvier, 1996, 2007). Furthermore, both basal placoderms and osteostracans have a shoulder girdle with a single endoskeletal element in articulation (Janvier, 1996, 2007; Coates, 2003). These observations suggest that the primitive gnathostome condition is a paired pectoral fin with a single skeletal element connecting the fin to the girdle. This finding contrasts with the fin-fold hypothesis, which predicts a lateral fold that gives rise simultaneously to both anterior and posterior fins, each composed of multiple radials.

Although the full details of the origin of paired fins, whether directly from median fin folds or via lateral fin folds (Figure 1.1, B), remain to be determined, it seems likely that a

redeployment of the median fin developmental program occurred in the origin of paired appendages. Although we know a great deal about paired appendage development, little is known of median fin initiation and patterning. Comparative analyses of gene expression and regulation in median fins may provide us with new clues as to the origins of paired fins.

1.4 Shh and Hox gene networks in fins and limbs

C*is*-regulatory regions are responsible for the controlled expression of genes that may pattern various tissues during distinct periods of development. A growing body of work suggests that *cis*-regulatory modifications in key gene networks may result in morphological innovations (Gompel et al., 2005; Davidson and Erwin, 2006; Carroll, 2008; Chan et al., 2010; Frankel et al., 2011). Due to the modular nature of *cis*-regulatory elements, evolutionary processes can act upon these regions, thus bypassing the negative pleiotropic effects that would be associated with modifications of coding regions (Stern, 2000). Furthermore, this modularity permits the establishment of independent developmental cascades that pattern a particular structure without affecting other aspects of an organism's development (Wagner et al., 2007). Comparing the developmental gene regulatory networks between organisms could help us understand how differences in the network contribute to morphology.

Tetrapod fore- and hind limbs are homologous to the pectoral and pelvic fins of chondrichthyans and osteichthyans (cartilaginous and bony fish, respectively) (Owen, 1849; Coates, 1994; Shubin et al., 1997). The implication of this relationship is that shared developmental mechanisms may be involved in appendage outgrowth (Ruvinsky and Gibson-Brown, 2000). In zebrafish (*Danio rerio*), pectoral fins arise from mesenchymal proliferations that originate from the lateral plate mesoderm, analogous to limb development in tetrapods (reviewed in Tanaka, 2013). Developing fish fin buds and tetrapod limb buds show remarkable

molecular resemblances within particular domains, such as the zone of polarizing activity (ZPA) and the apical ectodermal ridge (AER) which help demarcate the anteroposterior (AP), proximodistal, and dorsoventral axes via Shh and Fgf signaling (Grandel and Schulte-Merker, 1998; Yano et al., 2012; Zuniga, 2015). In developing limbs and fins, *Shh* originates from the ZPA, located at the posterior margin of the limb mesenchyme (Krauss et al., 1993; Riddle et al., 1993). *Shh* is activated and controlled by a network of transcription factors resulting in an asymmetric distribution of the Shh protein (Tanaka and Tickle, 2007; Butterfield et al., 2010). In the posterior region of the limb, high levels of Shh inhibit the processing of Gli3 to the cleaved transcriptional repressor, Gli3R, creating a gradient which functions to regulate the expression of patterning genes along the AP axis (Wang et al., 2000).

A number of regulatory genes have been shown to ablate or amplify *Shh* expression in the tetrapod limb, highlighting the complex gene regulatory logic mediating *Shh* expression. Capellini and colleagues (2006) found that $Pbx1^{-/-}/Pbx2^{+/-}$ mouse (*Mus musculus*) mutants exhibit abnormal fore- and hind limbs, and *Shh* expression is absent in the hind limb. Pbx is known to partner with 5' HoxD proteins in the limb and together these mediate *Shh* expression and influence AP limb morphology (Kmita et al., 2005; Capellini et al., 2006; Mao et al., 2009; Zhu et al., 2010; Lettice et al., 2012; Kozhemyakina et al., 2014). In zebrafish $Pbx4^{-/-}$ mutants lack pectoral fins and fail to express genes involved in fin-bud outgrowth, including *Shh* (Pöpperl et al., 2000). Although it has been challenging to parse out the role of Hox genes because of positive Hox-Shh cross-regulation during limb development, there is evidence that *HoxD* and *HoxA* genes are important in the proper maintenance of AER Fgf expression during mouse early limb development, independent of their role in controlling *Shh* expression (Sheth et

al., 2013). These observations support the role of *Pbx* and *Hox* genes in the regulation of *Shh* expression in vertebrate appendages.

Hand2, the basic helix-loop-helix (bHLH) transcription factor, is an upstream activator of *Shh* which binds to the ZPA regulatory sequence (ZRS) enhancer as part of a protein complex with HoxD13 in order to induce *Shh* expression (Lettice et al., 2003; Galli et al., 2010; Osterwalder et al., 2014). During limb outgrowth in mice, *Hand2* expression is localized to a broad domain in the posterior limb bud, encompassing the region of *Shh* expression. In homozygous *Hand2* mutants, limb buds are malformed and *Shh* expression ablated (Charité et al., 2000). In mice with ectopic *Hand2* expression, forelimbs showed mirror-image duplications of posterior elements and a second domain of *Shh* expression resulting in polydacytlous hind limbs (Charité et al., 2000). Similarly, zebrafish *hand2* mutants exhibit AP patterning defects in their pectoral fins, and *Shh* expression is absent (Yelon et al., 2000).

In contrast to *Hand2*, *Twist1* is required to inhibit *Shh* expression in the anterior limb bud mesenchyme. *Twist1* mutants exhibit ectopic anterior expression of *Shh* and up-regulation of downstream targets of Shh signaling such as *Gli1* and *Ptc1* resulting in polydactylous limbs (Charité et al., 2000; Zhang et al., 2010b). Additional analyses reveal that Twist1, along with two ETS transcription factors, Etv4 and Etv5, synergistically repress anterior *Shh* expression (Zhang et al., 2010b; Lettice et al., 2014). Zebrafish have four *twist* paralogs (*twist1a, twist1b, 2,* and *3*) and all but *twist2* are expressed during pectoral fin development (Germanguz et al., 2007; Yeo et al., 2009). However, their potential role in regulating *Shh* expression during fin development is not known.

Retinoic acid plays an important role in limb development as evidenced by its polarizing activity when applied to the anterior region of the wing buds of chicks, inducing supernumerary

digit formation through an ectopic anterior domain of *Shh* expression (Tickle, 1981; Riddle et al., 1993). In zebrafish, RA functions similarly and AP patterning of the fin is established using an orthologous gene network as seen in other vertebrates (reviewed in Mercader, 2007). For example, RA treatment at 24-30 hours post-fertilization (hpf) is sufficient to induce an ectopic *Shh* expression domain in the anterior region of the pectoral fin bud 2-3 days post fertilization (dpf) (Akimenko and Ekker, 1995; Hoffman et al., 2002). In mouse and zebrafish which lack the RA synthesis enzyme, raldh2, embryos fail to develop limbs/fins (Niederreither et al., 1997; Grandel et al., 2002). However, RA-deficient zebrafish pectoral fin and mouse hind limb development can be rescued with an Fgf receptor antagonist and this has been interpreted as demonstrating that RA is not required for appendage patterning but rather initiation (Zhao et al., 2009). However, this conclusion has been contested by others (Roselló-Díez et al., 2014). Nevertheless, similarities in RA responsiveness and *Shh* expression have been found in cartilaginous fish (Dahn et al., 2007; Sakamoto et al., 2009). Thus, the fundamental role of *Shh* in AP appendage patterning seems to be deeply conserved across vertebrates.

Like *Shh, HoxA/D* expression and regulation has been studied extensively in both paired fins and limbs revealing important differences in gene expression (Sordino et al., 1995; Davis et al., 2007; Freitas et al., 2007; Johanson et al., 2007; Zakany and Duboule, 2007). Studies in mouse have identified two phases of 5'*HoxD* expression: an early phase responsible for patterning more proximal limb structures (stylopod, zeugopod), and a late phase which patterns the distal portion (autopod) of the limb (Zakany and Duboule, 2007) through reverse colinear gene expression (nested expression of 5' *HoxD* genes with *HoxD13* being broadest). However, patterns of late phase expression in fish are distinct from what have been observed in mouse,

making it difficult to homologize gene expression across taxa and the skeletal structures they build.

During mouse limb development, *HoxD10, 12, and 13* genes are concomitantly expressed in a reverse colinear manner during late phase expression (Tarchini et al., 2006). Reports of late phase expression in catshark have instead shown that *HoxD10* is expressed at an earlier developmental period than *HoxD12* and *13* (Freitas et al., 2007; Tanaka, 2016). Other important differences in expression relate to the overlapping expression domains of *hoxa11* and *hoxa13* seen in zebrafish (Ahn and Ho, 2008), catshark (Sakamoto et al., 2009), and paddlefish (Metscher et al., 2005). These patterns are distinct from the separate domains seen in mouse and chick (*Gallus gallus*) limb development, where *HoxA11* is restricted to the presumptive zeugopod and *HoxA13* to the autopod (reviewed in Schneider and Shubin, 2013).

Given the differences in gene expression patterns in tetrapods and fish, understanding the role of *Hox* bi-modal expression during the fin-to-limb transition has been challenging. Recent work has instead focused on characterizing the regulatory elements controlling *HoxA/D* gene expression as well at the epigenetic landscape of the *HoxA/D* locus. On the telomeric (3') end of the murine *HoxD* locus, there is a gene desert that contains enhancer sequences that govern early, collinear gene expression (Andrey et al., 2013; Braasch et al., 2016). Within this desert are two functionally conserved enhancer sequences, CNS65 and CNS39, present in both gar (*Lepisosteus oculatus*) and zebrafish genomes (Braasch et al., 2016). Later in development, a conformational change in chromatin structure occurs, permitting access to enhancers located on the 5' side of the cluster to regulate late, reverse collinear *HoxD* expression (Montavon et al., 2011; Andrey et al., 2013). Subsequent efforts have further characterized the activity of the enhancers lying within

this desert in order to better understand the regulatory mechanisms shared between paired limbs and fins.

Comparative analyses of late phase regulatory elements reveal that *HoxD* Island I and CsB, as well as the *HoxA* element e16 are present in the genomes of both gar, a non-teleost actinopterygian, and skate, a chondrichthyan (Schneider et al., 2011; Gehrke et al., 2015). Furthermore, transgenic assays of these regulatory elements drive distal reporter expression in similar patterns to their murine orthologs in the developing mouse autopod. These results support the notion that regulation of *HoxD* late phase expression in paired appendages is a feature present in the last common ancestor of bony fish (Osteichthyes) (Gehrke et al., 2015).

1.5 Overview of thesis

This dissertation stems from my interests in obtaining a deeper understanding of genetic and developmental mechanisms that generate different morphologies. I focus on the development of limbs and fins because of their morphological diversity and wealth of data collected in model organisms. As an evo-devo biologist, my experimental approach is comparative, where I seek to understand the similarities and differences of gene expression in chondrichthyan and actinopterygian organisms (Chapter II). I characterize the expression of Hox genes in both pectoral and dorsal fins of skate and paddlefish and propose that a common developmental module is responsible for both median and paired fin patterning. While gene expression is largely descriptive, the analytical contribution of my work includes one of the first portrayals of the role of *hoxa13* in the dorsal fin of zebrafish though CRISPR/Cas9 genome editing.

In Chapter III, I study the functional conservation of the ZRS, a long-range regulatory element responsible for *Shh* expression in fin and limb development. I analyze reporter expression patterns of the ZRS in zebrafish and mouse transgenics from a variety of distantly

related donor organisms. Through this phylogenetic framework I find support for the hypothesis that the ZRS originated in the gnathostome lineage. I also characterize the phenotypes of ZRS medaka mutants carrying a 401 bp deletion, which generally exhibit fewer than 4 proximal radials in their pectoral fins. This evidence provides support for *Shh* playing a role in specifying the number of endoskeletal elements in the fin.

Collectively, these studies act to: (i) elucidate features of median fin patterning and development, which also sheds light on the common developmental module between paired and median fins, and (ii) illuminate *Shh* regulation, including the origin of the ZRS and the first functional analysis of this regulatory element in a fish model.

In Chapter IV, I conclude by revisiting the concept of homology introduced in Chapter I and postulate that to test hypotheses concerning evolutionary transformations and the origin of paired appendages, a holistic experimental approach must be taken, incorporating paleontological evidence and modern developmental and genomic tools. Specifically, detailed knowledge of the full suite of regulatory networks during fin, limb, and gill arch development may help biologists understand the origin of paired appendages. Moreover, performing such work in phylogenetically relevant organisms will perhaps identify common evolutionary trends that apply to broader themes of organogenesis.

Finally, in Appendix I, I summarize my work studying the reporter expression patterns of two additional *Shh* long-range enhancers, MACS1 and MFCS4, in zebrafish endodermal derivatives in an attempt to address the evolutionary conservation of these elements. In Appendix II, I summarize my efforts in generating a *shhb* CRISPR/Cas9 zebrafish mutant that can be later used to study the contribution of *shhb* expression to appendage development, a critical comparison to its single-copy homolog in mouse.

CHAPTER II

A COMMON DEVELOPMENTAL MODULE PATTERNS BOTH MEDIAN AND PAIRED FINS

2.1 Author contributions

The work reported in this chapter was completed through collaboration with Tetsuya Nakamura and Jeff Klomp. The analyses of skate pectoral fin development (Figure 2.6 and 2.7) were published as part of Nakamura, T., Klomp, J., Pieretti, J., Schneider, I., Gehrke, A.R., and Shubin, N.H. 2015. Molecular mechanisms underlying the exceptional adaptations of batoid fins. Proc. Natl. Acad. Sci. U. S. A. *112*, 15940–15945.

J. Klomp assembled the *L. erinacea* transcriptome. T. Nakamura and J. Pieretti isolated RNA from *L. erinacea* embryos used for RNA-seq. T. Nakamura generated, genotyped, and analyzed the pectoral fins of the CRISPR-Cas9 *hoxa13a*$^{-/-}$/*hoxa13b*$^{-/-}$ zebrafish mutants (Figure 2.9, B). John Westlund illustrated the organisms presented in Figure 2.1. All other data reported in this chapter was generated by J. Pieretti.

2.2 Abstract

Time and again, scientists have discovered that deeply conserved developmental networks often build seemingly disparate morphological structures. These biological networks exhibit modular organization that, through the operation of evolutionary processes, often results in co-option. A key example of this modular organization can be found in the development of vertebrate appendages. Fins and limbs exhibit a great diversity in their size, shape and position along the body axis, suggestive of a developmental module that has been deployed in many

instances. While there has been much work to understand tetrapod limb formation, it is important to consider other models of appendage development in order to fully distinguish the structure of developmental modularity in vertebrate appendages. Here I demonstrate that despite different embryonic origins, paired and dorsal fins share features of *Hox* gene expression in a basal actinopterygian, paddlefish, and a cartilaginous fish, the little skate. Moreover, functional evidence derived from *hoxa13* mutant zebrafish reveals that *hoxa13* is necessary for proper dorsal fin development. The shared anatomical and developmental similarities of dorsal and paired fins support the hypothesis that they are built via a shared developmental module and inform the origin of paired fins.

2.3 Introduction

One of the fundamental challenges in comparative biology lies in understanding the relationships between shared developmental programs and their influence on phenotypic diversity. Because of their functional importance and unique morphological features, the paired appendages of vertebrates have been at the center of much genetic and developmental work. As homologous structures, paired fins and tetrapod limbs have been comparatively analyzed to understand topics such as pattern formation and the evolution of novelty. These studies have revealed impressive conservation between the signaling molecules and regulatory networks used to build and shape paired fins and limbs (reviewed in Schneider and Shubin, 2013; Shubin et al., 2009; Yano and Tamura, 2013). While there has been significant experimental evidence dedicated to gene expression and regulation of these gene networks during tetrapod limb patterning, it is important to consider other models of appendage development. Specifically, there is a need to expand the body of experimental evidence in the unpaired fins of phylogenetically informative non-model organisms. Fishes exhibit great morphological diversity,

especially in the variation of the size, shape, and position of their fins. Studying the extent to which developmental and genetic modules are conserved and altered in different tissues will elucidate the mechanisms that contribute to fin diversity. In this context, evo-devo research is a powerful lens that can bring into focus the shared features of appendages and of the developmental and genetic processes that shape them (Braasch et al., 2016).

Extant gnathostomes display both median (dorsal, anal, caudal) and paired (pectoral and pelvic) fins. However, agnathans like lamprey possess median fins and lack paired appendages. Remarkably, it is thought that median (unpaired) fins arose prior to paired fins, approximately 400 million years ago (Coates, 1994; Mabee et al., 2002). The fossil record shows that among early stem-gnathostomes, including galeaspids and *Euphanerops longaevus,* there were representatives in which median fins were present, but paired appendages were absent (Janvier, 1996; Coates, 2003; Sansom, 2010). According to these phylogenetic interpretations, it can be hypothesized that the developmental mechanisms present in median fins may be ancestral to those in paired appendages, and these mechanisms may later have been co-opted in the evolution of paired fins (Mabee et al., 2002).

Researchers have long been fascinated by *Homeobox* (*Hox*) genes, largely due to their robust conservation across bilaterians and critical role in patterning the vertebrate body plan, including paired appendages (Duboule and Dollé, 1989; Favier and Dollé, 1997; Kmita et al., 2005). Through whole genome duplication events, *Hox* clusters have multiplied, providing a greater opportunity for diversification of function. Tetrapods, for example, have at least four clusters of paralogous *Hox* genes due to two whole genome duplication events early in the vertebrate lineage (Garcia-Fernandez, 2005; Kuraku and Meyer, 2009; Amemiya et al., 2010). However, much variability exists within the vertebrate group. Teleosts typically have seven or

eight *Hox* clusters due to a third round of whole-genome duplication (Hoegg et al., 2004), although there has also been a constellation of lineage-specific genome duplication and gene loss therein (Kurosawa et al., 2006; Mungpakdee et al., 2008; Kuraku and Meyer, 2009) (Figure 2.1). Among agnathans and basal actinopterygians such as lamprey and paddlefish, independent lineage-specific duplication events have resulted in a unique complement of paralogs (Crow et al., 2012; Mehta et al., 2013).

A unique feature of *Hox* genes is their spatiotemporal colinearity, reflected in the arrangement of the genes within a cluster and their AP expression in vertebrate embryos, including paraxial mesoderm, neural crest, and branchial arches (reviewed in Krumlauf, 1994). Genes on the 3' end of the cluster are broadly expressed in anterior domains, later followed by expression of 5' genes in more restricted, posterior regions. A similar phenomenon is observed during limb development where 3' *HoxA* and *HoxD* gene activity patterns proximal regions of the limb, the stylopod and zeugopod. This pattern in paired appendages is later followed by a second, inverted phase of gene activity, where genes from the 5' end now lead expression in distal mesenchyme in progressively more restricted domains to pattern the autopod (Tarchini and Duboule, 2006; Zakany and Duboule, 2007). Evidence from *HoxA13* gene knockouts in mice has shown an important role for these paralogs in endochondral bone formation during limb development (Fromental-Ramain et al., 1996b; Zakany and Duboule, 2007), but similar functional work in fish is sorely needed to distinguish the conserved and unique roles of *Hox* genes in fin development.

The evolutionary and mechanistic underpinnings of 'reverse colinear' or 'late phase' *HoxD* expression has been studied extensively, considering its influence in patterning an innovative feature of the limb—the distal autopod (Woltering et al., 2014). Comparative analyses

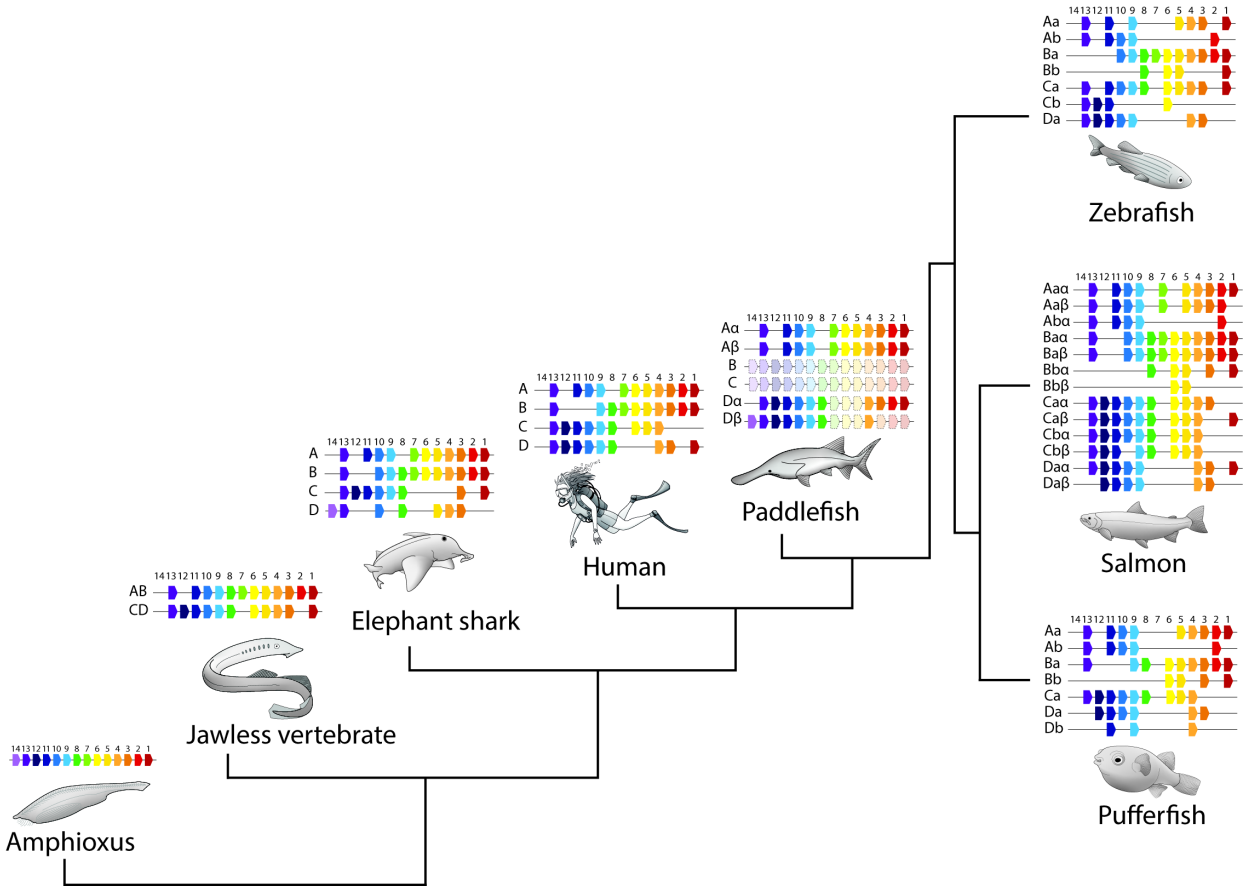

Figure 2.1 - Vertebrate phylogeny depicting *Hox* cluster duplications. *Hox* clusters have been duplicated in the gnathostome lineage through WGDs. Elephant shark and human both have 4 clusters. Paddlefish underwent a lineage-specific WGD separate from the teleost (zebrafish, salmon, pufferfish) WGD. Pale-colored *Hox* genes in paddlefish represent unknown data. α and β nomenclature is used to indicdate nonfirst-order paralogy with teleost *Hox* genes.

between tetrapod limb and pectoral fin development prompted the hypothesis that the acquisition of *HoxD* late phase expression was a necessary step in the fin-to-limb transition (Shubin et al., 1997; Wagner and Chiu, 2001). Subsequent developmental studies have challenged this view, though heed should be taken in their interpretation. Initially, late phase HoxD expression was detected in the basal actinopyterygian, *Polyodon spathula* (Davis et al., 2007), though more recent evidence no longer supports this claim (Tulenko et al., 2016). The reverse is true for zebrafish. While late phase *Hox* expression was not detected during zebrafish development (Sordino et al., 1995), a reevaluation at later developmental periods led Ahn and Ho (2008) to conclude that a distal expansion of *HoxD* expression, reminiscent of tetrapod late phase expression, was present. Additional gene expression analyses in catshark (Freitas et al., 2007) and lungfish (Johanson et al., 2007) also revealed late phase-like expression patterns during fin development suggesting an evolutionarily older role of late phase expression, prior to the origin of the autopod. However, other studies in catshark have not reported late phase *Hox* expression at similar developmental stages (Sakamoto et al., 2009) causing further ambiguity in these conclusions.

Recent studies have instead focused on the regulatory and epigenetic mechanisms responsible for both colinear and late phase expression patterns. In the case of the HoxD cluster in the mouse limb, enhancers embedded within a 3' gene desert adjacent to the cluster govern early, colinear expression. Later, a conformational change in chromatin structure permits access to enhancers located on the 5' side of the cluster and regulates late, reverse colinear HoxD expression (Montavon et al., 2011; Andrey et al., 2013). Experimental efforts have further characterized the activity of these enhancers, thus shedding light on the origin of late phase enhancers and shared regulatory mechanisms between paired fins and limbs.

Comparative analyses of regulatory elements 5' to the *HoxD* cluster have shown high conservation among jawed vertebrates including a non-teleost actinopterygian (spotted gar) and a chondrichthyan (little skate) (Spitz et al., 2003; Schneider et al., 2011; Schneider and Shubin, 2013; Gehrke et al., 2015). Recently, transgenic assays of orthologous zebrafish and gar late phase regulatory elements show that *hoxd* elements Island I and CsB, and the *hoxa* element, e16, are capable of driving distal expression in zebrafish fins (Schneider et al., 2011; Gehrke et al., 2015). Furthermore, these gar enhancers drive distal expression in similar patterns to their murine orthologs in the developing mouse autopod. Together these results support the notion that regulation of *HoxD* late phase expression in paired appendages is a feature present in the last common ancestor of bony fish (Osteichthyes) (Gehrke et al., 2015). However, regulatory elements responsible for median fin expression have yet to be identified.

Investigations in non-model organisms like gar (*Lepisosteus oculatus*) as well as paddlefish (*Polyodon spathula*) and the little skate (*Leucoraja erinacea*), can help to elucidate the developmental and genetic networks that underlie paired and median fin patterning. Analyzing paddlefish and skate fin development in a phylogenetic framework can provide context to hypotheses of fin evolution. Paddlefish are basal actinopterygians and members of the well-supported clade of acipenseriform fishes, which also includes sturgeons (Janvier, 1996; Inoue et al., 2003). The cartilaginous fish, little skate, is a representative of the elasmobranch clade and exhibits both derived and ancestral traits such as wing-like pectoral fins and two dorsal fins, which is considered an ancestral gnathostome trait (Janvier, 1996). Unlike teleosts, both chondrichthyans and paddlefish retain a tri-basal pectoral fin consisting of a propteryigum, mesopterygium, and metapterygium—a feature considered the plesiomorphic condition for extant gnathostomes (Coates, 1994; Mabee et al., 2002).

Gene tree analyses of *HoxA* genes led to the proposal that paddlefish had not been a part of the teleost-specific genome duplication (Metscher et al., 2005). However, it was later established that paddlefish did undergo a separate lineage-specific genome duplication, leading to orthologs of the *HoxA* and *HoxD* genes (Crow et al., 2012). As such, previous reports on *Hox* expression are confounded without detailed gene expression analyses of duplicated *Hox* genes during fin development.

To understand the relationship between paired and median fin development, *Hox* gene expression in both *P. spathula* and *L. erinacea* fins were analyzed. Additionally, dorsal fin morphology of *D. rerio hoxa13* mutants was analyzed using μCT scanning. These results show that a common developmental module is deployed in both paired pectoral and dorsal fins, and provide experimental support for the hypothesis that this developmental control module originated in the midline and was later co-opted in development of paired fins (Freitas et al., 2006).

2.4 Results

HoxA and *HoxD* gene expression during paddlefish paired fin development

In light of the whole genome duplication event in the paddlefish lineage, it was important to reevaluate the expression data of *Hox* gene paralogues during paddlefish paired and median development. Published genomic data of BAC regions encompassing the *HoxA* and *HoxD* clusters (Crow et al., 2012) were used to design probes against *Alpha* (α) and *Beta* (β) paralogues in the two clusters (Figure 2.1). These probes were used to assess the genes' spatiotemporal activity across three developmental stages via whole mount *in situ* hybridization. Given the high sequence identity between certain paralogues, such as *HoxA11α* and *HoxA11β* (97.9%) instances of cross-reactivity between the probes cannot be strictly ruled out.

Gene expression was studied at Stage 41 during early pectoral fin development, Stage 43.5 during the onset of endoskeletal radial formation, and Stage 46 when the fin has differentiated endochondral and dermal components. At Stage 41, *HoxD10* transcripts were not detected via whole mount *in situ* hybridization (Figure 2.2). However, at Stage 43.5 *HoxD10* expression was detected in a band along the distal pectoral fin bud. At Stage 46, *HoxD10* expression continued and the domain became more posteriorly restricted. Unlike *HoxD10*, both *HoxA11α* and *HoxA11β* transcripts were detected in Stage 41 paddlefish pectoral fin buds. While *HoxA11α* was expressed weakly throughout the fin bud, *HoxA11β* trancripts localized to the posterior half of the fin bud mesenchyme (Figure 2.2). At Stage 43.5, *HoxA11α* expression persisted throughout much of the fin fold. In older embryos (Stage 46), *HoxA11α* transcripts appeared along a distal strip along the margin of the pectoral fin bud (Figure 2.2). In contrast, the paralog *HoxA11β,* exhibited posteriorly localized expression within the pectoral fin fold in both Stg 43.5 and 46 paddlefish embryos (Figure 2.2). The expression patterns of *HoxA13* α and β paralogs were quite similar until Stage 46. Early in fin development (Stage 41) both genes have weak expression that is distally restricted, albeit *HoxA13α* appears more diffuse than *HoxA13β* (see arrowhead in Figure 2.2). At Stage 43.5, *HoxA13α* and *HoxA13b* transcripts are both expressed in a broad strip along the distal margin of the fin bud mesenchyme. In Stage 46 embryos, *HoxA13α* expression becomes more retricted than at Stage 43.5 and it is expressed both in the posterior distal fin bud and fin fold. In contrast, *HoxA13β* faint signal is present along the posterior distal margin of the endochondral disk.

In addition to characterizing *Hox* paralog expression in the pectoral fins, pelvic fin expression was also evaluated. Stage 43.5 paddlefish pelvic fins exhibited expression of both

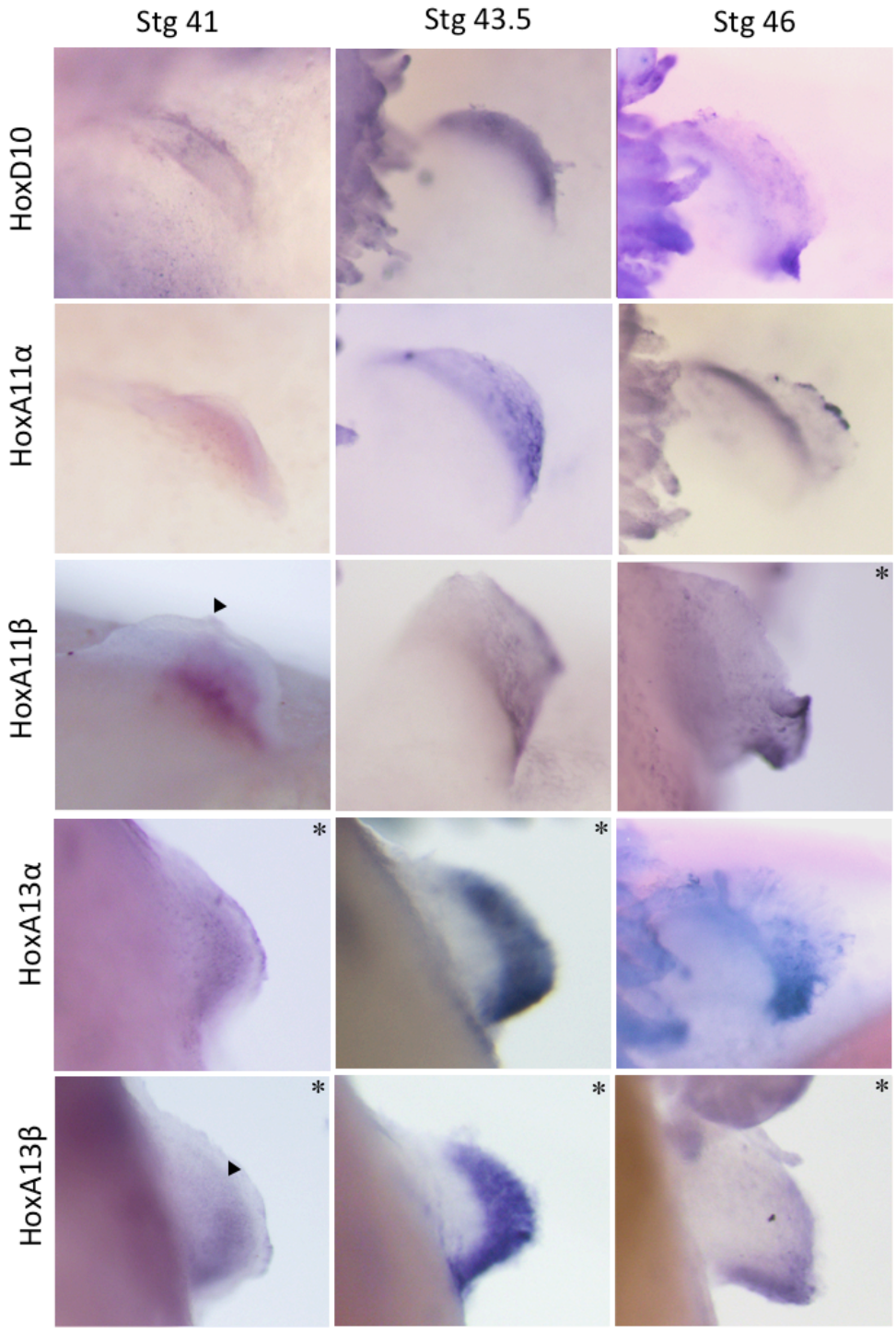

Figure 2.2 - *Hox* expression in *P. spathula* pectoral fins. Whole-mount *in situ* hybridizations for *HoxD10, HoxA11α, HoxA11β, HoxA13α*, and *HoxA13β* across developmental stages 40, 43.5, and 46. Lateral views shown, with anterior to the left, and distal is up except where noted. Asterisk (*) denotes a dorsal view of the fin where anterior is up and distal is to the right. Arrowheads mark anterior boundaries of expression. Genes are marked in rows and stages are marked in columns.

Shh, a developmental gene involved in A-P polarity, and *HoxD10* in a posteriorly restricted pattern at the base of the pelvic fin buds (Figure 2.3, A, arrowheads). By contrast, *HoxA11α* expression was harder to detect, though it may be expressed diffusely within the pelvic fin bud mesenchyme (Figure 2.3, A). However, expression of *HoxA11β* was more robustly expressed throughout the pelvic fin buds (Figure 2.3, A). Expression of both *HoxA13α* and *HoxA13β* paralogs was observed throughout the pelvic fin bud mesenchyme, though robust localization towards the base of the buds was noted (Figure 2.3, A). A lateral view of the embryo shows the tapering of *HoxA13β* expression in the anterior pelvic fins (Figure 2.3, B). Notably, expression in the caudal fin web was also observed and might be localized in the fin fold mesemchyme. However, this expression pattern did not persist at Stage 46 (Figure 2. 3, B).

In sum, *HoxD10*, *HoxA11* paralogs, and *HoxA13* paralogs exhibit distal expression along the margin of the pectoral fin, which becomes posteriorly restricted at later stages (Figure 2.2). In pelvic fins, both *Shh* and *HoxD10* expression is observed in distinct posterior domains, while *HoxA11β*, and *HoxA13* paralogs are expressed more broadly at Stage 43.5 (Figure 2.3, A).

HoxA and _HoxD_ expression during paddlefish median fin development

In an effort to determine the developmental modularity of fins as a whole, *Hox* gene expression was also assayed during median fin development. At Stage 43.5 weak *HoxA10a* expression can be broadly detected in the dorsal fin fold (dff) as well as the fin mesenchyme (Figure 2.4, A). Expression of both *HoxA11α* and *HoxA11β* was detected at low levels encompassing the dff and the muscle buds. Relative to *HoxA11α,* the signal for *HoxA11β* appeared to be more robust. Like other HoxA genes assayed, *HoxA13α* and *HoxA13β* expression

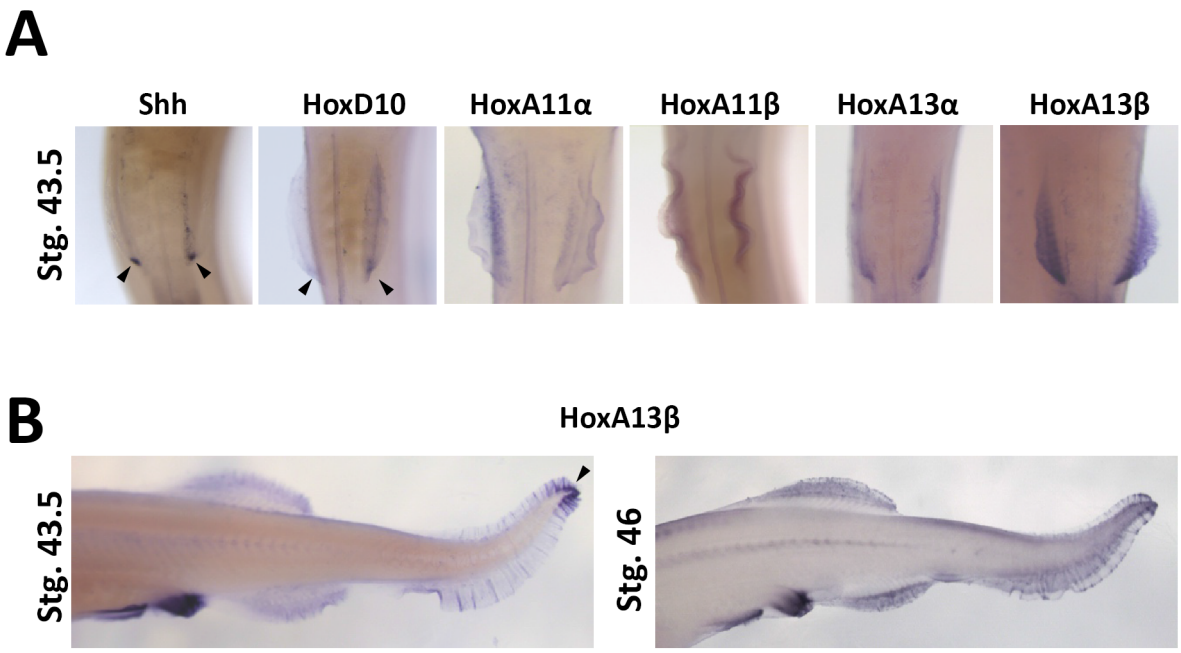

Figure 2.3 - Expression of *Shh* and *Hox* genes in *P. spathula* pelvic fins and median fins. (A) Whole-mount *in situ* hybridization of *Shh* and *Hox* cluster genes in Stage 43.5 pelvic fins. Ventral view is shown, anterior is up. Arrow denotes posteriorly localized *HoxD10* expression. **(B)** Paddlefish *HoxA13β* expression in the posterior half of the body. Anterior is to the left. Expression can be seen in the fin fold of the dorsal and anal fins. Note expression in the fin web of the developing caudal fin at Stage 43.5 (arrow). Another angle of pelvic fin expression is provided. Note expression in the vent (equivalent to urethra) at both stages.

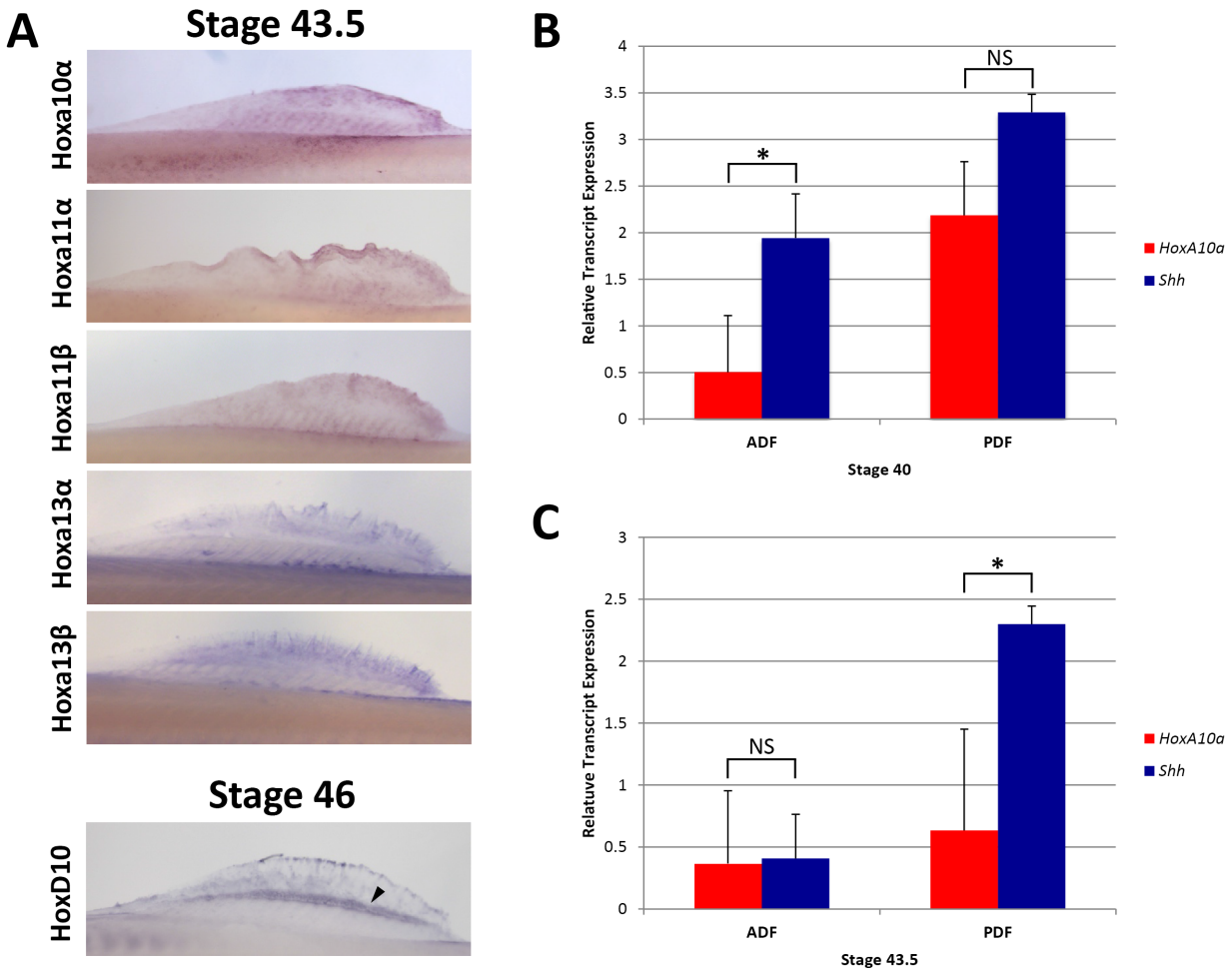

Figure 2.4 - *P. spathula Hox* gene expression in dorsal fins. (A) Whole mount *in situ* hybridizations for *HoxA* α and β cluster genes. Note *HoxA10α, HoxA11β*, and *HoxA13α* expression in muscle buds. Weak expression can also be seen in the fin fold of the dorsal fin. At Stage 46, HoxD10 is expressed along distal margin of the dorsal fin bud. Preliminary qRT-PCR data for *Shh* and *HoxA10α* expression in the anterior dorsal fin (ADF) and posterior dorsal fin (PDF) at Stage 40 **(B)** and Stage 43.5 **(C)** embryos (N=15). Expression was normalized to the housekeeping gene β-*actin*. At Stage 40, ADF *HoxA10a* expression is 0.50-fold below expression relative to *β-actin* and *Shh* expression is 1.94-fold greater. PDF *HoxA10a* expression is 2.18-fold greater and PDF *Shh* expression is 3.29-fold greater relative to β-*actin*. The difference in expression between *HoxA10a* and *Shh* expression in the ADF is statistically significant (t-test $p < 0.05$). However, Stage 40 *HoxA10a* and *Shh* PDF expression is not statistically significantly different. At Stage 43.5, ADF *HoxA10a* expression is 0.36-fold below expression relative to *β-actin*, and *Shh* expression is 0.41-fold below. The difference in ADF expression between *HoxA10a* and *Shh* is not statistically significant (t-test $p > 0.05$). *HoxA101a* PDF expression at Stage 43.5 is 0.64-fold below and PDF *Shh* expression is 2.30-fold greater. The difference between Stage 43.5 *HoxA10a* and *Shh* expression in the PDF is significant (t-test $p < 0.05$). Positive standard error bars are shown.

was weak and primarily found in the dff. However, some localized *HoxA13α* expression was detected at the base of the fin and may be localized to the fin mesenchyme. While *HoxD10* transcripts could not be detected in dorsal fins at Stage 43.5, trancripts were subsequently detected along the distal edge of the dorsal fin bud at Stage 46. As a control, in situ hybridization using sense probes in both median and pectoral fins were performed and background was generally weak or absent (Figure 2.5).

In the case that transcript levels of genes like *Sonic hedgehog* (*Shh*) were too low to be detectable by *in situ* hybridzation, qRT-PCR was performed. *Shh* is expressed in a posteriorly localized domain in paired appendages, and is a key gene for establishing A-P polarity (Riddle et al., 1993). This preliminary analysis indicated that *Shh* transcripts were enriched over 3-fold in the posterior dorsal fin (PDF) relative to *β-actin* expression at Stage 40 (Figure 2.4, B). Later, at Stage 43.5, *Shh* transcripts were enriched 2.3-fold in the PDF (Figure 2.4, C). Earlier in development, at Stage 40, *HoxA10a* expression was 2.18-fold greater than *β-actin* in the PDF, and 0.50-fold below in the ADF (Figure 2.4, B). Transcripts of *HoxA10a* were detectable throughout the dorsal fin via *in situ* hybridization and RT-PCR results indicated that relative transcript levels were low throughout the fin at Stage 43.5 (Figure 2.4, C). *HoxA10a* expression was 0.34-fold below *β-actin* expression in the ADF and 0.64-below in the PDF. These preliminary qRT-PCR results suggest that *Shh* expression in the ADF may be down regulated as development progresses while high levels of expression are sustained in the PDF

Gene profile during skate pectoral fin development

During embryogenesis, the skate pectoral fin undergoes a unique transformation where the small, semi-circular fin dramatically extends anteriorly and fuses to the head, forming a

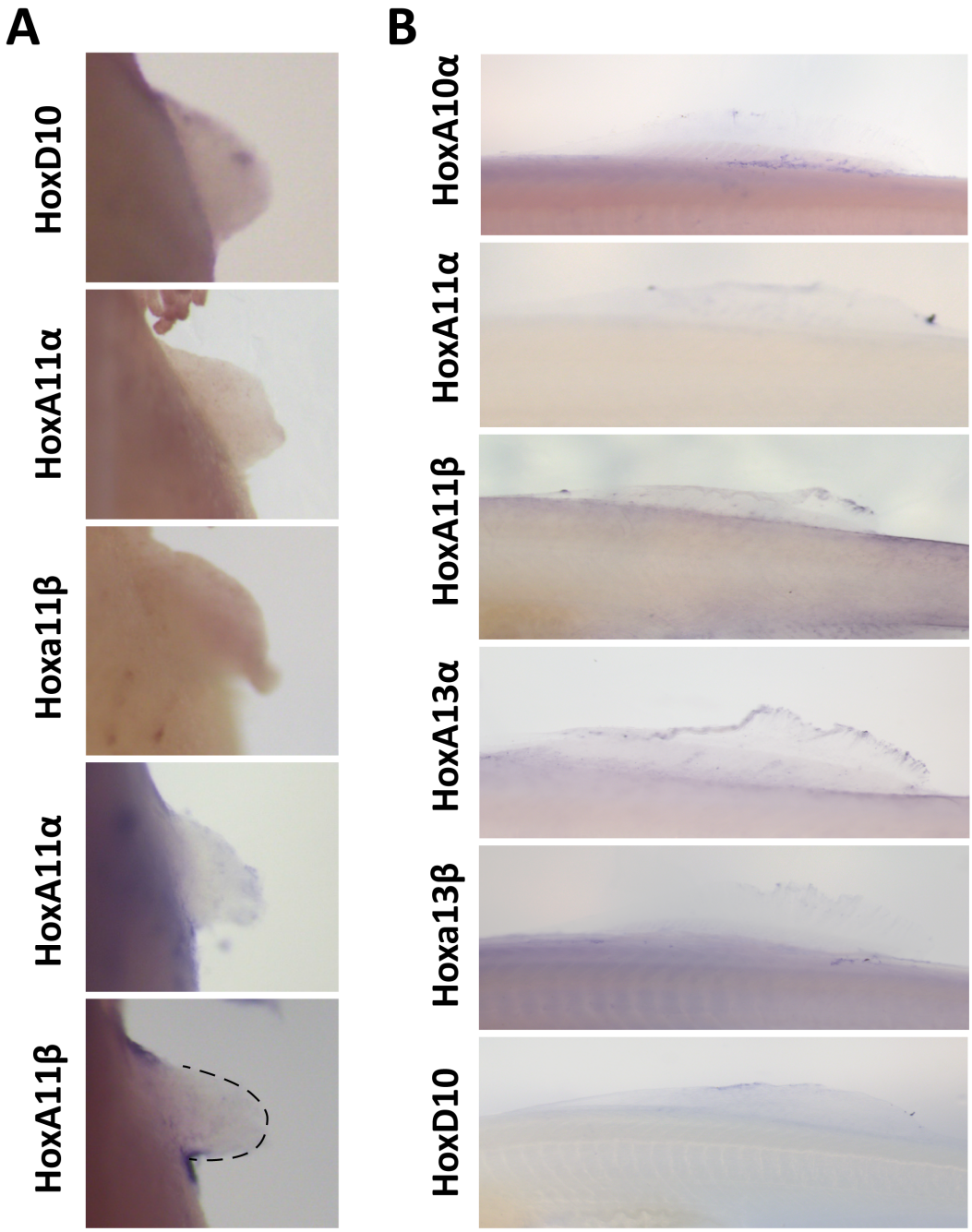

Figure 2.5 - Control *in situs* for *P. spathula* fins. (A) Sense dig-labeled RNA probe *in situ* hybridization in Stg. 43.5 pectoral fins **(B)** Sense dig-labeled RNA probe *in situ* hybridization in Stg. 43.5 embryos.

broad wing-like fin suited for benthic life (Maxwell et al., 2008). In order to characterize the temporal and spatial profile of genes expressed during skate fin development, RNA-seq was performed on three portions of the pectoral fin (anterior, central, and posterior) at three different stages (Stages 29, 30, and 31) (Figure 2.6; see Figure 2.7 for Stages 29 and 31). In lieu of a skate genome, each mRNA was annotated using the zebrafish genome. RNA-seq identified *Alx4* and *Pax9* (known anterior-specific limb genes in tetrapods) (Takahashi et al., 1998; LeClair et al., 1999) in the anterior pectoral fin, indicating the efficacy of this technique to identify site-specific gene activity (Figure 2.6, A). RNA-seq also revealed a number of genes that were significantly enriched in the posterior portion of the fin (Figure 2.6, A and B). These include genes involved in paired appendage development, including *Hox*, *Fgf* (*Fibroblast growth factor*), and *Wnt* (*Wingless-type MMTV integration site family*).

We performed in situ hybridization of a subset of the genes identified via RNA-seq to characterize their expression patterns during skate pectoral fin development. Expression of the *Shh* target gene, *Ptc2* (Marigo et al., 1996), was localized to the posterior mesenchyme (Figure 2.6, C). This pectoral fin expression is identical to previous reports of *Ptc2* expression in skate (Dahn et al., 2007). *Fgf8*-*Fgf10*, which maintain the apical ectodermal ridge (AER) in tetrapods (Ohuchi et al., 1997) and are expressed in the apical fold (AF) during fin bud outgrowth and regeneration (Yano et al., 2012), are expressed in the posterior half of skate pectoral fins. *Fgf8* expression is restricted to the posterior ectoderm, whereas *Fgf10* is expressed in the posterior mesenchyme (Figure 2.6, C). Transcripts of *And2,* a molecular marker of cells that contribute to the AF in teleosts (Zhang et al., 2010a), are also expressed along the distal margin of the fin. *HoxA11* appeared to have three domains of expression including the muscle buds spanning the fin and weak expression in the both anterior and posterior mesenchyme (Figure 2.6, C, arrows).

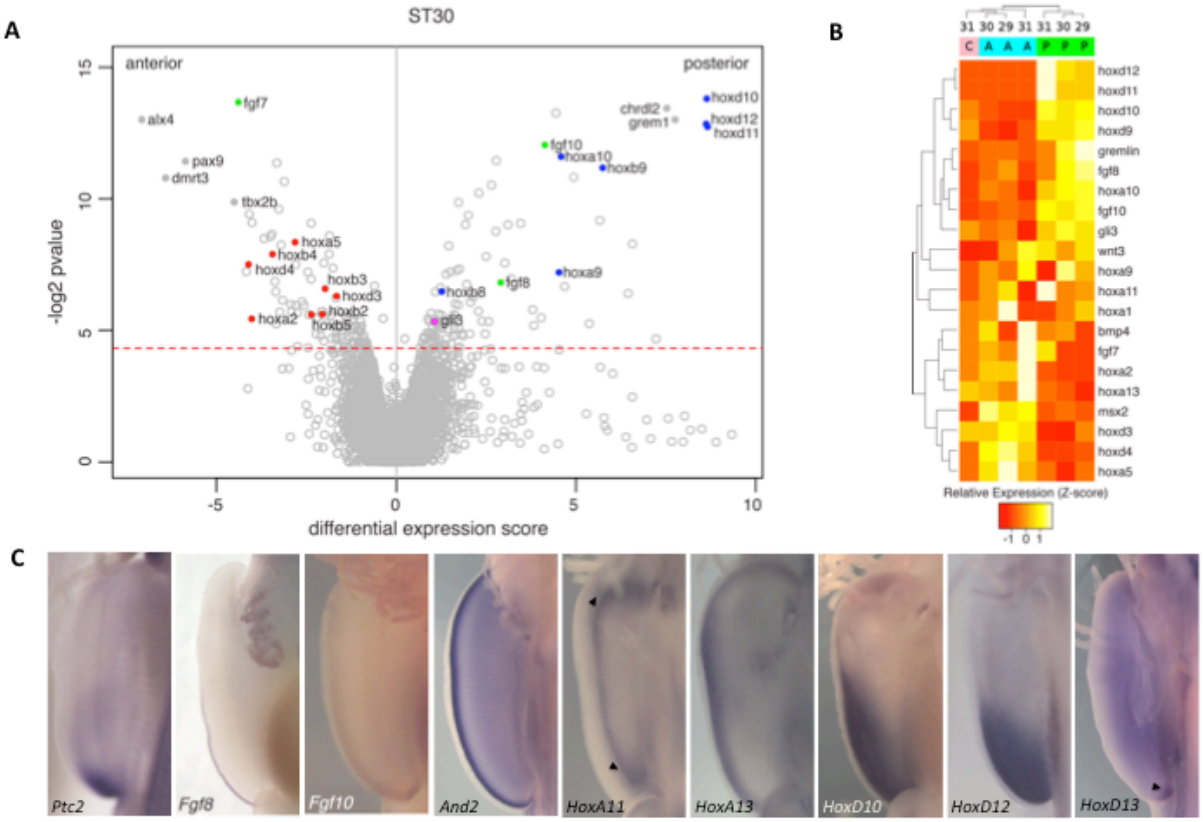

Figure 2.6 - RNA-Seq and whole mount in situ in *L. erinacea* pectoral fins. (A) Differential expression of transcripts assembled from RNA-seq of anterior and posterior fin tissue samples of Stage 30 skates. Differential expression score is derived from multiple A–P comparisons of transcript abundance (n = 3). Above the red dotted line corresponds to P values < 0.05. Blue, *5'Hox* genes; green, *Fgf* genes; purple, *Gli3*; red, *3'Hox* genes. **(B)** Standardized read counts (z-scores) for selected transcripts in the pectoral fin at three developmental stages and locations of the pectoral fin. Transcripts were median-summarized according to their annotations. A, anterior fin; C, center fin; P, posterior fin. Sample developmental stages are listed at the top, and clustering is based on relative expression levels. **(C)** Whole-mount in situ hybridization for 'tool-kit' developmental genes at stage 30.

Note: The data analysis in **(A)** and **(B)** was performed by J. Klomp. The *Fgf8* and *Fgf10 in situ* hybridizations in **(C)** were performed by T. Nakamura.

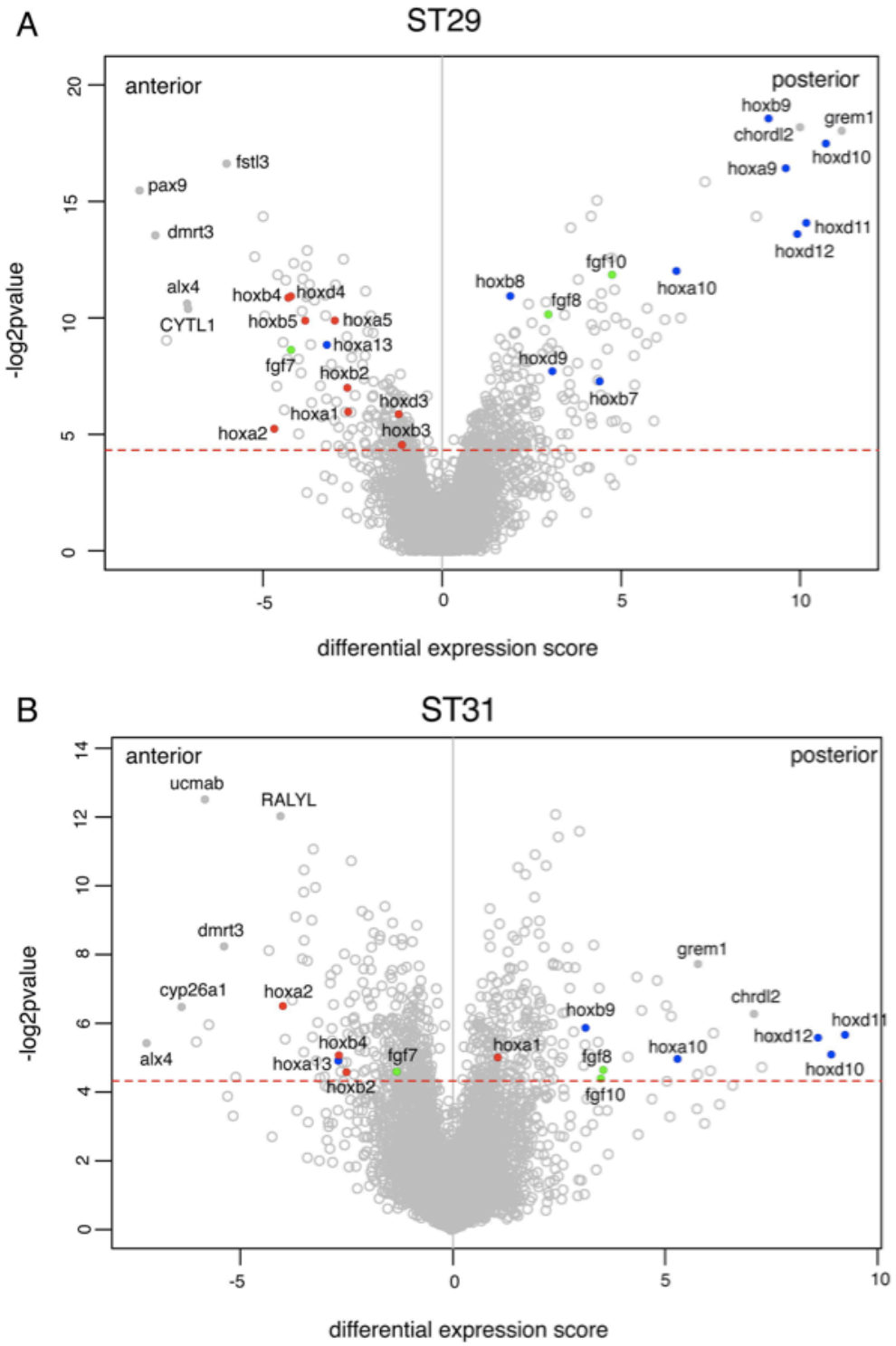

Figure 2.7 - Volcano plots of *L. erinacea* differential expression in Stages 29 and 30 pectoral fins. Differential expression of transcripts assembled from RNA-seq of anterior and posterior fin tissue samples of **(A)** Stage 29 and **(B)** Stage 30 skates. Differential expression score is derived from multiple A–P comparisons of transcript abundance (n = 3). Above the red dotted line corresponds to P values < 0.05. Blue, *5'Hox* genes; green, *Fgf* genes; red, *3'Hox* genes; grey, genes with known activity in anterior or posterior limb development.

This is in agreement with the RNA-seq data of *HoxA11* expression at Stage 30 (Figure 2.6, B). *HoxA13* gene expression was restricted to the distal margin of the fin bud mesenchyme (Figure 2.6, C). Finally, 5′ *HoxD* (*HoxD10*, *12*, and *13*) genes localized to the posterior fin, consistent with the pattern described in tetrapod limbs and zebrafish fins (Figure 2.6, C). These data demonstrate that the developmental genes that pattern the skate pectoral fin are comparable to those of the paired fins of teleosts and limbs of tetrapods.

Hox gene expression during skate median fin development

Hox expression was also assayed in the dorsal fins of the skate to determine if median fins of skate and paddlefish share common patterning mechanisms. Expression was examined at Stage 29, where dorsal fins can be easily distinguished and the posterior edge of the second dorsal fin has an acute angle relative to the body axis (Maxwell et al., 2008). Interestingly, at this stage *HoxA13* expression spans the distal margin of the dorsal fin buds in a pattern similar to what is observed during late phase expression of posterior *HoxA* genes in mouse (Fromental-Ramain et al., 1996a). Transcripts of *HoxD9, HoxD12*, and *HoxD13* were restricted to the posterior end of the dorsal fins, forming a nested, colinear pattern of expression (Figure 2.8, A).

In mice, *Hand2* is required for proper limb bud development though activation of *Shh* by forming a protein complex with HoxD13 (Galli et al., 2010). In skate, transcripts of *Hand2* were restricted to the posterior domain of the dorsal fins. However, in Stage 29 embryos *Shh* was not detected in the dorsal fins, despite its expression in other tissues at this stage (Gillis et al., 2009), and previous reports of dorsal fin expression (Figure 2.8, B) (Dahn et al., 2007). The lack of *Shh* expression in dorsal fins may be explained by slight staging differences in Stage 29-30 embryos, as their development is strongly influenced by water temperature, and developmental stages span a window of several weeks (Maxwell et al., 2008).

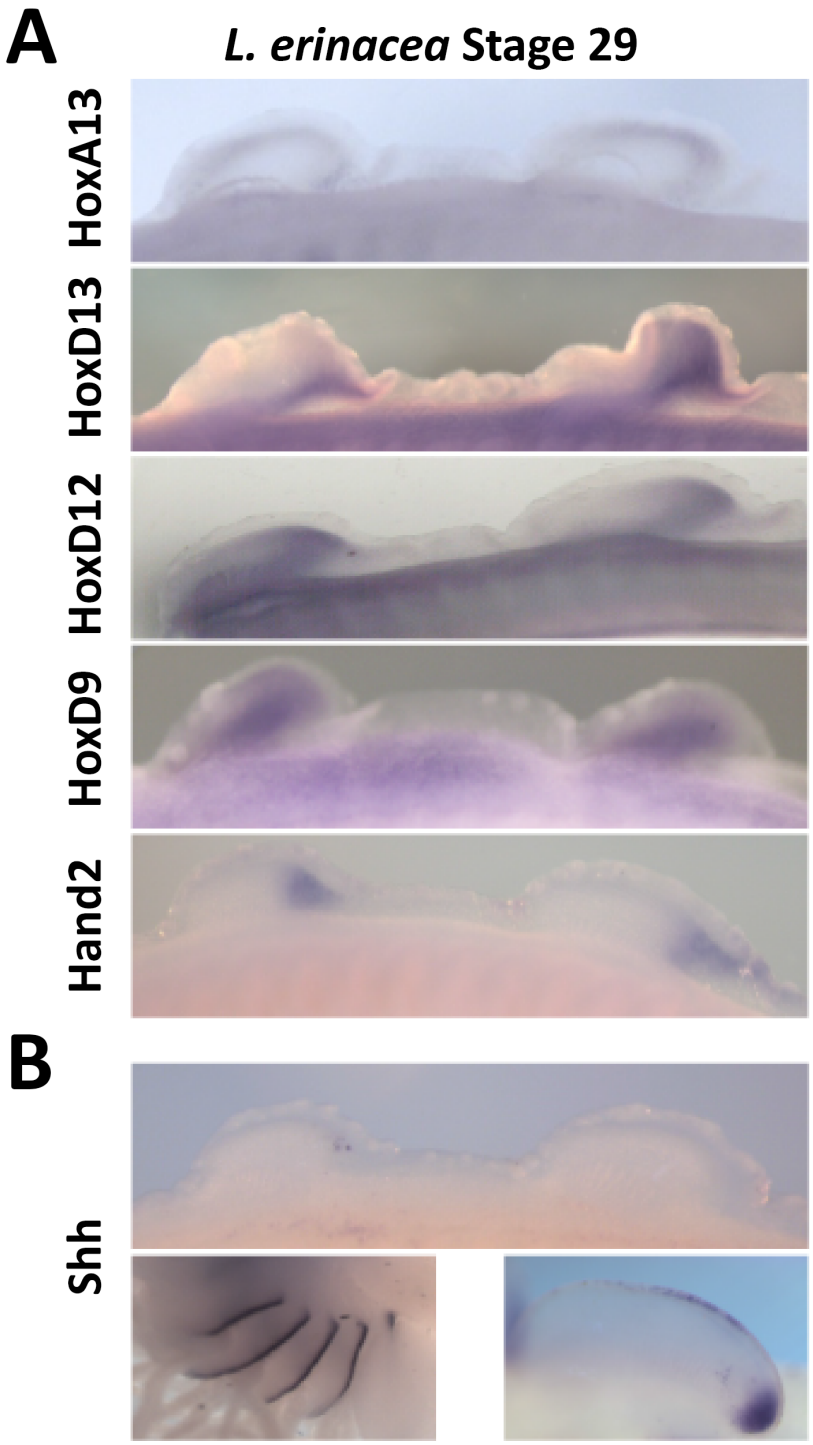

Figure 2.8 - *Hox, Hand2,* and *Shh* gene expression in *L. erinacea.* (A) Whole-mount in situ hybridization of *HoxA13*, *HoxD13*, *HoxD12, HoxD9*, and *Hand2* skate dorsal fin expression at Stage 29. Note *HoxA13* distal expression along the margin of the dorsal fin bud. *HoxD13*, *HoxD12, HoxD9*, and *Hand2* dorsal fin expression are posteriorly localized in both dorsal fins. A nested, colinear pattern of expression is observed among *HoxD9-HoxD13* genes. **(B)** *Shh* expression in the dorsal fins was not detected, though it has been reported previously (Dahn et al., 2007). However, robust expression can be seen in the branchial arches (left) and pelvic fin (right).

Altered dorsal fin morphology in *Danio rerio hoxa13a*$^{-/-}$ and *hoxa13b*$^{-/-}$ mutants

In order to assay the functional role of *Hox* genes in patterning dorsal and pectoral fins, CRISPR-Cas9 technology was used to disrupt the coding region of *hoxa13a* and *hoxa13b* genes in *Danio rerio* (T. Nakamura generated stable-germ line mutants carrying a frameshift mutation within the first exon upstream of the homeodomain). *D. rerio* have a single dorsal fin with eight radials, although the number of radials can range from seven to nine (Bird and Mabee, 2003). According to Bird and Mabee (2003) the radials segment proximodistally, resulting in a larger proximal radial and a smaller distal radial, which articulates directly with adjacent lepidotrichia (fin rays). Using μCT-scanning to garner a greater level of detail than clearing and staining, I observed further segmentation of radials in both wildtype and mutant specimens, where a second distal radial lies between the larger proximal radial and smaller distal radial that articulates with the fin ray (Figure 2.9, A). The number of fin rays also varies, though generally there is an "N+2" rule where N equals the number of proximal radials (Bird and Mabee, 2003). At approximately four months of age, homozygous mutant fish exhibit altered dorsal fin morphology where the dermal fin rays were considerably shortened and appeared more ossified than their wildtype counterparts (Figure 2.9, A). The proximal radials with extended rods and vanes (also called pterygiophores) appeared relatively unaffected. Paired appendages were also affected in *hoxa13* mutants, exhibiting truncated finrays and an increased number of distal radials (Figure 2.9, B) (Nakamura et al., submitted).

2.5 Discussion

The vertebrate appendage has long been considered an exemplar developmental module, defined by its autonomy from other parts of the body and expression of specific sets of genes. Whether discussing developmental, genetic, or variational modules (Wagner and Mezey, 2004),

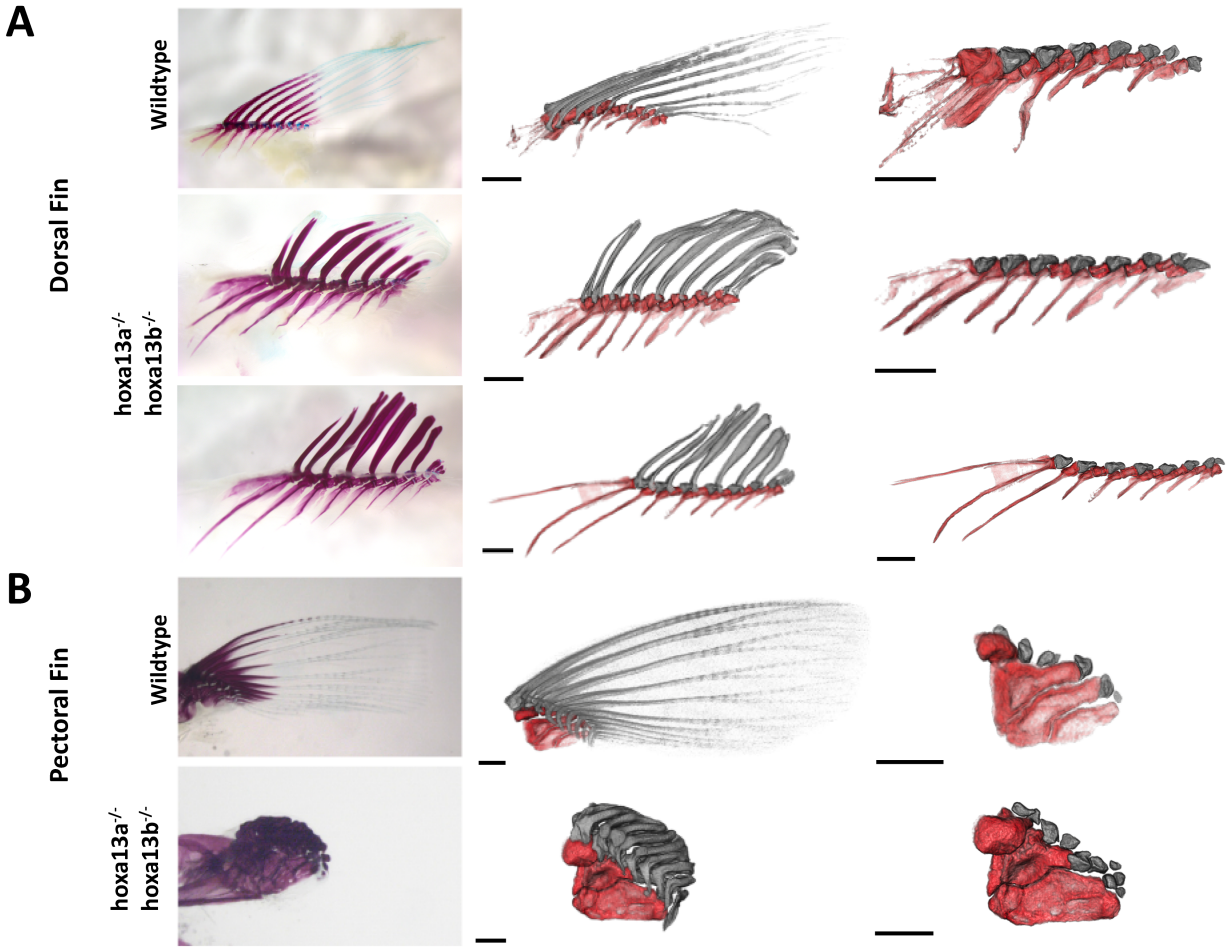

Figure 2.9 - *D. rerio* fin phenotype in *hoxa13* mutants. (A) Leftmost panels show cleared and stained dorsal fins from adult wildtype and *hoxa13a*$^{-/-}$/*hoxa13b*$^{-/-}$ specimens. Middle panels show µCT images of dorsal fin specimens with endochondral radials (red) and dermal fin rays (grey). Right panels show endochondral component only, where distal radials are shown in grey**.** Note truncated fin rays in mutant. **(B)** Leftmost panels show cleared and stained pectoral fins from adult wildtype and mutant specimens. Middle panels show µCT images of pectoral fins with endochondral component (red) and dermal fin rays (grey). Right panels show endochondral component only, where distal radials are shown in grey. Note truncated fin rays and additional distal radials in mutant. Scale bars = 500µm

Note: T. Nakamura generated the *D. rerio hoxa13a*$^{-/-}$/*hoxa13b*$^{-/-}$ mutants and analyzed pectoral fins seen in **(B)**

these modular units of organization allow for the action of evolutionary processes including dissociative processes like heterotopy, duplication and divergence, and co-option (Raff, 1996; Wagner and Altenberg, 1996; Mabee et al., 2002). Since modular units are dynamic and undergo evolutionary change, they can be recognized as modified homologous traits across taxa (Raff, 1996) and their study can lead to a better understanding of the impact of modularity on morphological evolution.

The evidence presented in this study suggests that there is a fin developmental module present in both dorsal and paired fins. In paddlefish pectoral fins, *Hox* paralogs are deployed in a nested, colinear manner consistent with reported data in both tetrapod and fish (reviewed in Schneider and Shubin, 2013) (Figure 2.10, A). At Stage 43.5 paddlefish *HoxD10* pectoral fin expression is reminiscent of distally localized mouse limb *HoxD10* expression (Akiyama et al., 2015). The data presented here are also in agreement with previous developmental studies of distally localized paddlefish *HoxA11* and *HoxA13* expression, prior to the knowledge that the cluster was duplicated (Davis et al., 2007). Remarkably, late phase *HoxD* expression in other paddlefish structures like the barbel, has been reported (Archambeault et al., 2014). However, based on the gene expression data presented here it appears that late phase expression in fins, considered a distinctive feature of autopod development, is absent in paddlefish, in accordance with a recent report (Tulenko et al., 2016). Future efforts to characterize the regulatory features that govern paddlefish *Hox* gene expression may reveal as yet unknown conserved *cis*-regulatory elements in this basal actinopterygian. Combined data on gene expression and regulation may provide more conclusive evidence on the presence or absence of late phase *Hox* expression.

The gene tool-kit used in skate pectoral fins suggests that it is functionally congruent to the paired fins of teleosts and tetrapod limbs due to the conserved expression of *HoxD* genes.

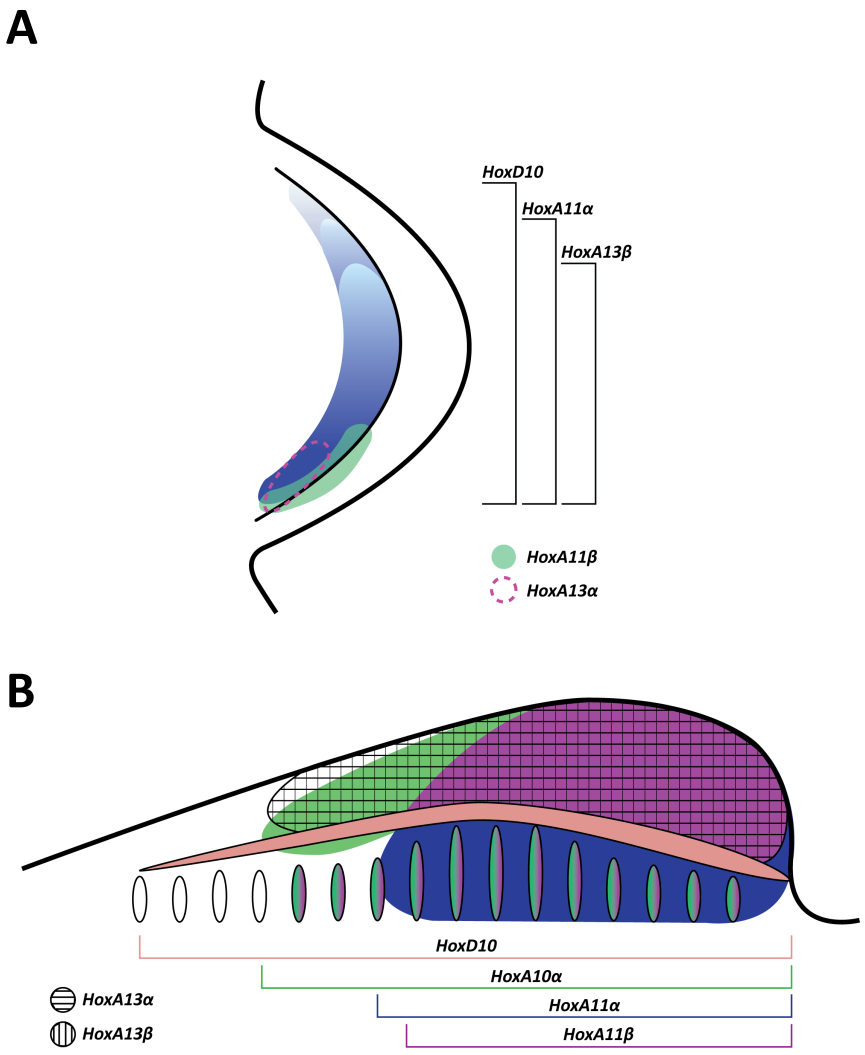

Figure 2.10 - Schematic of *Hox* expression in *P. spathula* pectoral and dorsal fins. Summary of gene expression results in **(A)** pectoral fins (at Stage 46) and **(B)** median fins (Stage 43.5; except for *HoxD10*, which is expressed at Stage 46). Gene domains are approximate in median fins given the diffuse patterns of transcripts.

Skate pectoral fins also exhibit *HoxA11* and *HoxA13* gene expression similar to reported expression patterns in *Scyliorhinus canicula* (catshark) embryos, another chondrichthyan representative (Sakamoto et al., 2009), though there was no overlap of these genes in the distal mesenchyme of the skate fin at the observed stage. *And2* expression, a feature of the dermal compartment of the fin is also equivalent to expression seen in catshark embryos (Tulenko et al., 2016). The most startling difference of skate pectoral fin development, however, is the development of an extra AER-like tissue in the anterior portion of the fin, which is maintained by a *3′ Hox-Fgf7-Wnt3* module (Nakamura et al., 2015). When *Wnt3* was disrupted in skate pectoral fins, the anteriormost endoskeletal component, the propterygium, was reduced and failed to elongate anteriorly (Nakamura et al., 2015). This is suggestive of an anterior developmental module in the skate fin. While the maintenance of a second, anterior AER-like tissue may be a derived feature of skate pectoral fin development, it highlights the capacity of a developmental module to be parceled out, i.e. gene functions in the module can be partitioned without severely affecting other regions of activity. A way by which parcellation of modules can occur is through gene duplication and subsequent subfunctionalization of duplicated genes (Force et al., 1999, 2004). Nakamura and colleagues (2015) hypothesize that *Wnt3* may have played an ancestral role in maintaining the AER and this role was later reassigned to different *Wnt3* members via gene duplication and divergence. This scenario likely played out in case of *Wnt3* and *Wnt3a*, which maintain the AER in mice and chicken, respectively (Barrow et al., 2002; Narita et al., 2007).

The results presented in this study demonstrate that a suite of conserved *Hox* genes associated with paired fin development is also deployed in the dorsal fins of paddlefish and skate. *HoxA10α, HoxA11,* and *HoxA13* paddlefish paralogs exhibit diffuse expression in the

dorsal fin fold of paddlefish, while *HoxA10α* and *HoxA11* paralogs were also expressed in the dorsal fin bud mesenchyme (Figure 2.10, B). In skate dorsal fins, a nested, colinear pattern of expression was observed among *HoxD9-HoxD13* genes. While late phase *Hox* expression has not been reported in median fins, it is intriguing that skate *HoxA13* was expressed in a distally restricted pattern along the margin of the dorsal fin bud. Future work should focus on characterizing this developmental module more fully. For example, determining if factors such as *T-box* genes initiate fin bud outgrowth as they do in paired appendages, and identifying the *Hox* gene enhancers that drive median fin expression. 5' *Hox* genes would also need to be evaluated at multiple stages to determine if late phase expression occurs during skate dorsal fin development.

Preliminary qRT-PCR analyses suggest that *Shh* is expressed in the dorsal fins of paddlefish, and while transcripts were not detected in skate pectoral fins in this study, previous work has shown that there is a ZPA-like domain present in the dorsal fins of both skate and bamboo shark embryos (Dahn et al., 2007). In order to better understand how broadly *Shh* expression in the dorsal fins of jawed vertebrates, additional expression analyses of *Shh* during median fin development must be performed including that of actinopterygians such as medaka and zebrafish, and lobe-finned fishes such as the lungfish. To date, *Shh* expression has not been reported in the median fins of any actinopterygian though previous work suggests that at least in the zebrafish caudal fin, *Shh* signaling may emanate from the notochord and not a ZPA-like domain (Hadzhiev et al., 2007). Similarly in agnathans, effort is need to investigate whether *Hh* genes are expressed in the median fin of lamprey or hagfish embryos. It may be possible that a source of *Shh* signaling exists in the dorsal fins of many actinopterygians as well as the median

fins of agnathans, but has not yet been formally reported. Discovery of such a domain will strengthen the hypothesis of a common developmental module in both paired and median fins.

Evidence of truncated fin rays and potentially fused distal radials of *D. rerio hoxa13a*$^{-/-}$ /*hoxa13b*$^{-/-}$ dorsal fins show that *hoxa13* is necessary for proper development of the dorsal, as well as pectoral fins (Nakamura et. al., submitted). These data provide functional support for the existence of a fin developmental module in both dorsal and paired fins. This is consistent with some models of paired fin origin, which proposed that the pectoral fins originated by the redeployment of median fin modules in the lateral plate mesoderm (Coates and Cohn, 1998; Freitas et al., 2006). Freitas and colleagues (2006) offered a hypothesis proposing that the mechanisms of fin and limb development were present in the median fin fold prior to the origin of vertebrates based on their study of gene expression in lamprey and catshark median fins. Analyses of *dlx* and *msx* expression in the paired and median fins of zebrafish may also be viewed as evidence of co-option of this developmental module (Akimenko et al., 1994, 1995). Moreover, the competency to induce an apical ectodermal ridge (AER) in the lateral flank of dogfish and zebrafish (Abe et al., 2007; Yonei-Tamura et al., 2008) supports the existence of a fin developmental program (i.e. module) that contributes to variations in position and morphology of fins. It may be that the morphological diversity of fish fins is a byproduct of their developmental modularity, which is considered an important property that influences the evolvability of a system (Raff, 1996; Wagner and Altenberg, 1996). For instance, a genetic or regulatory change to a particular module will have pleiotropic effects on a set of related traits, but will interfere less with traits outside of this module (Wagner et al., 2007).

Interestingly, *HoxA13β* expression is found in the caudal fin web of Stage 43.5 embryos. Adult acipenseriforms exhibit diverse heterocercal caudal fin morphologies, including the

relatively equal dorsal and ventral caudal fin lobes of adult paddlefish, versus the highly asymmetric caudal fin lobes of *Scaphirhynchus platorynchus* (shovelnose sturgeon), that are associated with a variety of swimming and feeding functions (Bemis and Grande, 1999). Moriyama and Takeda (2013) describe a sclerotome-rich cell population that gives rise to caudal skeletal components in teleosts and suggest that *HoxA13* might specify this cell population. Further comparative analyses of *HoxA13* expression and functional testing via CRISPR-Cas9 technology in actinopterygians may give insights into caudal fin development and its contribution to morphological diversity.

In an analysis of conserved phylogenetic patterns of fin differentiation in actinopterygians, Mabee and colleagues (2002) inferred that dorsal and anal fins are part of two positioning and patterning modules based on the symmetric position of the dorsal and anal fin along the AP axis and observed similarity between radial and ray formation in both types of fins. Interestingly, these modules may be primitively retained in paddlefish (Mabee et al., 2002). However, a recent geometric morphometric study on the variational modularity of fin positioning in the actinopterygian fish, *Danio rerio* and the Northern redbelly dace (*Chrosomus eos)* led the authors to conclude that dorsal and anal fins may a form a single positional module along with the caudal fin and posterior portion of the trunk (Larouche et al., 2015). However, both patterns of co-variation and modularity can evolve; therefore the conclusions made by Larouche et al. (2015) may not represent an ancestral condition, or a true model for the origin of parts. Additionally, a high degree of shared developmental similarity between fins might be a derived feature whereby fins have converged on similar forms due to common functional demands and constraints on morphology (Stewart et al., 2014). These different experimental approaches highlight both the challenges and need to investigate the influence of modularity on several

levels of biological organization from position and patterning of morphological structures to the function of molecules within a cell.

Instances of co-option at multiple levels of organization and across seemingly disparate structures have been observed before (Gao and Davidson, 2008; Moczek and Rose, 2009; Shubin et al., 2009; Wang et al., 2013). Another example comes from embryological work done in *L. erinacea*. It has been shown that in the little skate, a Shh-Fgf feedback loop patterns both paired pectoral fins and the gill arches (Gillis et al., 2009). Developmental modules, however, can be influenced by dissociative processes including heterochrony and heterotopy, thus complicating interpretations of morphological transformations like that described in the gill-arch theory for the origin of paired appendages. While support for the gill-arch hypothesis remains equivocal (Pieretti et al., 2015), the results from this study support the use of recursive developmental mechanisms to pattern similar morphological structures.

2.6 Materials & Methods

Animal Husbandry and Staging

All animal procedures were performed in accordance with the University of Chicago IACUC policies (ACUP #71033). Fertilized eggs of the American paddlefish, *Polyodon spathula* were purchased from Osage Catfisheries, Inc. (Osage Beach, MO) and raised to desired stages. Approximately 1,500 embryos were incubated at 18°C (12 h:12 h light:dark cycle) in reverse osmosis water with water hardness approximating 100ppm. After hatching, the temperature was gradually increased to 22°C and juveniles were fed live brine shrimp. At 22°C, *P. spathula* development between stages 36 (hatching) and stage 46 (feeding; yolk exhaustion) proceed at approximately one stage every 24 hours (Davis et al., 2004). Staging of *P. spathula* was based on Ballard and Needham (1964) and Bemis and Grande (1992). At desired stages, *P. spathula* were

euthanized in a lethal dose of MS-222 (Tricaine) and fixed at 4°C for at least 24 hours in Modified Carnoy's Fixative (6 volumes of 100% ethanol: 3 volumes of 37% formaldehyde: 1 volume of glacial acetic acid).

Leucoraja erinacea embryos were purchased from the Marine Resource Center of The Marine Biological Laboratory (Woods Hole, MA). Embryos were kept at 15°C in reconstituted Instant Ocean (Aquarium systems) in reverse osmosis water with a 12 h:12 h light:dark cycle. Staging of embryos was based on (Maxwell et al., 2008). At desired stages, embryos were euthanized with a lethal dose of MS-222 (Tricaine) and fixed at 4°C for at least 24 hours in 4% (wt/vol) paraformaldehyde (PFA).

Isolation of *P. spathula* and *L. erinacea* genes

P. spathula RNA was extracted from Stage 38-46 embryos using the RNeasy® Mini Kit (Qiagen) following the manufacturer's instructions. *L. erinacea* RNA was extracted from Stage 29 and 30 embryos also using the RNeasy® Mini Kit (Qiagen). Prepared RNA was then used as a template for first strand cDNA synthesis using the iScript™ (Biorad) kit. PCR primers were designed using *P. spathula* gene sequences published in Crow et al., (2012) and Davis et al., (2007) (see Table 2.1 for primers used). PCR primers used to amplify *L. erinacea* genes are listed in Table 2.1. Next, gene fragments were amplified and then integrated into pCRII-TOPO (Invitrogen). Plasmid clones were purified and sequenced by the University of Chicago Sequencing Facility to confirm accuracy and orientation of insert.

***In situ* hybridization**

Sense and antisense digoxigenin-labeled probes were generated using T7 or SP6 polymerases (Promega) and dUTP (Roche). In situ hybridizations in paddlefish were performed as described in Modrell et al., (2011) with the following modifications: Post-hybridization washes consisted

of two one-hour washes of 50% formamide, 5X SSC, and 1% SDS followed by two 30 minutes washes with 50% formamide and 2X SSC, and a 20 minute wash with 50% formamide, 1X SSC, and 0.1% Tween-20; embryos were washed for an additional day in MABT after anti-digoxigenin incubation; after color development specimens were washed in several washes of PBS, postfixed in 4% paraformaldehyde, and stored in TE buffer. Skate in situ hybridizations were performed as described in O'Neill et al., (2007), except for a 60°C incubation for hybridizing the *Fgf7* probe.

***L. erinacea* RNA-Seq**

Total RNA was extracted from three biological replicates from two domains (anterior and posterior fin) of *L. erinacea* embryos at Stages 29 and 30 and three domains (anterior, center, and posterior fin) at Stage 31 using the Qiagen RNeasy kit. RNA-seq libraries were generated using the TruSeq Stranded mRNA kit (Illumina). Libraries were multiplexed and 100-bp paired-end sequencing was conducted on an Illumina HiSeq2000 sequencer at the University of Chicago Genomics Facility.

Data preprocessing

Quality control of raw sequencing data was conducted using FASTQC v0.10.1 (Andrews, 2010). Barcodes and contaminating adapter sequences with > 5bp overlap were removed using CUTADAPT v1.1(Martin, 2011). Removal of low quality reads and extraction of orphaned reads were conducted using SICKLE (Joshi and Fass, 2011). Overlapping pairs of sequencing reads were merged using FLASH v1.2.2 (Magoč and Salzberg, 2011).

***L. erinacea* Transcriptome assembly and annotation**

Preprocessed RNA-seq data were assembled using the ABYSS v1.3.5 assembler (Birol et al., 2009; Simpson et al., 2009) and the tiled sub-read (kmer) length that optimized the N50 was

estimated as 35 nucleotides. Coding sequences and Ensembl gene IDs for Danio rerio (Zv10) were downloaded from Ensembl. The BLASTSUITE v34 tools (Camacho et al., 2009) were used to generate BLAST databases and conduct searches. Annotation of transcripts was completed in two steps. The translated largest open reading frame (ORF) from each *L. erinacea* transcript was used to query the *Danio rerio* coding sequences with tBLASTn (max e-value = 0.01) and hits from the reference database within 20 bp were merged. For each *L. erinacea* contig, the largest difference in log-2 e-values of the BLAST hits was chosen as the cutoff. For *L. erinacea* contigs of interest with greater than one BLAST hit, a reciprocal tBLASTn of the matching *D. rerio* genes was conducted in the *L. erinacea* transcriptome and the *D. rerio* gene with the lowest mean e-value was chosen as the annotation. For *L. erinacea* contigs without ORFs greater than 150 nucleotides or unannotated from the previous tBLASTn, a tBLASTx search was conducted in the *D. rerio* coding sequences. The annotations provided with the assembled transcriptome fasta file include the Ensembl gene IDs, gene descriptions, and BLAST e-values.

***L. erinacea* Alignment and differential expression**

We used BOWTIE2 v2.0.0 (Langmead & Salzberg, 2012) for sequence alignment and SAMTOOLS v0.1.18 suite (Li et al., 2009) for sorting, converting, removing duplicate, and indexing reads. The statistical environment R and Bioconductor packages were used for differential expression analysis. Biostrings v2.26.3 (Pages et al., 2009) was used for handling sequencing data. Transcripts less than 300 nucleotides in length were excluded. Transcripts that were unable to be annotated using the aforementioned methods were excluded such that 18,521 transcripts were included in the analyses. Log-2 RPKM (reads per kilobase of transcript per million mapped reads) values were computed for each transcript. Comparisons to identify differential expression were conducted essentially as in (Klomp et al., 2015). However, the

magnitude of differential expression (residuals) for individual transcript comparisons (linear regression) was modified to correct for irregular distribution. An apex was chosen at 1.02 times the maximum transcript score and the angular distance was used to weight individual transcript residuals.

***P. spathula* relative qRT-PCR in dorsal fin**

Anterior and posterior halves of *P. spathula* dorsal fins were dissected from Stage 40 and Stage 43.5 embryos stored in RNAlater reagent (Qiagen). RNA was isolated from pooled samples (N=15) of anterior and dorsal fin halves using the RNeasy® Mini Kit with DNAse digestion. Next, first-strand cDNA was synthesized using iScript™ (Biorad). Primers were designed to target products <200bp from *hoxa10a,* and *shh* genes (see Table 2.1 for oligos used). *β-actin* primers were obtained from Xiaoni et al., (2012). *β-actin* expression was analyzed as a reference gene to normalize expression. Real time PCR was run on an Applied Biosystems 7300 system using SYBR Green PCR Master Mix (Invitrogen). A standard curve for each set of primers was prepared using whole body cDNA from Stage 40 or Stage 43.5 *P. spathula* based on the stage analyzed in each plate. Expression levels were quantified and compared using the $2^{-\Delta\Delta CT}$ method (Livak and Schmittgen, 2001). Expression was visualized relative to B-actin expression, which was set = 1. Two plates for each stage (40, 43.5) containing triplicate technical reactions for each gene were pooled and analyzed.

Hoxa13a/hoxa13b* CRISPR-Cas9 in *Danio rerio

T. Nakamura generated stable germline mutants carrying frameshift mutations in *hoxa13a* and *hoxa13b.* Two mutations were simultaneously introduced into the first exon of each *hox13* gene by CRISPR/Cas9 system as previously described in *Xenopus tropicalis* (Nakayama et al., 2013). Briefly, two gRNAs matching the exon 1 sequence of each *hox13* gene were designed using

ZiFiT, http://zifit.partners.org/ZiFiT/*)*. Forward and reverse oligonucleotides unique to each target sequence were synthesized by Integrated DNA Technologies, Inc. (IDT) (see Table 2.1). Subsequently, each forward and reverse oligonucleotide was hybridized, and double stranded products were individually amplified by PCR with primers that included a T7 RNA promoter sequence, followed by DNA purification using NucleoSpin Gel and PCR Clean-up Kit (Macherey-Nagel). Each gRNA was synthesized from the purified PCR products by *in vitro* transcription with the MEGAscript T7 Transcription kit (Ambion). Cas9 mRNA was synthesized by mMESSAGE mMACHINE SP6 Transcription Kit according to the manufacturer's instructions (Ambion).

CRISPR/Cas9 injection and mutant selection

Two gRNAs targeting exon 1 of each *hox* gene were injected with *Cas9* mRNA into zebrafish eggs at the one cell stage. Approximately 2nL of the injection solution (5µl solution containing 500ng of each gRNA and 500ng Cas9 diluted in nuclease-free water) was injected into a one-cell stage embryo. Injected embryos were raised to adulthood, and at three months the fish were genotyped by extracting DNA from fin clips. Briefly, zebrafish were anesthetized using Tricaine (0.004%) and tips of the caudal fin (2-3mm^2) were removed and placed in a microcentrifuge tube. The tissue was lysed in standard lysis buffer (10 mM Tris pH 8.2, 10 mM EDTA, 200 mM NaCl, 0.5% SDS, 200 ug/mL proteinase K) in a 55°C water bath and DNA recovered by ethanol precipitation. Approximately 800-1100 bp of exon 1 from each gene was amplified by PCR using primers found in Table 2.1. To determine if mutations were present, PCR products were analyzed using the T7E1 (T7 endonuclease1) assay as previously reported (Jao et al., 2013). PCR fragments positive for mismatches were cloned into the pCRII-TOPO vector (Invitrogen) for further mutation analysis. After identification of mutant fish via the T7E1 assay, detailed

analysis of mutation indels were performed by sequencing at the University of Chicago Sequencing Facility.

Adult *Danio rerio* skeletal staining

Skeletal staining was performed as previously described (Bird and Mabee, 2003). Briefly, fish were fixed by 10% neutral-buffered formalin overnight. After washing with distilled & deionized water (ddH_2O), specimens were placed in a graded series to of 70% EtOH followed by 30% acetic acid/70%EtOH. Cartilage was stained overnight using a 0.02% Alcian blue solution in 30% acetic acid /70%EtOH. Specimens were then briefly rinsed using ddH_2O and the solution was changed to a 30% saturated sodium borate solution and incubated for an hour. After, specimens were immersed in a 1% trypsin/30% saturated sodium borate and incubated at room temperature for eight hours. Following another ddH_2O rinse, specimens were transferred into a 1% KOH solution with 0.005% Alzarin Red S. On the following day, specimens were rinsed in ddH_2O and subjected to a graded glycerol series for photographing and storage. Photographs were taken using a Leica M205FA microscope.

PMA staining and µCT scanning

After skeletal staining, dorsal fins were separated from the body. Fins were stained using a 0.5% (weight/volume) PMA (Phosphomolybdic acid) stain for 17 hours followed by two washes using ddH_2O. Specimens were placed into 1.5mL microcentrifuge tubes with ddH_2O and kept overnight to settle. On the following day, specimens were scanned using the UChicago PaleoCT (GE Phoenix v/tome/x 240kv/180kv scanner) (http://luo-lab.uchicago.edu/paleoCT.html), at 50

P. spathula Gene Target	Forward (5') Primer	Reverse (3') Primer
HoxD10	tgccgtctcttggtaaaagg	tcggtgaggttcacactctg
HoxA10α	aacggaacgagggtaactcc	gttctcccggctcatttttct
HoxA11α/ β	tgatgagcgagtttctgtgg	gcgcttctccttgttgatgt
Bts1 enzyme cuts *HoxA11α*, Product size:		128 bp, 208, 373 bp
HoxA13α	catggaaggatttgcaggag	cggctgtgtttgctccttag
HoxA13β	gacccggtgatgttccttta	gtcgaaatgagccgacatct
Shh	taaagctgagggtcacggaa	tgggtgaaacgagcccttat
HoxD10	tgccgtctcttggtaaaagg	tcggtgaggttcacactctg
P. spathula RT-PCR	**Forward (5') Primer**	**Reverse (3') Primer**
HoxA10α	agagaccgacgcttcttcag	ccagttggcagtgctttca
Shh	gtgattgaaacggaggagcc	tgacggaatgaaaaccagcg
B-actin		
L. erinacea Gene Target	**Forward (5') Primer**	**Reverse (3') Primer**
Ptc2	ttctgggcatttccttcaac	ggtacagcccatcatgaacc
Fgf8	accaactctacagccgcact	gagcgaggttatggttgagg
Fgf10	tgcggtctccaaatatcaca	tgcttccagataaatgcgtgt
And2	ggggtgaggctggattct	gtccttcttggggtcacagg
HoxA11	ccagcctgccttcatttta	cggtcggttaaattgagcat
HoxA13	gaacttcaccgcaaaccaat	tgatgccgatatcctccttc
HoxD9	ggcaggagacagaggacttg	acttgccgctcggtaagatt
HoxD10	ggaatgcagacctgtggact	gggcatctctttttccttcc
HoxD12	gccgtacacaaagcaacaga	aagtgaagagtcacggagcaa
HoxD13	ctgcatttggagcacatcac	gtctttcggtgaggttggtg
Hand2	tggaggatttcctcatcacc	ttcagttccaaagcccagac
Shh	acaagcaattcatcccgaac	ttctgctttcaccgagcagt
D. rerio CRISPR-Cas9	**gRNA #1**	**gRNA#2**
hoxa13a	aattaatacgactcactatagggcaatcacaaccagtggagttttagagctagaaatagc	aattaatacgactcactataggcagtaaagactcatgtcggttttagagagctagaaatagc
hoxa13b	aattaatacgactcactataggacacttctgtttctggaggttttagagctagaaatagc	aattaatacgactcactataggacacttctgtttctggaggttttagagagctagaaatagc
D. rerio T7 Assay	**Forward (5') Primer**	**Reverse (3') Primer**
hoxa13a	ctgcagcgggtgattctg	ctcctttacccgtcggtttt
Product size:		810bp
hoxa13b	gaagcttatcactagaatctttacagc	ttttctcagggcctaaaggt
Product size:		1089bp

Table 2.1 - List of oligos used in Chapter II. Primer sequences for gene cloning, RT-PCR, and the T7 endonuclease1 assay.

kVp, 160 μA, no filtration, 5x-averaging, exposure timing of 1000 ms per image, and a resolution of 6.000 μm per slice (216 μm^3 per voxel). Scanned images were analyzed and segmented using Amira 3D Software 6.0 (FEI).

2.6 Acknowledgements

Sincere thanks go to N. Adachi, and T. Stewart for helpful comments. Thank you to T. Nakamura for feedback and generously sharing his CRISPR-Cas9 *hoxa13a*$^{-/-}$/*hoxa13b*$^{-/-}$ mutant zebrafish. Thank you to J. Lemberg for helping use of the UChicago PaleoCT scanner. Thank you to the University of Chicago Genomics Facility for the *L. erinacea* RNA-sequencing. This work was supported by The Brinson Foundation and the University of Chicago Biological Sciences Division (to N.H.S.); a Japanese Society for the Promotion of Science (JSPS) Postdoctoral Fellowship for Research Abroad, Uehara Memorial Foundation Research Fellowship, and Marine Biological Laboratory Research Grant (to T.N.); National Science Foundation Grant IOS-1355057 (to J.K.); Graduate Assistance in Areas of National Need Grant P200A120178 (to J.P.).

CHAPTER III

THE ZRS, A *SONIC HEDGEHOG* REGULATORY ELEMENT, IS AN EVOLUTIONARILY CONSERVED FEATURE OF GNATHOSTOME PAIRED APPENDAGE DEVELOPMENT

3.1 Author contributions

The work presented in in this chapter was completed in collaboration with Igor Schneider Joaquín Letelier, Elisa de la Calle-Mustienes, Ignacio Maeso, Juan Ramón Martinez Morales, José Luis Gómez-Skarmeta, and Neil Shubin. I.S. selected the two lamprey genomic regions to test for ZRS regulatory potential. Except for lamprey (I.S.), and amphioxus (E.C-M, I.M.), J. Pieretti generated the ZRS entry vectors used for zebrafish transgenesis. Transfer of ZRS elements into final destination vectors and generation of zebrafish F1 ZRS transgenics was completed by E.C-M and I.M (Figure 3.3). J.Pieretti generated the constructs used for mouse transgenesis presented in Figure 3.4 J. Letelier generated, genotyped, and analyzed gene expression and proximal radial number in the medaka ZRS mutants presented in Figure 3.5, and Figure 3.6. J. Pieretti analyzed the ZRS pectoral fin phenotypes using μCT reconstruction shown in Figure 3.7 John Westlund designed Figure 3.2 with input from J. Pieretti. J. Westlund generated the animal illustrations presented in Figure 3.1.

3.2 Abstract

Vertebrate paired appendages have become an excellent model for the study of spatiotemporal gene regulation and morphological evolution because of their rich legacy in experimental analysis and research literature. Studies in mouse have revealed a complex network of regulatory factors that mediate expression of developmental genes including *Sonic hedgehog*

(*Shh*). It is likely that a single long-range *cis*-regulatory element, termed the "ZRS" is solely responsible for coordinating *Shh* expression in limbs (Lettice et al., 2002), and this element is present in the genomes of tetrapods and cartilaginous fish, lineages that diverged at least 423 mya. In order to determine the functional activity of the ZRS across large evolutionary distances, we performed a broad phylogenetic survey of the ZRS in vertebrates, as well as agnathans and cephalochordate representatives, and assayed the function of these elements using mouse and zebrafish transgenics. We find that the ZRS from all tested gnathostomes is functional in both mouse limbs and zebrafish fins, and propose that the ZRS is a conserved feature of all jawed vertebrates. Additionally, in a functional assay of the ZRS via CRISPR-Cas9 genome editing, we find that *Shh* expression influences the number of proximal radials in medaka. These data suggest that the regulatory underpinnings mediating *Shh* expression in paired appendages are conserved among gnathostomes and that *Shh* influences the number of skeletal elements along the anteroposterior axis.

3.3 Introduction

Despite the anatomical differences between the tetrapod limb and fish fin, the genetic networks responsible for their outgrowth are highly conserved. Due to this extensive conservation, research has concentrated on the *cis*-regulatory elements that mediate the spatiotemporal expression of genes. Among these conserved gene networks, *Sonic hedgehog* (*Shh*) is a key developmental gene with a rich investigative history in both tetrapod and fish models, where it is known to mediate anteroposterior (AP) signaling, and the development and identity of digits (Riddle et al., 1993; Neumann et al., 1999). Surprisingly, the *cis*-regulatory element responsible for *Shh* expression in the limb is present in the genomes of tetrapods and cartilaginous fish, suggesting an ancient and conserved regulatory potential for this element

(Dahn et al., 2007). However, it is unknown whether and to what extent this element is functionally conserved in vertebrate appendage development.

In developing limbs and fins, *Shh* originates from a domain called the zone of polarizing activity (ZPA) (Krauss et al., 1993; Riddle et al., 1993; Neumann et al., 1999). Studies in mice have shown that *Shh* expression is initiated by a long-range *cis*-regulatory element, termed the "ZPA regulatory sequence" (ZRS) (Lettice et al., 2003; Sagai et al., 2004). The ZRS element is one of at least seven long-range enhancers that control tissue-specific *Shh* expression and is located approximately 1 Mb from the *Shh* transcriptional start site in the 5th intron of the *Lmbr1* gene. Both the presence of the ZRS and its position within the 5th *Lmbr1* intron are conserved features in osteichthyans and chondrichthyans alike. When comparing across such large timescales of vertebrate evolution, phylogenetically informed functional studies of gene regulation provide insight on the evolution of regulatory elements. This method identifies signatures of conserved non-coding elements (CNEs) that may be of functional significance and can be used to determine how changes in *cis*-regulatory elements or transcription factors influence expression patterns of key developmental genes like *Shh*.

The ZRS is the only regulatory element responsible for *Shh* expression in the limb (Lettice et al., 2002, 2003; Sagai et al., 2004, 2005). In mice, ZRS knockouts show a complete loss of *Shh* expression and deformed distal elements of the limb, a phenotype similar to the *Shh* knockout (Chiang et al., 1996; Sagai et al., 2005). Interestingly, human, mouse, cat, and chick polydactylous limb mutants have been linked to several point mutations across the ZRS resulting in anterior ectopic expression of *Shh* (Lettice et al., 2003, 2008; Sagai et al., 2004, 2005; Maas et al., 2011). Recently, deletion analyses have shown that the ZRS is composed of a 5' region responsible for eliciting most of the expression activity and a 3' region that is required to

facilitate long-range activity (Lettice et al., 2014). Furthermore, a number of transcription factors have been implicated in mouse *Shh* regulation via interactions with the ZRS including HOX, PBX, ETS1, and HAND2 activating factors and TWIST1, ETV4/5, and GATA factors, which serve to repress anterior ectopic expression (Kmita et al., 2005; Capellini et al., 2006; Mao et al., 2009; Galli et al., 2010; Zhang et al., 2010b; Lettice et al., 2012, 2014; Kozhemyakina et al., 2014; Osterwalder et al., 2014). With the advent of genome-editing technologies like CRISPR-Cas9, ZRS function can now be assayed in non-tetrapod models by generating insertion-deletion (indel) germline mutations in key transcription factor binding sites that govern *Shh* expression.

Shh expression emanating from the ZPA domain functions in a dose-dependent manner to specify tetrapod limb structures (Harfe et al., 2004; Scherz et al., 2007; Suzuki, 2013). In chondrichthyans, *Shh* ZPA expression in the paired fins of little skate (*Leucoraja erinacea*) and the brownbanded bamboo shark (*Chiloscyllium punctatum*) suggest that the mechanisms controlling polarized *Shh* expression are ancient and deeply conserved among gnathostomes (Dahn et al., 2007). A previous study demonstrated that a putative ZRS from pufferfish (*Fugu rubripes*) drove reporter expression in mouse limbs in a ZPA-like pattern, indicating that *Shh* expression is being regulated similarly in fins and limbs (Lettice et al., 2003). While the functional conservation of this element has been amply researched in tetrapods, its deeper evolutionary history has not been extensively addressed. It is unknown to what degree evolutionary processes have altered *Shh* regulation via the ZRS along non-tetrapod lineages.

In this study, I have sought to broaden comparative developmental analyses of the ZRS using the following phylogenetically relevant taxa: amphioxus (*Branchiostoma lanceolatum*), an invertebrate chordate; sea lamprey (*Petromyzon marinus*), an agnathan; little skate (*Leucoraja erinacea*), a chondrichthyan; spotted gar (*Lepisosteus oculatus*), a non-teleost actinopterygian;

zebrafish (*Danio rerio*), an actinopterygian teleost; coelacanth (*Latimeria menadoensis*), a sarcopterygian; and the tetrapod representatives anole (*Anolis carolinensis*), and mouse (*Mus musculus*) (Figure 3.1). In collaboration with the Skarmeta lab, I also characterize the pectoral fin phenotype of a medaka (*Oryzias latipes)* ZRS mutant containing a deletion in a conserved ETS1 binding site responsible for *Shh* activation.

Through functional investigations of these putative ZRS elements in zebrafish and mouse transgenesis assays, we address the evolutionary origins of the ZRS. Coupled with the phenotypic analysis of the ZRS, we find that the ZRS is an evolutionarily conserved feature of gnathostome paired appendage development (Figure 3.1).

3.4 Results

To frame the evolution of the ZRS in a phylogenetic context, we first sought to identify putative ZRS elements from a variety of tetrapod and fish representatives. Using phylogenetic footprinting, we aligned homologous chromosomal regions from different species in order to uncover the ZRS conserved non-coding element (CNE) located within the *Lmbr1* intron (Figure 3.2, A). We identified ZRS orthologues from species in key phylogenetic positions, including organisms like the African coelacanth, whose slow evolving genome provides insight on the composition of the ZRS from a basal sarcopterygian perspective (Amemiya et al., 2013) and the spotted gar, whose lineage diverged prior to the teleost whole genome duplication (Amores et al., 2011).

To deepen the prospective evolutionary origins of the ZRS, we used the genome from amphioxus, an invertebrate chordate with a single median fin, to identify a putative ZRS element. In amphioxus, the unduplicated *Hh* gene is expressed during the development of the central nervous system, notochord, tail bud, and pharyngeal endoderm. We could not find any

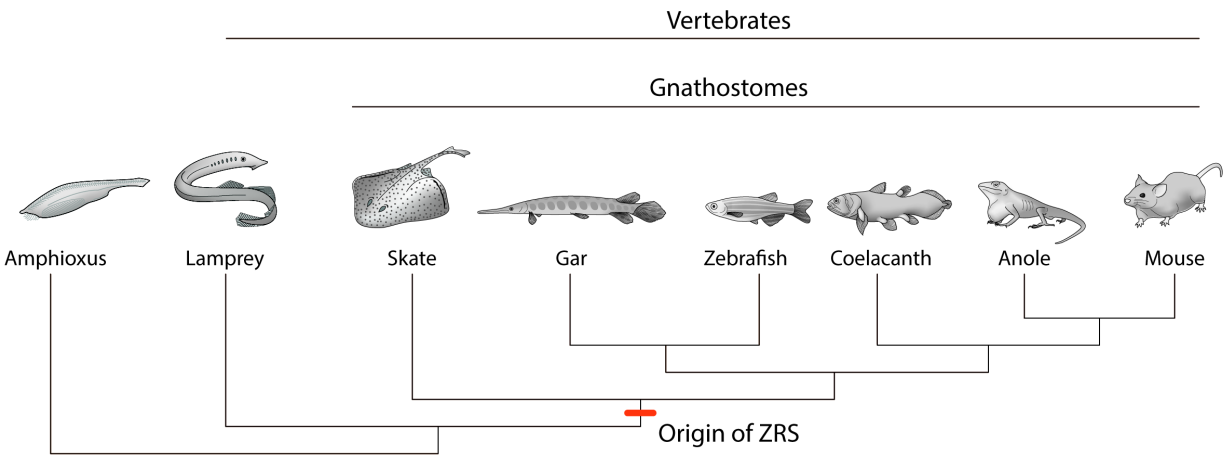

Figure 3.1 - Origin of ZRS in gnathostomes. Cladogram featuring cephalochordate, agnathan, and gnathostome representatives (chondrichthyans, actinopterygians, sarcopterygians). Proposed origin of ZRS is marked in red.

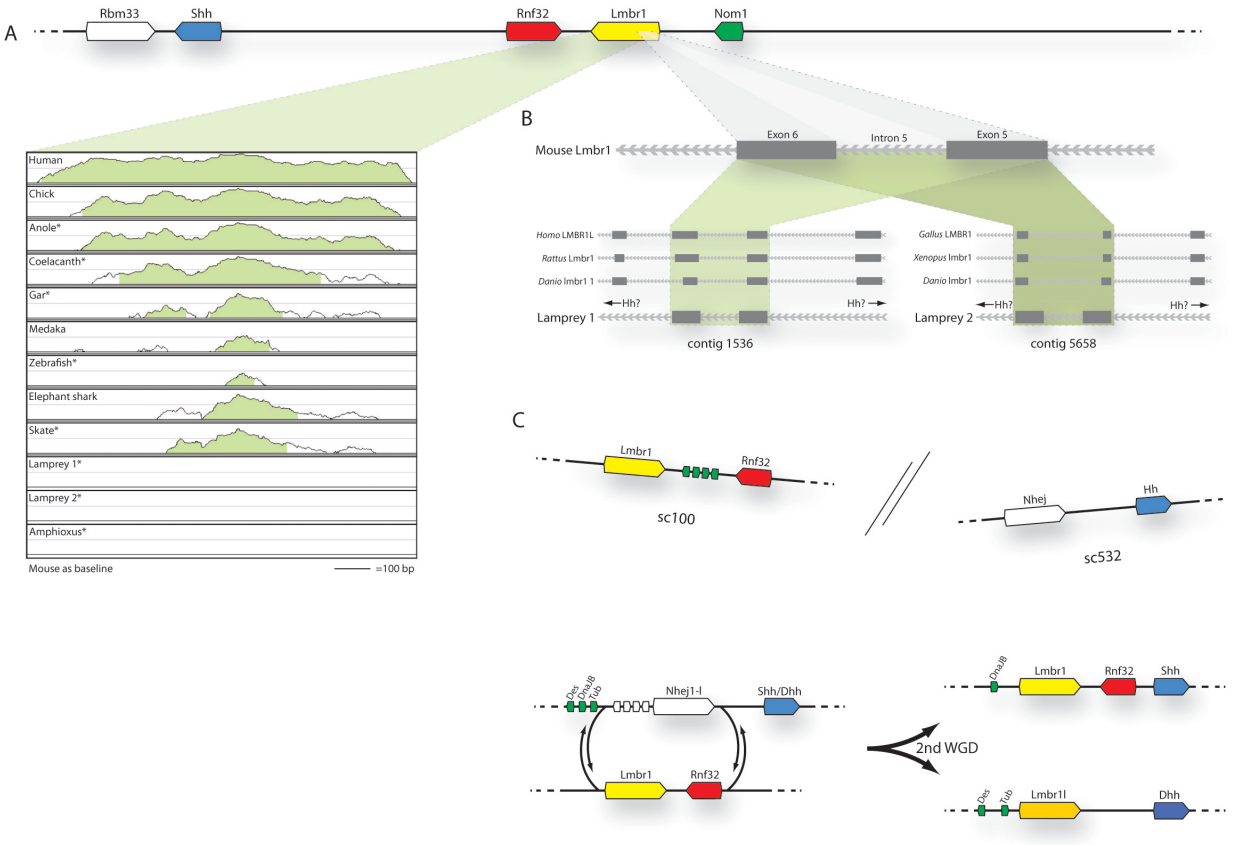

Figure 3.2 - Conservation ZRS *Shh* enhancer in *Lmbr1*. (A) Genomic arrangement of *Shh* locus in a vertebrate representative. Below, an mVista Shuffle-LAGAN alignment shows ZRS sequence conservation across selected species within *Lmbr1* (100bp window and minimum conservation identity of 70%). Note the lack of visible sequence conservation in sea lamprey and amphioxus sequences (inset). **(B)** Sequence homology to *Lmbr1* exons identifies two candidate introns in the marine lamprey genome assembly. **(C)** In the cephalochordate amphioxus the syntenic arrangement of the single-copy *Hh* gene is remarkably different. *Lmbr1* is not associated with *Hh* and these genes are located on different genomic scaffolds (sc100 and sc532). Data presented in C were adapted from (Irimia et al., 2012).

overt sequence conservation in orthologous *Lmbr1* intronic regions harboring ZRS regulatory potential in amphioxus nor lamprey (Figure 3.2, B). Because of divergence in CNEs over long evolutionary time spans, putative enhancers can become difficult to identify simply through sequence conservation. However, sequence conservation is not always indicative of functional conservation (reviewed in Nelson and Wardle, 2013), and so we sought to test these regions first through zebrafish transgenesis.

Interestingly, the amphioxus orthologous *Hedgehog* locus is arranged differently than in gnathostomes. It has been suggested that the genomic landscape surrounding the *Hh* locus in amphioxus is representative of an ancient linkage group that was subsequently rearranged during gnathostome evolution (Irimia et al., 2012). Gnathostome genomic reorganization may have occurred through two whole genome duplications (WGD), creating the familiar arrangement where *Lmbr1* (and the ZRS) reside upstream of *Shh* (Figure 3.2, C). In this scenario, the ZRS may have become associated with *Shh* regulation after the first gnathostome WGD through the genomic reshuffling of the vertebrate *Hh* paralogs and the neighboring genes, *Lmbr1* and *Rnf32*.

Lamprey and amphioxus ZRS sequences do not drive reporter expression in zebrafish pectoral fins

Given the distinct arrangement of *Lmbr1* and *Hh* in amphioxus, we sought to characterize a putative ZRS element with which to assay expression activity in transgenic zebrafish. Based on sequence conservation of neighboring *Lmbr1* exons, we identified a ~1kb region that could harbor the ZRS enhancer. When tested in multiple stable transgenic zebrafish lines, we found that this region did not drive reporter expression in fins. Strong expression in the midbrain was observed, however, due to an enhancer present in the vector, which served as a positive transgenesis control (de la Calle-Mustienes et al., 2005)(Figure 3.3, A).

Through sequence conservation of the *Lmbr1* exons in the lamprey genome, we identified two introns containing putative ZRS elements (Figure 3.2, B), which diverged from the lineage leading to gnathostomes prior to the origin of paired appendages. Lamprey lack paired fins, but their median fin shares patterning mechanisms characteristic of paired appendages, including nested expression of 5' *Hox* genes (Freitas et al., 2006). However, *Hh* expression has not been observed during lamprey median fin development. In our assays, we find that the two lamprey regions tested for *ZRS* activity fail to drive reporter expression in zebrafish fins (Figure 3.3 B, C). This suggests that the lamprey genome does not have a ZRS regulatory element tasked with regulating *Hh* expression in fins, likely because the ZRS originated after the divergence of this lineage from gnathostomes (see Discussion).

Gnathostome ZRS elements drive ZPA expression in zebrafish

All tested gnathostome ZRS elements (skate, gar, coelacanth, gar, anole, mouse) drive GFP reporter expression in the posteriorly localized ZPA domain of zebrafish fins, revealed by GFP *in situ* hybridizations (Figure 3.3, D-I). The tested elements drive nearly indistinguishable expression patterns relative to the native zebrafish ZRS element (Figure 3.3, F). Although the chondrichthyan ZRS element elicits a fainter signal than other ZRS elements in the zebrafish fin, it is still posteriorly localized. These results provide strong evidence that the zebrafish ZRS is the regulatory element responsible for localized *Shh* expression in the developing fin bud, and that all tested gnathostome orthologues are functionally conserved. These results also show that the *trans* environment (that is, the transcription factors that bind to the *cis* regulatory element) of the host (zebrafish) is able to properly "decode" the information from the different donor gnathostome *cis* elements and elicit a ZPA pattern.

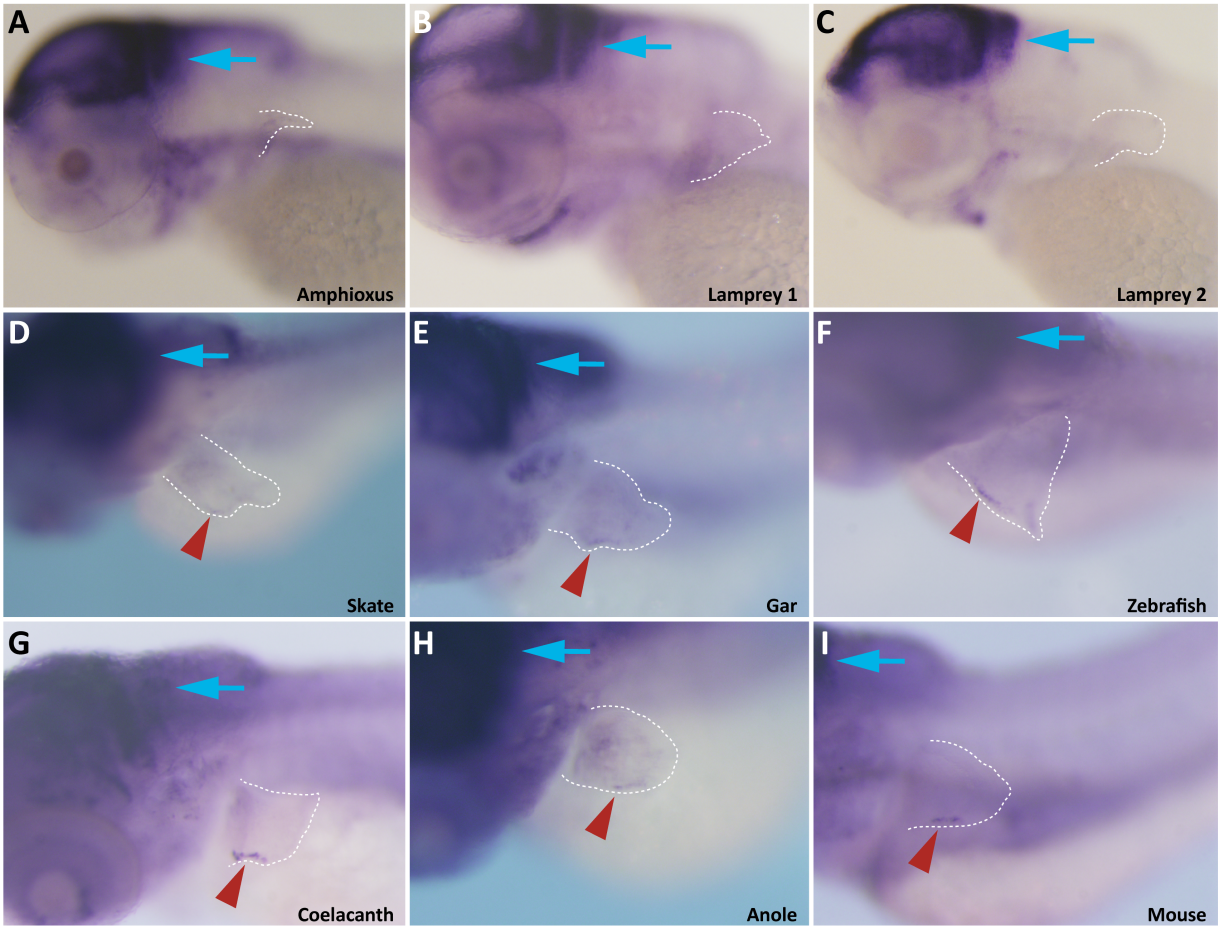

Figure 3.3 - Gnathostome ZRS elements drive distal expression in *D. rerio* fins. GFP in situ hybridization of zebrafish transgenic embryos at 72 hours post fertilization (hpf). Each letter corresponds to a tested orthologous ZRS element noted at the bottom right of each image. Midbrain expression (blue arrows) driven by the Z48 zebrafish enhancer confirms genomic integration of the insert. Note the absence of expression in fins in the amphioxus and lamprey transgenic lines (A-C), and the localization of GFP protein in the ZPA domain (D-I; red arrowheads).

Note: E. de la Calle-Mustienes and I. Maeso generated the data presented in this figure.

Gnathostome ZRS elements drive ZPA expression in mouse limbs

To further test the potential of ZRS elements to drive appendage expression in a tetrapod, we cloned the ZRS elements from all species except amphioxus into a Hsp68-LacZ vector to assess its function in a mouse transgenic assay. We chose not to test the amphioxus sequence based on the lack of expression in zebrafish fins and the chromosomal arrangement of *Lmbr1* and *Hh* (Figure 3.2, C). We found that the two putative ZRS lamprey sequences, which failed to drive expression in zebrafish fins, also failed to drive reporter expression in mice (Fig 3.4, A-B). On the other hand, the ZRS elements from all gnathostomes (skate, gar, zebrafish, coelacanth, and anole) drove expression in mouse limbs in a ZPA-like domain (Figure 3.4, C-G), suggesting that *Shh* regulation via the ZRS in fish and tetrapods is an ancestral characteristic of jawed vertebrates. Notably, the skate ZRS had a wider area of expression in the mouse limb relative to the other transgenics, which is interesting given the larger size of the skate fin. However, given the small sample size of skate transgenics, this result is difficult to interpret (5 PCR positive embryos, 4 embryos with LacZ staining, 1 embryo with limb expression).

Reduced number of proximal radials in the medaka ZRS mutant

In order to assay the functional role of the ZRS during pectoral fin development, we used CRISPR-Cas9 technology to disrupt a conserved ETS1 binding site in the ZRS enhancer of medaka (*O. latipes*). Members of the ETS family have been shown to regulate *Shh* expression in mouse limbs by controlling the ZPA spatial boundary and restricting anterior *Shh* activity (Lettice et al., 2012). Unlike the zebrafish genome, the medaka genome has only one copy of *Shh,* making it more amenable to deletion analyses. In collaboration with the Skarmeta lab, J. Letelier generated stable germ-line medaka mutants carrying a 401 bp deletion that modestly reduced *Shh* expression temporarily at 3dpf before reaching normal expression (Figure 3.5).

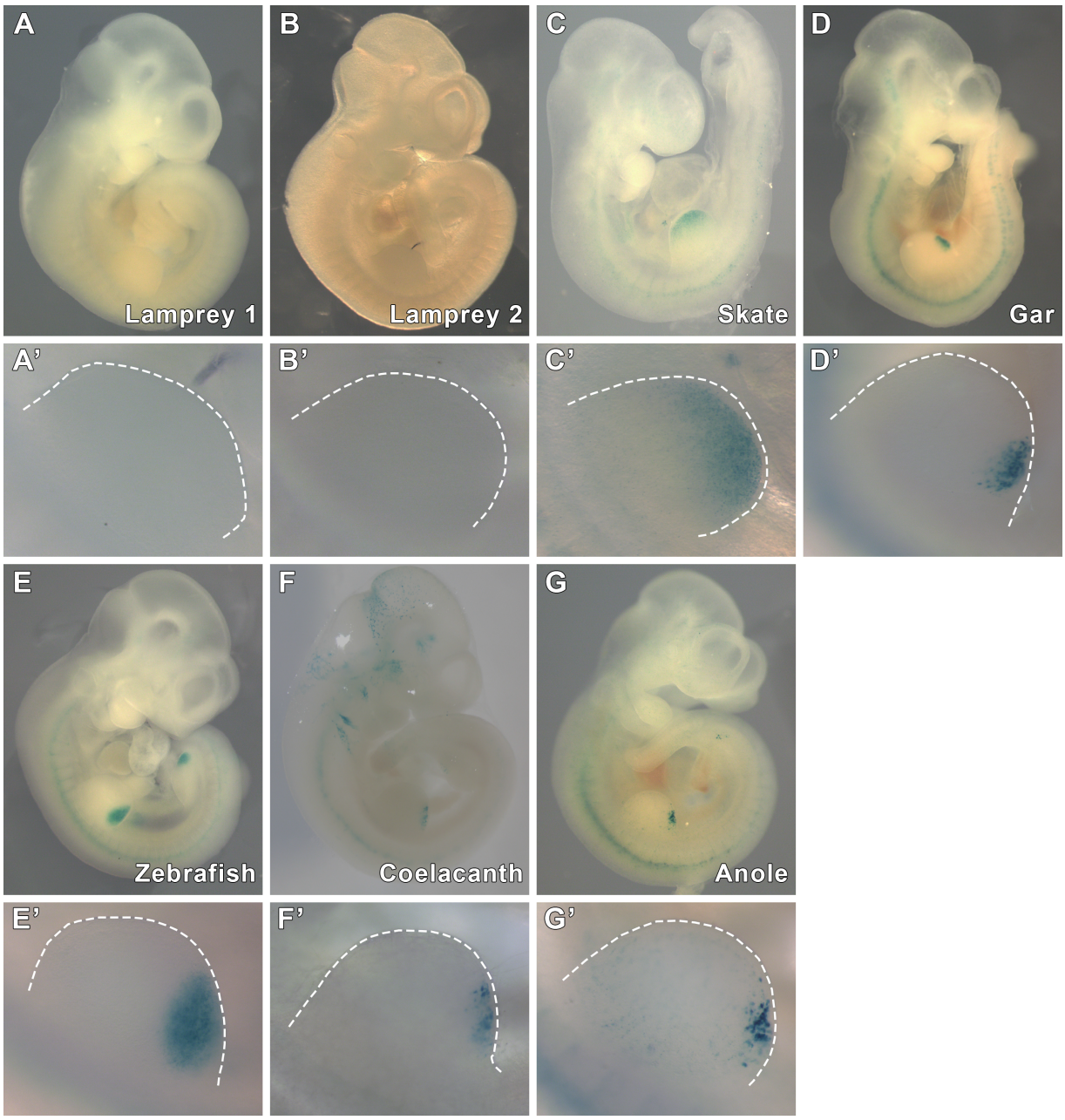

Figure 3.4 - Gnathostome ZRS elements drive distal expression in *M. musculus* limbs. Reciprocal transgenic analyses of orthologous ZRS elements in E10.5 mouse embryos. Each letter corresponds to a LacZ stained whole embryo and panels designated with a prime symbol show the higher magnification of the forelimb, directly underneath. Proximal is to the left. ZRS donor species are indicated at the bottom right of the panel. Note the lack of expression in A and B. Gnathostome ZRS elements (C-G) drive posteriorly localized expression akin to the ZPA domain. The ratio of embryos positive for the limb pattern to number of transgenic specimens analyzed are as follows: Lamprey 1: 0/4; Lamprey 2: 0/4; Skate: 1/4; Gar: 1/3; Zebrafish: 6/11; Coelacanth: 1/2; Anole: 3/4.

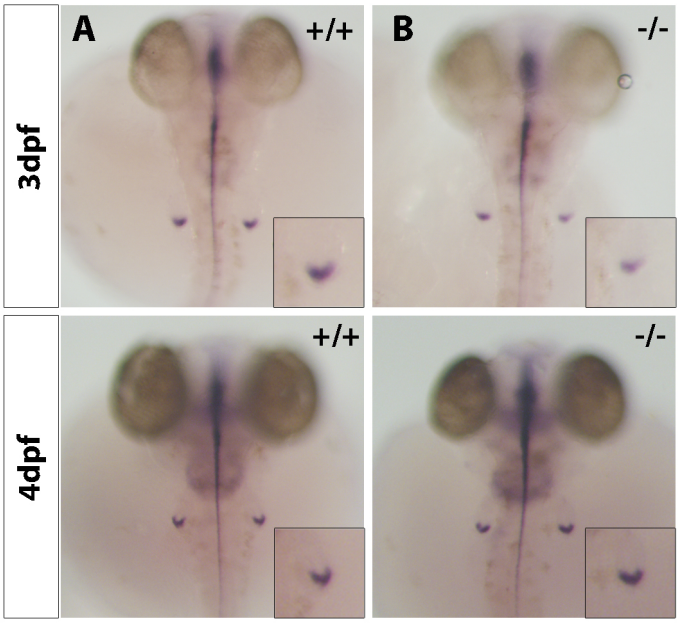

Figure 3.5 - *Shh* expression in *O. Latipes* wildtype and ZRS mutants. (A) *Shh in situ* hybridization (ISH) in wildtype embryos at 3dpf and 4dpf. Signal is comparable at both stages (see pectoral fin inset). **(B)** *Shh* ISH in 401bp ZRS deletion mutant. Note reduced pectoral fin expression relative to WT at 3dpf. At 4dpf expression is comparable to wildtype embryo.

Note: J. Letelier generated the data presented in this figure.

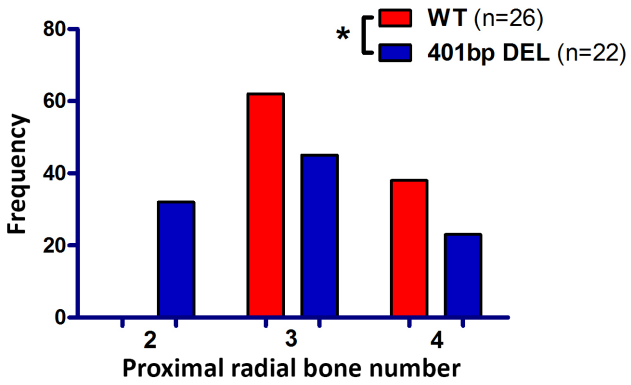

Figure 3.6 - Number of proximal radials in *O. latipes* wildtype and ZRS mutants. Frequency of medaka wildtype and ZRS mutants displaying 2, 3, or 4 proximal radials. Difference in number of radials between WT and mutant is statistically significant (t test $p < 0.05$).

Note: J. Letelier generated the data presented in this figure.

Normally, medaka have four small, square-shaped proximal radials which support the fin rays and have no distal radials (Iwamatsu, 2013). We found that wildtype (WT) medaka display a normal range of radials (3 to 4) but never exhibit only two radials, while homozygous ZRS mutants display 2 to 4 proximal radials (Figure 3.6).

To obtain a better resolution of the mutant radial phenotype, we analyzed the pectoral fins from three-month-old wildtype and ZRS mutant medaka in both cleared-and-stained imaging and μCT-derived reconstructions. ZRS mutants show a minimum of two radials, and some appear to be fused (Figure 3.7). Preliminary volumetric analyses do not show a significant difference in the total volume of the radials in the mutants compared to WT, however, this may be a result of small sample size (ZRS mutant, N=6; WT, N=3) (data not shown).

3.5 Discussion

Evolutionary implications of lamprey and amphioxus ZRS elements

Using donor *cis* regulatory elements from amphioxus and lamprey, we found that the putative *cis* regulatory elements from these taxa failed to drive expression in both zebrafish pectoral fins and mouse limbs. Some important caveats must be considered when interpreting these results. These experiments cannot capture the full scope of evolution in *cis* or *trans*, because the *cis* regulatory elements from the donors (amphioxus, lamprey) have not been tested in their native *trans* environment. In non-model organisms like amphioxus and lamprey, it is experimentally challenging to test the function of a *cis* regulatory element in its endogenous *trans* environment (Parker et al., 2014a). Therefore, it cannot be ruled out that evolutionary divergence between the *cis* element donor and host (zebrafish and mouse) genomes has occurred, leading to lineage-specific changes either in the *trans* environment of the host and/or the *cis* element from the non-model donor (Gordon and Ruvinsky, 2012). In either case, this would lead

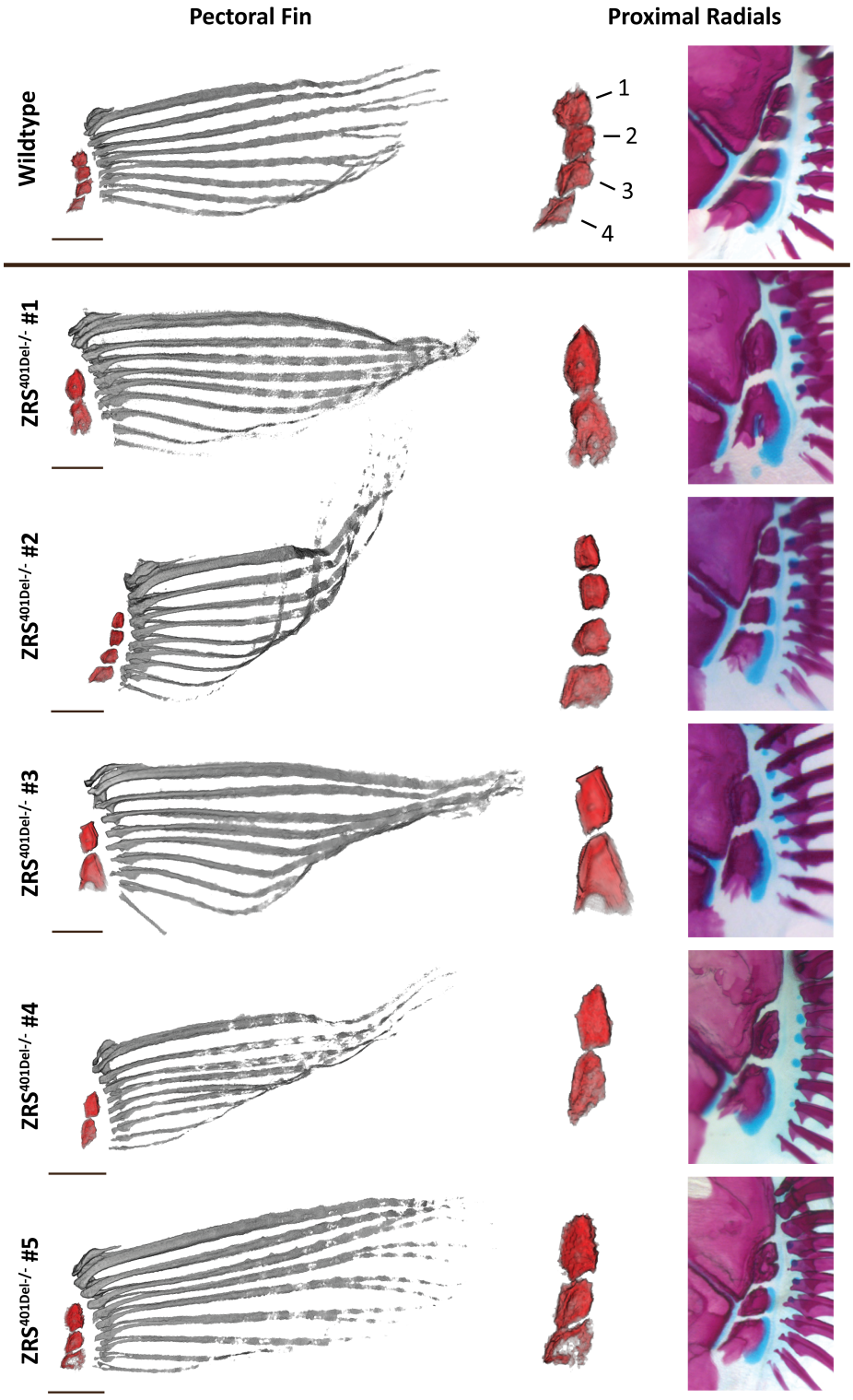

Figure 3.7 - µCT reconstruction of *O. latipes* wildtype and ZRS mutant pectoral fins. Wildtype exhibit 4 proximal radials as seen in the first row. Mutants exhibit a range in the number of proximal radials as shown in representatives #1-5. Note presence of only two

Figure 3.7, continued. radials in mutants #1, #3,and #4. In mutants with fewer than 4 radials, the endochondral elements appear more triangular in shape than in wildtype. Proximal radials are numbered in WT with 1 being the anteriormost radial. Scale = 500μm.

to an incompatibility between the host's *trans* environment and the putative ZRS element from the donor, resulting in the observed lack of expression. Without knowing the expression pattern activity of the *cis* element in its native organism (e.g. lamprey *cis* element in lamprey), the mode of evolution (*cis, trans,* or both) cannot be parsed out (Gordon and Ruvinsky, 2012). While testing a *cis* regulatory element in its native *trans* environment is an ideal experiment, this is not always feasible. Moreover, the lamprey genome has not been completely sequenced making identification of regulatory elements all the more challenging. We cannot rule out that a lamprey ZRS element lies elsewhere in the genome, but feel confident in the selection of the regions tested based on *Lmbr1* sequence conservation.

Given the genomic arrangement between *Lmbr1* and *Hh* in amphioxus (Irimia et al., 2012), it could be inferred that *Lmbr1* may not yet have been incorporated into the regulatory architecture of *Hh* in early chordate evolution. One possibility is that this region may not have the necessary complement of transcription factor binding sites to regulate *Hh* expression in fins.

Similarly, both lamprey putative *ZRS* elements failed to drive reporter expression in zebrafish and mouse hosts and this may indicate that the lamprey lineage does not have a ZRS element associated with polarized *Hh* expression, though it is uncertain if the ZRS originated in the ancestor to vertebrates and was subsequently lost in the lamprey lineage, or diverged in function in this lineage. Recently, transient transgenesis assays in sea lamprey were reported (Parker et al., 2014b), making it possible to test the putative ZRS regions from lamprey in their native context in future studies, though preliminary work to detect *Hh* expression in the median

fin should first be performed. Analyses of *Hh* gene expression in the river lamprey (*Lampetra fluvitalis*) show that *Hh* paralogs are expressed in a gnathostome *Shh*-like manner in the forebrain, notochord and floor plate, but median fin expression has not yet been reported (Kano et al., 2010). If median fin *Hh* expression were detected in future analyses, it would warrant a search for the regulatory element responsible for such expression. Given the number of tissue specific enhancers regulating *Shh* expression in vertebrates (Irimia et al., 2012), it may be another regulatory element distinct from the ZRS is responsible for *Hh*/*Shh* median fin expression in non-tetrapod vertebrates

Identification and testing of a putative ZRS element residing in the *Lmbr1* ortholog of hagfish, the extant sister group to lamprey, could clarify the observed lack of expression seen with the lamprey elements, but genome analyses and developmental genetics techniques are also limited in this organism (Shimeld and Donoghue, 2012). In light of the absence of reporter activity from the amphioxus element in zebrafish and the lamprey elements in both zebrafish and mouse, the most parsimonious explanation is that the ZRS originated after the split of these lineages from a chordate ancestor.

Gnathostome ZRS expression activity is conserved in both zebrafish fin and mouse limbs

Based on our results, ZRS elements from all tested gnathostome species drive reporter expression in the ZPA domain of zebrafish fins (Figure 3.3, D-I) and mouse limbs (Figure 3.4, C-G). Together these data support the hypothesis that the ZRS elements of all jawed vertebrates are functionally conserved. As the tetrapod limb is considered a vertebrate novelty that facilitated the water-to-land transition, these results suggest that despite the structural novelty of the limb, the underlying regulatory circuitry of *Shh* was pre-established in fins. Furthermore, the data from lamprey suggest that the ZRS originated after the divergence of agnathans and gnathostomes and

is strictly associated with ZPA expression in paired appendages. This suggests that the regulatory function of the ZRS originated in the ancestor of gnathostomes. With *Shh* expression now in the posterior region of the appendage, recruitment of the downstream *Shh* signaling factors was therefore possible.

The ZRS is part of a network that regulates digit number in tetrapods and proximal radial number in fish

Localized expression of *Shh* is required for the proper patterning and outgrowth of the appendages. In mice, modifications to the *Shh* signaling pathway create a range of digit phenotypes, from a single distinguishable digit (Litingtung et al., 2002; Lettice et al., 2014) to poldactyly (Litingtung et al., 2002; te Welscher et al., 2002; Galli et al., 2010). These polydactylous phenotypes strongly resemble ZRS mutants in mouse, cat, and chick (Lettice et al., 2002, 2008; Sagai et al., 2005; Maas et al., 2011). Studies in zebrafish tell a similar story—loss or downregulation of *Shh* expression results in little to no outgrowth of the fin (van Eeden et al., 1996; Schauerte et al., 1998), and a larger fin size is observed when *Shh* expression is upregulated (Koudijs et al., 2005; Sakamoto et al., 2009).

Much like in mouse ZRS mutants (Lettice et al., 2014), deletion of an ETS1 site in the medaka ZRS enhancer leads to a reduction in the number of skeletal elements in the fin. This raises an interesting possibility that endochondral proximal radials and tetrapod digit number are similarly influenced by *Shh* regulation via the ETS site of the ZRS. Further testing of this hypothesis could be done by generating a complete ZRS deletion in a fish model and observing endochondral phenotypes. Such experiments may reveal a complete loss of *Shh* expression and failure of all endoskeletal elements to develop, or loss of radials only. These results could be compared to what is known in loss-of-function mutants. Intriguingly, in zebrafish *Shh* null

mutants do not form any endoskeletal elements while *Shh* hypomorphs develop all elements, through cell number is reduced and the elements are smaller than in wildtype pectoral fins (Neumann et al., 1999). Reduced cell number is especially apparent in the endoskeletal disc, from which the radials are derived (Neumann et al., 1999). Putative transcription factor biding sites within the ZRS could also be identified using the "Assay for Transposable Accessible Chromatin" ATAC-seq (Buenrostro et al., 2013) in a fish model with a good quality genome such as medaka or zebrafish. Next, characterization of candidate factors such TWIST1 or ETV binding sites could be explored, where derepression via CRISPR-Cas9 mutations in medaka might reveal a similar polydactylous phenotype as seen in mouse, where the mutant medaka develops more than 4 proximal radials. Another line of inquiry would be to test the extent of shared regulatory inputs again in a transgenic context by using a modified fish ZRS element (i.e. mutating an essential activator binding site) and replacing the endogenous mouse ZRS with the modified fish ZRS to see if digit number is reduced. This would be highly suggestive of similar regulatory inputs responsible for driving *Shh* expression, and the most parsimonious explanation for this would be due to deep homology in the patterning of both digits and radials.

Our data demonstrate that *Shh* regulation in paired limbs and fins are conserved features of jawed vertebrates. Moreover, phenotypic analyses of medaka mutants suggest that there is a relationship between ZRS regulation of *Shh* expression and the patterning and identity of the appendage skeleton. Further studies should seek to characterize the Shh signaling pathway in fish fins in more detail to determine how spatial and temporal exposure to SHH affects proximal radial number and AP identity.

3.6 Materials and Methods

Phylogenetic analyses and isolation of ZRS orthologues

To identify and confirm the presence of the ZRS element, equivalent regions were identified within intron five of the *Lmbr1* gene using the UCSC genome database (http://genome.ucsc.edu), the gar genome from the ENSEMBL database (http://www.ensembl.org/index.html), and the skate genome from Skatebase (http://skatebase.org). Sequence alignments and conservation peaks were visualized using the mVista program Shuffle-LAGAN. Putative ZRS elements were isolated from: mouse (*Mus musculus*), anole (*Anolis carolinensis*), coelacanth (*Latimeria menadoensis*), zebrafish (*Danio rerio*), gar (*Lepisosteus oculatus*), skate (*Leucoraja erinacea*), marine lamprey (*Petromyzon marinus*) and amphioxus *(Branchiostoma lanceolatum)*. Using mouse or zebrafish as the reference genome, two *Lmbr1*-like genes were identified in the marine lamprey genome by I. Schneider and the intronic region spanning exons five and six was subsequently tested for regulatory activity in transgenic assays. Table 3.1 lists the oligonucleotide sequences used to amplify the genomic fragments from their corresponding genomes. An orthologous ~1kb *Lmbr1* intronic region from amphioxus was kindly provided by the lab of J.L. Gómez-Skarmeta. Genomic DNA fragments ranging from 0.7 to 1.5kb were isolated using the Platinum® *Taq* DNA polymerase High Fidelity Kit (Life Technologies). Fragments were cloned into an entry vector (PCR8/GW/TOPO; except for *D. rerio*, which was cloned into pENTR/D-TOPO) and transferred to the appropriate destination vectors using the Gateway® LR recombination reaction (Invitrogen).

Zebrafish transgenesis

After subcloning in the appropriate entry vector, the DNA inserts were transferred to the

Organism	ZRS Forward (5') Primer	ZRS Reverse (3') Primer
M. musculus	AGTTCAAGAAACCGCACACC	GACAGCAACATCCTGACCAA
A. carolinensis	GGCAGAGACAGACGTGATGA	TGGCATGCTTTTCCTAGCTT
L. menadoensis	CAGCAAAGACCCCCAAATAG	GGAAAAAGACATTTTTAGTGTCTCC
D. rerio	AACACGGGACAATTTTGAGC	TTTCTGCTGCTGGCATACAAAT
L. oculatus	ATGGATCATCAATGGGGAGA	TTTGAGTTGACCATGCAAGC
***P. marinus* (1)**	GTGATGTTGGTTGTCGTTGTG	CTAAGTCACGTGGGAAAGCTG
***P. marinus* (2)**	ACTTGGTCTTCTTGTGCTCCA	CGAGGTCAAGTAGTGCCTCAC
B. lanceolatum	ATCGTGCTGAGGAAGGTGAC	TGTGCCTCTACGCATTCAAG

Table 3.1 - List of oligos used in Chapter III.

Zebrafish Enhancer Detector (ZED) insulator vector, which contains the midbrain enhancer 3' of the GFP reporter to serve as a positive control for transgenesis (Bessa et al., 2009). Zebrafish transgenic embryos were generated using the Tol2 transposon/transposase method (Kawakami et al., 2004) with minor modifications. One-cell embryos were injected with: 2 nl of 25 ng/µl of transposase mRNA, 20 ng/µl of phenol:chloroform-purified constructs and 0.05% phenol red solution. Three or more independent stable transgenic lines were generated for each construct.

Zebrafish in situ hybridization

Antisense digoxigenin-labeled (Boehringer-Mannheim) RNA probes were prepared from cDNA. Zebrafish specimens were prepared, hybridized, and stained as previously described (Jowett and Lettice, 1994). Specimens were visualized with and Olympus SZX16 binocular microscope and photographed with an Olympus DP71 camera.

Mouse transgenesis

After subcloning into the entry vector, the DNA inserts were transferred to a destination vector containing the human minimal β-globin promoter upstream of the LacZ/SV40polyA reporter gene (for coelacanth fragment), or a vector containing the mouse hsp68 minimal promoter (all other organisms) and LacZ/SV40polyA (a kind gift of Marcelo Nobrega). Final destination vectors were confirmed by restriction digest and sequencing. Cyagen Biosciences (Cyagen.com) performed injections and LacZ staining for all DNA elements except for zebrafish, which was performed by I. Schneider. Purified, linearized plasmid DNA containing the zebrafish ZRS was used for pronuclear injections of CD1 mouse embryos in accordance with standard protocols approved by the University of Chicago through the Transgenics/ES Cell Technology Mouse Core Facility. Mouse embryos were harvested, stained and fixed as per (Schneider et al., 2011). Embryos were analyzed and imaged using a Leica M205FA microscope.

Adult *O. latipes* skeletal staining

Skeletal staining was performed as previously described (Bird and Mabee, 2003). Briefly, fish were fixed by 10% neutral-buffered formalin overnight. After washing with distilled & deionized water (ddH_2O), specimens were placed in a graded series of 70% EtOH followed by 30% acetic acid/70%EtOH. Cartilage was stained overnight using a 0.02% Alcian blue solution in 30% acetic acid /70%EtOH. Specimens were then briefly rinsed using ddH_2O and the solution was changed to a 30% saturated sodium borate solution and incubated for an hour. After, specimens were immersed in a 1% trypsin/30% saturated sodium borate and incubated at room temperature for eight hours. Following another ddH_2O rinse, specimens were transferred into 1% KOH solution with 0.005% Alizarin Red S. On the following day, specimens were rinsed in ddH_2O and subjected to a graded glycerol series for photographing using a Leica M205FA microscope followed by storage.

PMA staining and µCT scanning

After skeletal staining, dorsal fins were separated from the body. Fins were stained using a 0.5% (weight/volume) PMA (Phosphomolybdic acid) stain for 17 hours followed by two washes using ddH_2O. Specimens were placed into 1.5mL microcentrifuge tubes with ddH_2O and kept overnight to settle. On the following day, specimens were scanned using the UChicago PaleoCT (GE Phoenix v/tome/x 240kv/180kv scanner) (http://luo-lab.uchicago.edu/paleoCT.html), at 50 kVp, 160 µA, no filtration, 5x-averaging, exposure timing

of 1000 ms per image, and a resolution of 6.000 μm per slice (216 μm^3 per voxel). Scanned images were analyzed and segmented using Amira 3D Software 6.0 (FEI).

3.7 Acknowledgements

Sincere thanks go to Daniela H. Palmer and Tetsuya Nakamura for critical reading of the text and John Westlund for figure design, assistance, and animal illustrations. This work was supported the Spanish and Andalusian Governments grant BFU2010-14839, BFU2013-41322-P and Proyecto de Excelencia BIO-396 (J.L.G-S), the Graduate Assistance in Areas of National Need Grant P200A120178 (J.P.), and the Brinson Foundation and the University of Chicago Biological Sciences Division (N.H.S.).

CHAPTER IV

DISCUSSION

4.1 Summary

The work reported in this thesis provides insight on the shared features of the underlying gene network that builds median fins and the paired fins and limbs of jawed vertebrates. Based on gene expression experiments in the paired and dorsal fins of paddlefish and skate I propose that a common developmental module featuring 5' *Hox* genes is responsible for building both paired and median fins in fish. To determine the contribution of a 5' *Hox* gene candidate *hoxa13*, I analyzed the dorsal fin phenotype of *hoxa13a*$^{-/-}$/*hoxa13b*$^{-/-}$ and wildtype zebrafish, and found that fin rays were severely truncated in mutants. This is comparable to the phenotype seen in mutant pectoral fins, where dermal fin rays are also drastically reduced. These results suggest a role for *hoxa13* in specifying proper pectoral and dorsal fin ray development. These findings also lend developmental support to the lateral fin fold hypothesis, as will be discussed in the next section.

To address the level of functional conservation of the ZRS *cis*-regulatory element, I took a comparative approach using transgenic reporter assays in zebrafish and mouse. Through these experiments I found that the ZRS regulates *Shh* expression in both paired fins and limbs, and this element likely originated in the lineage that gave rise to gnathostomes. In analyzing the skeletal phenotype of a medaka *Shh* hypomorph carrying a 401 bp ZRS deletion, I found that the number of pectoral fin proximal radials was reduced and mutants exhibited a minimum of two, or the WT complement of four proximal radials. This finding in an actinopterygian system is intriguing, given the importance of *Shh* expression in mediating tetrapod digit number and

identity (Suzuki, 2013). This is suggestive of a deep conservation of *Shh* regulatory mechanisms in both tetrapod digit and fin radial formation. From these studies, I reflect on the broader implications to the field of evo-devo in the sections below.

4.2 Developmental modularity and levels of homology

From classical studies of anatomy and embryology to recent technological advances in genetics and genomics, research has long focused on addressing the origin and development of the vertebrate appendage. The significance of this work lies not only in understanding how complex gene networks shape such a structure, but also important are its broader applications in understanding the evolutionary patterns and processes of organogenesis. With respect to the vertebrate appendage, are the same gene networks implicated in the development of paired and median fins? If yes, what mechanisms make them different? Similarly, to what degree are the gene networks that pattern pectoral fins and tetrapod forelimbs conserved? No discussion on the origin and patterning of morphological features is complete without mention of the concepts of homology and modularity. And so, the answers to these questions involve addressing the hierarchical features of developmental modularity and levels of homology at a genetic and structural level.

According to the fin-fold hypothesis developed by Thacher (1877), Mivart (1879), and Balfour (1881), paired fins arose from a set of continuous lateral fin folds, similar to the embryonic precursor of median fins. Median fins, which form along the midline and include dorsal, caudal, and anal fins, are structurally similar to paired fins. Like paired fins, median fins exhibit endochondral skeletal supports, radials, and dermal fin rays consisting of lepidotrichia that make up the exoskeleton (Bird and Mabee, 2003). While definitive conclusions on the origin of paired vertebrate appendages remain equivocal (Pieretti et al., 2015), developmental evidence

reported in this thesis and by others (Tanaka et al., 2002; Freitas et al., 2006; Yonei-Tamura et al., 2008), indirectly supports lateral fin fold hypothesis for the origin of paired appendages, short of physically finding an embryonic fold (see Bemis and Grande, 1999). This would suggest that the developmental module of median fins might have been co-opted in paired appendage development, though the precise mechanism is unclear.

Paired appendages primarily develop from lateral plate mesoderm (LPM) while unpaired appendages derive from somitic mesoderm. The boundary between these two populations, named the lateral somitic frontier (LSF) demarcates a region formed by structures derived from somitic cells (the primaxial region) such as the median fins, and an abaxial region consisting of somitic and LPM-derived cells. (Burke and Nowicki, 2003; Shearman and Burke, 2009). Paired fins are derived from LPM, though migratory somitic cells also contribute to appendicular musculature. Although paired and median fins originate primarily from these two distinct populations, it has been suggested that these structures may have shared a similar embryonic origin in the primaxial domain because early fossil agnathans exhibit fin-like structures which extend dorsally (unlike LPM-derived paired fins) and lack mesodermally derived endoskeleton and girdles (Johanson, 2010; Freitas et al., 2014). If paired and median fins both originated from the primaxial domain, then this evolutionary scenario may have permitted genetic redeployment of the median fin module to paired appendages within the same tissue (Freitas et al., 2014).

Given the similar anatomical properties of paired and median fins, it is not surprising that a common developmental module patterns both kinds of structures. Developmental modules are dynamic entities subject to evolutionary processes, and can thus undergo temporal, spatial, and other types of transformations (Raff, 1996). For co-option of this fin module to have occurred, a type of dissociation event likely happened whereby the gene expression program was shifted

from one site to another. While the causal mechanisms of this transformation are unknown, one scenario could involve a regulatory switch by which a master gene of this network was switched on and subsequently activated downstream effectors (reviewed in Peter and Davidson, 2011; Schlosser, 2004). This has been purported to be the mechanism for the co-option of the *Hh* regulatory circuit in butterfly eyespots (Keys et al., 1999). Some aspects of the signaling network between dorsal and median fins have been described (reviewed in Freitas et al., 2014), but more work is needed to characterize the complete dorsal fin network, including the *cis*-regulatory elements which control gene expression (see Future Directions).

Given the dynamic qualities of developmental modules, specifically their propensity for co-option and dissociation, assigning homology among structurally distinct features can be challenging and ultimately depends on the level of homology that is being discussed. For example, homology can be in reference to anatomical structures, genes, networks, or cell types. In an attempt to address the conceptual difficulties of homology, Wagner (2007) coined the phrase "Character Identity Network" (ChIN) to describe a conserved organ-specific gene regulatory program that defines the identity of a character. This regulatory program exhibits historical continuity and its output (i.e. character identity) is the sum of the interactions between the genes in the program. Considering the relationship between paired and median fins, if the same ChIN was executed in both paired fins and median fins, this would be strong evidence of deep homology of a fin developmental network in structures not considered taxic homologs.

The alternative hypothesis to the lateral-fin gold hypothesis is Gegenbaur's gill-arch hypothesis (1878), which suggests a transformational homology between gill arches and paired appendages. Other examples of transformational homologies are supported by paleontological data (e.g. malleus and incus of modern mammals and the articular and quadrate jaw bones in

early synapsids), providing robust evidence of an evolutionary transition. The case for the gill-arch hypothesis, however, is less clear. Recent evidence provides developmental support for this hypothesis in that features of vertebrate limb development were found in chondrichthyan gill arches, where patterning and outgrowth is mediated via *Fgf8* and *Shh* signaling, while also exhibiting responsiveness to RA (Gillis et al., 2009; Gillis and Hall, 2016). In order to confirm a transformational homology between arches and paired fins, strong evidence will likely rely on additional developmental data exposing a ChIN that specifies both gill arches and paired appendages, but has no role in patterning other structures (McCune and Schimenti, 2012).

However, it is possible that over long periods, a ChIN can evolve beyond recognition, muddling support for transformational homology or co-option. In these instances, one approach to tackle this issue could involve studying the hierarchy within ChINs and investigating whether high level regulators are more conserved than downstream effectors (Arthur, 2002). Additionally, support from paleontology and phylogenetics may aid in understanding the evolutionary relationship between the morphological structures being compared. Through phylogenetics we can determine dates of divergence to help constrain when certain morphologies evolved giving insight perhaps to when the underlying genetic mechanisms first evolved (Organ et al., 2015). Furthermore, phylogenetics helps us establish the directionality of evolution, allowing us to learn the order in which related developmental and morphological features evolved (Raff, 2000; Organ et al., 2015).

Assigning homology between skeletal components of the tetrapod limb and fins of bony fish has also been met with controversy (Sordino et al., 1995; Davis et al., 2007; Freitas et al., 2007; Woltering et al., 2014). Based on interpretation of fossil evidence, paired pectoral and pelvic fins are considered to be serial homologues (Wagner, 2014) and are homologous to

tetrapod fore- and hind limbs, respectively (Janvier, 1996). The autopod (wrist and digits; ankle and toes) is considered an evolutionary novelty of tetrapods, with no clear morphological antecedent in fish fins. In the absence of comparative anatomical support, recent work has sought to characterize the functionality of *Hox cis*-regulatory elements in both murine limbs and zebrafish fins. The findings that in transgenic mice, digit-specific *Hox* enhancers from gar and skate drive nearly identical expression to their murine counterparts is suggestive of equivalence between radials and digits (Schneider et al., 2011; Gehrke et al., 2015).

In a similar vein, in Chapter III we find disruption of the ZRS directly impacts the proximal radials of medaka, where reduced *Shh* expression leads to a reduction in the number of radials. This intriguing result suggests that radial and digit number are directly influenced by *Shh* regulation via the ZRS. This too points to a shared regulatory apparatus that patterns distal skeletal elements in fins/limbs. Moreover, a recent study described a Turing model that controls digit patterning in mouse limbs as well as the distal skeletal elements of catshark fins, suggesting an ancestral role of this patterning mechanism in pattering fish fins and tetrapod limbs (Onimaru et al., 2016). Further work to address the development and patterning of radials will be required to determine to what extent patterning mechanisms, gene networks and associated *cis*-regulatory elements are shared between the autopod and endoskeletal elements of the fin and how modifications to these components facilitated the fin-to-limb transition.

The study of gene networks, especially at a regulatory level, will help identify morphological transitions because it goes beyond gene expression and informs on the interactions between genes and associated regulatory elements that influence morphology. However, one caveat must be mentioned when discussing either deep or transformational homology and gene regulatory networks. Regulatory networks involved in multiple

developmental processes such as the Wnt signaling pathway or other signaling cascades, are not ideal candidates with which to identify transformational homology because they have been coopted and redeployed in various contexts (McCune and Schimenti, 2012). For gene networks to be informative for transformational homologies, they must be relatively specific to the tissues in question, or include unique interactions found only within that system.

4.3 Future Directions

In Chapter II, I proposed that a shared developmental module patterns median and paired fins based on gene expression data and functional tests via gene disruption. However, developmental and gene regulatory data on median fin morphogenesis is markedly incomplete. It is uncertain to what extent this common developmental module is tweaked to give rise to dorsal, caudal, and anal fin morphological diversity. Moreover, characterization of the fin regulatory network in both median and paired fins may provide crucial insight on the origin of paired appendages (described in section 4.1). To tackle these issues, a holistic experimental approach must be taken incorporating paleontological evidence, as well as developmental and epigenomic techniques (Figure 4.1), in order to test hypotheses concerning evolutionary transformations and deeply conserved features of organogenesis.

Identification and functional characterization of median fin, paired fin, and gill arch ChINs will help elucidate which evolutionary scenario was most plausible in the origin of paired appendages. For example, identifying a gene regulatory network that is critical to paired appendage and gill arch development would provide support for these structures being transformational homologues. Similarly, characterizing the ChINs of median and paired appendages may reveal that the evolution of novel regulatory element(s) permitted the co-option of the median fin module to the lateral plate mesoderm. A thorough examination of gill arch,

median fin, and paired fin development gene networks will help to weigh the evolutionary likelihood of either of the two classic hypotheses on the origin of paired appendages. In a similar vein, additional evidence of developmental modularity in median and paired appendage development may provide conclusive support of co-option and require revision of the lateral fin fold hypothesis.

An unprecedented depth of knowledge can now be accessed through the use of novel technologies to understand the pattern and process of evolutionary transitions. These technologies include: RNA-seq to characterize the transcriptomic expression profile in tissues of interest (Romero et al., 2012; Nakamura et al., 2015); identification of transcription factor binding sites and enhancer-promoter interactions though ChIP-seq and chromatin capture assays, respectively (Amano et al., 2009; Andrey et al., 2013; VanderMeer et al., 2014; Rotem et al., 2015); ATAC-seq to identify candidate regulatory elements in regions of open chromatin (Buenrostro et al., 2013; Gehrke et al., 2015); and finally, CRISPR/Cas9 to directly edit the genomes of model and non-model organisms alike (see Chapters II and III; Buenrostro et al., 2013) (Figure 4.1). A multifaceted experimental approach using these modern genomic technologies will help uncover the hierarchy of the regulatory networks which pattern gill arches, as well as median and paired appendages. The findings of this work will ultimately lend support to transformational homologies between arches and paired appendages or deep homology between median and paired appendages.

In addition to the use of powerful genomic technologies, a broader sampling of organisms will be a necessary part of research programs investigating the evolution of morphological traits, including paired appendages. While the choice of developmental model organisms (e.g. zebrafish, *Drosophila*) has been based on practical benefits from each species including

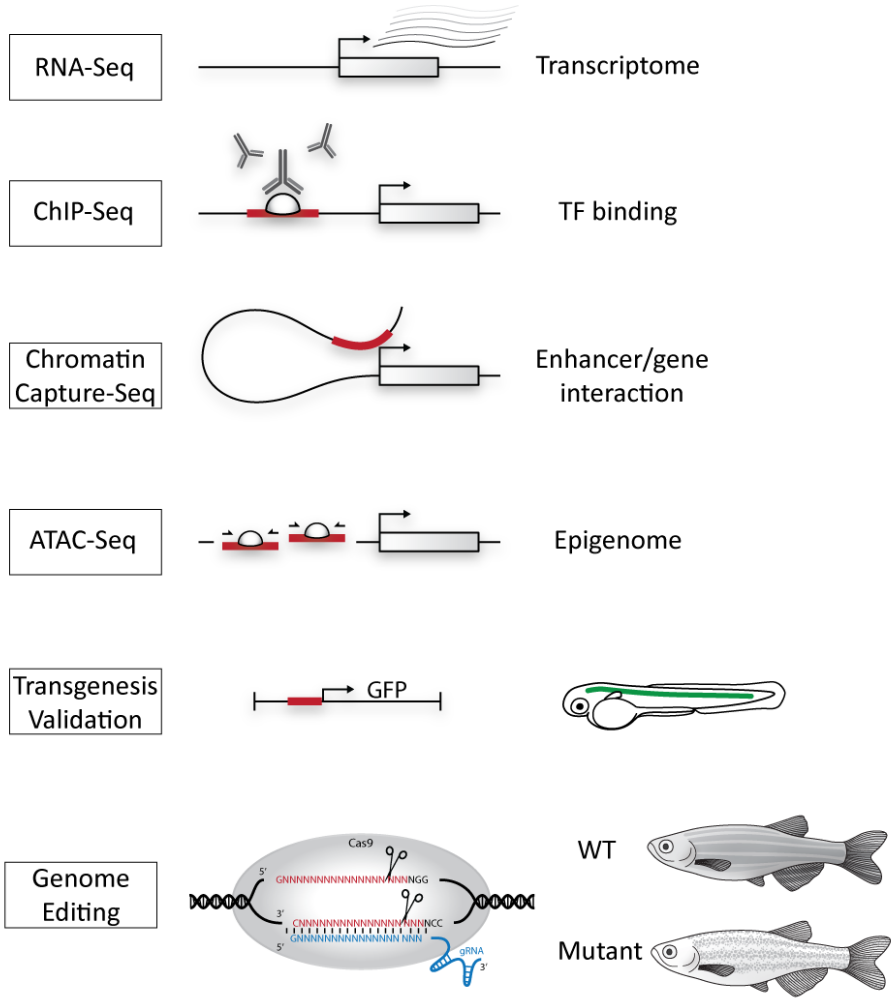

Figure 4.1 - Genetic and epigenomic technologies. Modern epigenomic techniques can identify candidate loci that contributed morphological transformations in the genome of extant organisms (Wang et al., 2009; Tena et al., 2011; Buenrostro et al., 2013; Woltering et al., 2014). These data can contribute to a model of phenotypic change that can then be tested by direct manipulations of the genome using CRISPR/Cas9 (Jinek et al., 2012) bringing us closer to understanding the evolutionary course of morphological transformations.

generation time, cost, transparency and size of embryo, etc., there are genuine concerns relating to how well representative these model organisms are of other taxa (Kellogg and Shaffer, 1993; Jenner and Wills, 2007). For example zebrafish are highly derived teleosts whose lineage underwent a third WGD (Taylor et al., 2003), making comparative analyses of gene function and regulation to non-teleost organisms more challenging. To remedy this, careful selection of additional organisms for comparative study will be necessary based on criteria such as: phylogenetic position, lineage branch length (rates of divergence), unique developmental or phenotypic variation, or whether they serve as reasonable proxies for the study of evolutionary features in lineages where such changes may have occurred (e.g. gar feeding mechanics to study feeding mechanisms in fossil tetrapods) (Jenner and Wills, 2007; Bolker, 2014).

This will inevitably require access to embryos and further development of molecular tools for phylogenetically important organisms, including chondrichthyans like skate and basal actinopterygians such as paddlefish, bowfin, and gar. To illustrate the value of such organisms, recent sequencing of the unduplicated gar genome has revealed conserved cryptic enhancers not detected in other teleosts via sequence conservation (Braasch et al., 2016), and the first genomic evidence of enamel proteins in an actinopterygian (Qu et al., 2015). Evaluating fin development in organisms such as gar and paddlefish may reveal deep commonalities to paired and median fin patterning which may be difficult to study using the duplicated genome of zebrafish.

Integrating modern epigenomic technologies with paleontological data will yield a more comprehensive understanding of the evolutionary course of morphological transformations (Pieretti et al., 2015). Through genomic manipulation researchers will be able to exhaustively test hypotheses on the interactions between genotype, phenotype, and the environment. By taking a comparative developmental genetics approach and a broad sampling of phylogenetically

relevant organisms, we will continue to obtain insight on the molecular controls of development that are responsible for morphological variation and evolution. We may find evidence in support of deeply conserved modules during key stages of development across taxa (Nelson and Wardle, 2013), and the mechanistic details of *cis*-regulatory changes to the morphological evolution of structures such as fins and limbs. Equipped with this knowledge, this will lead to new conceptualizations and novel investigative approaches in the field of evolutionary developmental biology.

APPENDIX I

DESCRIPTION AND TESTING OF THE CONSERVED *SONIC HEDGEHOG* REGULATORY ELEMENTS, MFCS4 AND MACS1

At least seven functional long-range *Sonic hedgehog* regulatory elements have been discovered in mice (*Mus musculus*), where they drive reporter expression in regions of known *Shh* activity (Jeong et al., 2006; Sagai et al., 2009) (Figure A1.1, A). Of these, the Mammal Amphibian Conserved Sequence 1 (MACS1) has been conserved in tetrapod genomes, and drives expression primarily in endodermal derivatives including the epithelial linings of the mouse gut and respiratory tubes (Sagai et al., 2009). Sagai and colleagues (2009) reported that MACS1 was not identified in teleost genomes through sequence conversation and suggest MACS1 may not be conserved in this lineage. However, no functional assays have determined if the MACS1 enhancer is truly absent in this lineage. Another regulatory element, Mammal Fish Conserved Sequence 4 (MFCS4) drives expression in derivatives of the pharyngeal endoderm (Sagai et al., 2009). Together, MFCS4 and MACS1 exhibit overlapping domains of expression in laryngeal cartilage derivatives of the pharyngeal arches. Despite the identification of these long-range regulatory elements in mice, little has been done to understand how well conserved this regulatory architecture might be in other taxa. For example, MACS1 and MFCS4 activity has not been characterized in teleost representatives like the zebrafish (*Danio rerio*).

To gain a more comprehensive understanding of the functional conservation of long-range enhancers governing *Shh* expression, I first sought to identify orthologues of MACS1 and MFCS4 in various non-tetrapod vertebrate representatives. I generated a multiple sequence alignment including osteichthyan and chondrichthyan genomes and found that MFCS4 showed

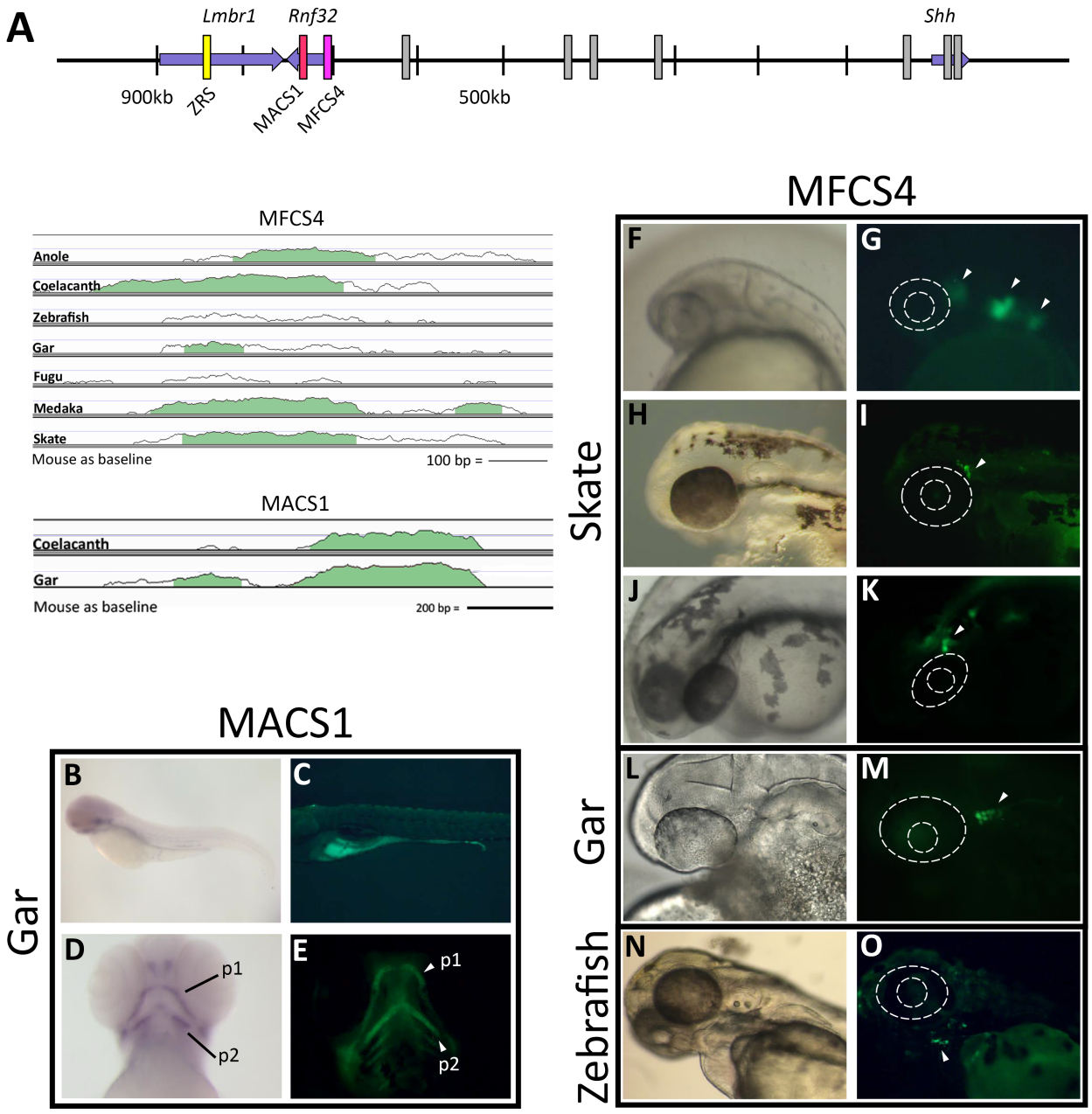

Figure A1.1 - GFP reporter expression of MACS1 and MFCS4 *Shh* regulatory elements. (A) Schematic representing genomic region featuring *Shh* and its long-range enhancers. The ZRS (yellow), MACS1 (red), and MFCS4 (pink) reside in the neighboring genes *Lmbr1* and *Rnf32* (other elements are shaded in grey). Below, sequence conservation plots ofMFCS4 and MACS1 from representative tetrapod and fish species. MACS1 ISH for GFP in 4 dpf embryos **(B, D)** and GFP reporter expression at 5 dpf **(C, E)**. MFCS4 reporter expression in three different founder lines – line 1 at 24 hpf, **(F, G)**, line 2 at 48 hpf **(H, I)** and line 3 at 48hpf **(J, K)**; gar MFCS4 reporter expression in 24 hpf embryos **(L, M)**; zebrafish transient GFP expression in 24hpf embryos **(N, O)**.

high sequence conservation among the selected tetrapods, as well as coelacanth (sarcopterygian), zebrafish (actinopterygian), and skate (elasmobranch) genomes (Figure A1.1, A). Surprisingly, the MACS1 sequence was also identified in both coelacanth and gar genomes, in contrast to Sagai and colleagues' (2009) previous findings (Figure A1.1, A).

Having identified putative enhancers via sequence conservation, I sought to characterize their activity in zebrafish through GFP reporter assays. Stable transgenic lines were raised for the skate MFCS4 and gar MACS1 and MFCS4 enhancers. Expression from the zebrafish MFCS4 enhancer reported is from transient mutants. Stable founders of gar MACS1 reporter drove GFP expression in the gut (Figure A1.1 B, C), after the digestive endoderm has fully differentiated (Wallace and Pack, 2003). GFP reporter expression and in situ hybridization using a GFP probe also showed that the protein is localized to derivatives of pharyngeal arches one (p1) and two (p2) (Meckel's and hyoid cartilages, respectively) at both 96 and 120hpf (Figure A1.1 D, E).

MFCS4 GFP reporter expression was more variable. Skate stable Line 1 exhibited GFP expression in presumptive rhombomeres 3, 4, and 5 at 24 hpf (Figure A1.1 F, G). Expression was also observed in the glial cells adjacent to the eye at 24 and 48hpf in Lines 2 and 3 (Figure A1.1 H-K). Gar MFCS4 drives reporter expression in a region similar to what is observed in skate MFCS4 Lines 2 and 3, where reporter expression is visible in the trigeminal ganglion (Figure A1.1 L, M). Zebrafish MFCS4 transgenics showed reporter expression in the anterior pharyngeal arches. Interestingly, this was in a pattern not observed in other MFCS4 transgenics (Figure A1.1 N, O, compare to F-M).

These preliminary data demonstrate that the gar MACS1 enhancer, as well as the skate and gar MFCS4 enhancers drive reproducible patterns of expression in regions of known *shh* activity (Piotrowski and Nüsslein-Volhard, 2000; Reichenbach et al., 2008). The gar MACS1

element elicits expression in the gut and pharyngeal region, similar to its murine counterpart (Sagai et al., 2009). While the zebrafish MFCS4 transients did not drive reporter expression in a pattern similar to its skate and gar counterparts, it is more similar to the murine MFCS4 element which was shown to also drive expression in pharyngeal tissues in mouse (Sagai et al., 2009) (Figure A1.1 N, O). However, drawing conclusions from inter-species comparisons is challenging, as the *trans* environment of the host (zebrafish) may be unable to properly interpret the MFCS4 donor elements due to lineage specific evolution. To remedy this issue, it will be necessary to establish stable lines of the native zebrafish MFCS4 enhancer (to reduce position effects) and perform dual-labeling of GFP and pharyngeal arch markers *hoxb2*, or *hand2* using antibodies to more accurately define the area of reporter activity. Furthermore, establishing stable transgenics in order to test the murine MACS1 and MFCS4 elements in zebrafish, as well as the inverse (reciprocal transgenics) will allow for more robust interpretation regarding *cis* and *trans* evolutionary changes of these regulatory elements (Gordon and Ruvinsky, 2012; Gehrke and Shubin, 2016).

These data suggest a role for MACS1 in patterning the zebrafish gut tube, though further work is necessary to assess the expression of the native zebrafish MACS1 element and characterize its function through CRISPR-Cas9 loss-of-function mutagenesis. Phenotypic analysis of *sonic-you* (*syu*) mutants suggests a role for *shha* in the development of the zebrafish digestive system, where both the esophagus and the pneumatic duct, the tissue homologue of the mammalian trachea, are malformed (Wallace and Pack, 2003). Future studies may reveal a role for MACS1 regulation of *Shha* in the digestive system of zebrafish, if a MACS1 deletion mutant exhibits gut malformation during development.

The pharyngeal arch region of vertebrates features multipotent cell populations from all

germ layers, as well as the neural crest. These cell populations contribute to the development of specialized organs such as the larynx of mammals, neuronal tissues, as well as craniofacial muscular and skeletal components. During zebrafish pharyngeal development, *shh* is expressed in pharyngeal endoderm and second pharyngeal arch (Piotrowski and Nüsslein-Volhard, 2000). Interestingly, *shh* mutants in zebrafish develop normal pharyngeal arches, suggesting that it is not required for the proper segmenting of the pharyngeal region (Schauerte et al., 1998; Piotrowski and Nüsslein-Volhard, 2000). However, *Shh* has been implicated in the maintenance and growth of the adjacent pouches in mice (Moore-Scott and Manley, 2005). Therefore, it is enticing to hypothesize that the reporter expression pattern of gar MACS1 may be suggestive of a role for *shh* in pharyngeal pouch maintenance. To address this possibility, further investigation of *shh* regulation and function at the level of individual regulatory elements is required.

I found that skate and gar MFCS4 elements drive GFP expression in a region posterior to the eye, interpreted as the trigeminal ganglion based on its location and shape. Interestingly, in an analysis of a zebrafish *shh* hypomorph, the trigeminal ganglion was unperturbed (Chandrasekhar et al., 1998). Studies in mouse, however, suggest *shh* plays a role in the migration of cells that contribute to the trigeminal placode (Fedtsova et al., 2003). Given the expression of skate and gar MFCS4 elements in this sensory tissue, it may be possible that *shh* is but one contributor to the formation of the trigeminal ganglion in zebrafish. Analyzing the expression of the native MFCS4 enhancer in stable lines will first be needed to assess the function of this element in zebrafish. Further assays such as CRISPR-Cas9 MFCS4 disruption may reveal as yet unknown contributions of *shh* function to the development of the trigeminal ganglion.

These results raise intriguing questions regarding the evolution of *Shh cis*-regulatory

architecture. However, more descriptive and detailed enhancer analyses via reciprocal transgenics are needed to obtain a better understanding of what and possibly how changes to *Shh* enhancers have affected morphological evolution. Finally, general principles of regulatory evolution may be found through these thorough assays of *Shh* regulation.

Materials & Methods

Vista Alignments

Anole (*Anolis carolinensis*), coelacanth (*Latimeria menadoensis*), zebrafish (*Danio rerio*), pufferfish (*Fugu rubripes*), and medaka (*Oryzias latipes*) genomic regions spanning intron 8 of *rnf32* (location of MACS1 in mouse), or adjacent to *rnf32* (location of MFCS4) were downloaded from the UCSC genome database (http://genome.ucsc.edu), the gar genome from the ENSEMBL database (http://www.ensembl.org/index.html), and the skate genome from Skatebase (Wyffels et al., 2014) (http://skatebase.org). Alignments were made using the mVista (LAGAN) program with the following parameters: Calculation window: 100 bps, Min Conservation Width: 100 bps, Conservation Identity: 70%. Mouse was used as a baseline for all alignments.

Enhancer Cloning

Putative enhancers were amplified using primers listed in Table A1.1 and PCR products were approximately ~1kb in length, spanning the conservation peaks and neighboring flanking sequence (Figure A1.1, A). Following amplification, the purified PCR products were subcloned into the PCR8/GW/TOPO vector. The MACS1 and MFCS4 enhancer elements were then cloned into the pXIG-cfos-eGFP destination vector (Fisher et al., 2006). The final destination vectors

were confirmed through restriction digest and sequencing at the University of Chicago Genomics Facility.

***Danio rerio* Transgenesis**

All experiments were performed in accordance with the University of Chicago ACUP protocol #72074. Zebrafish embryos (WT; strain *AB) were collected from natural spawning. Transposase RNA was synthesized from pCS2-zT2TP (Suster et al., 2011) using the mMessage mMachine® SP6 Kit (Ambion). The cytoplasm of one- or two-cell stage zebrafish were injected with a ~2nl solution containing transposase RNA and the destination vector and according to the protocol established by Fisher et al., (2006). Injected embryos were raised to adulthood (~3 months of age) and outcrossed to WT fish to identify GFP positive transgenic founders. See Table A1.2 for summary of zebrafish injections. GFP positive fish were imaged using a Leica M204FA microscope.

GFP in situ hybridization

Zebrafish embryos were staged according to (Kimmel et al., 1995). *In situ* hybridization was performed according to (Kopinke et al., 2006) with the following modifications: a solution of 50% formamide, 5×SSC pH4.5, 1% SDS, 500 μg/ml tRNA, 50 μg/ml heparin and 5 mM EDTA pH8.0 was used for RNA probe hybridization, and maleic acid buffer containing a 2% blocking reagent (Sigma-Aldrich) and 20% goat serum was used as blocking solution. The anti-DIG-AP antibody (1:5000 in blocking solution, Sigma-Aldrich) and BM purple (Sigma-Aldrich) were used for probe detection and color development, respectively. After color development, embryos were post-fixed in 4% PFA, washed in TE buffer, and photographed using a Leica M205FA microscope.

Organism	MACS1 Forward (5') Primer	MACS1 Reverse (3') Primer	Product size:
Gar	cccattaatctgggtttcctc	attttgaaaaccccgaaagt	1048
	MFCS4 Forward (5') Primer	**MFCS4 Reverse (3') Primer**	
Zebrafish	gcaacgcatgtgctgtagat	caacaaagaacaaagaggctatca	1091
Gar	aatgcgtggaatggagtgct	agctgcttctacaaggccag	971
Skate	cggatgatttgtttaaaggtttg	gccctgtctcacaaaggaac	842

Table A1.1 - List of oligos used in Appendix I. Primers used to amplify MGFC4 and MACS1 enhancer sequences from zebrafish, gar, and skate genomes.

Putative Enhancer	Total # Injected	GFP Signal -	GFP Signal +	% with signal	Founder line
Gar MACS1	113	89	24	21.2%	Yes
Gar MFCS4	165	148	17	10.3%	Yes
Skate MFCS4	141	123	18	12.7%	Yes
Zebrafish MFCS4	139	131	8	5.7%	No

Table A1.2 - Summary of MFCS4 and MACS1 transgenics.

APPENDIX II

MUTATIONS IN *SONIC HEDGEHOG B* CODING REGION USING CRISPR/CAS9 IN ZEBRAFISH

The teleost, *Danio rerio,* has five functional copies of *hedgehog* family genes, including two copies of *sonic hedgehog, shha* and *shhb.* Both paralogs exhibit similar patterns of expression in the floor plate of the neural tube and developing diencephalon (Ekker et al., 1995; Avaron et al., 2006). During fin bud development, *shha* and *shhb* are both expressed in similar domains, though there is a slight delay in the onset of *shhb* expression (Du and Dienhart, 2001; Avaron et al., 2006). To date, zebrafish *shhb* function has only been studied through morpholino knockdowns to better understand features of craniofacial development, where it serves as animal model for the human disorder of holoprosencephaly (Nasevicius and Ekker, 2000; Teraoka et al., 2006). Recently, clustered regularly interspaced short palindromic repeats (CRISPR)-Cas9 technology been proposed as a powerful tool to edit the genome and generate germ-line mutations in order to carefully assess knockdown or loss-of-function phenotypes in range of organisms, including zebrafish (Jao et al., 2013). Utilizing CRISPR-Cas9 technology to manipulate *shhb* function in zebrafish will help in understanding the phenotypic contribution of this gene to fins and other structures exhibiting *shhb* expression.

Large scale mutagenesis screens in zebrafish previously identified mutations in 11 genes, including *shha*, that affect larval and/or adult fin morphology (van Eeden et al., 1996). One allelic variant, *sonic-you* (*syu*), is an *shha* null mutant that carries a 7.5kb deletion encompassing the entire *shha* coding region (Schauerte et al., 1998). However, no *shhb* mutants have been

identified through mutagenesis screens. In order to assess the function of *shhb* during fin bud development, I used CRISPR-Cas9 technology to disrupt the *shhb* coding region.

I co-injected *shhb s*gRNA and Cas9 mRNA into WT zebrafish to induce insertion-deletion (indel) mutations within the first exon of *shhb* (Figure A2.1, A). After 24 hours, embryos were analyzed for basepair mismatches using the T7 endonuclease I assay as reported previously (Jao et al., 2013). As expected, the T7 enzyme did not cut the PCR product from the control embryos, but did cleave the amplicons derived from *shhb* sgRNA/Cas9 injected embryos. Mutagenesis rates were estimated to be 64% (7 out of 11 randomly selected embryos) indicative of successful disruption of the target site (Figure A2.1, B). Subcloning of these PCR products from individual embryos revealed a range of indels, supporting the results of the T7 assay. The remaining embryos were raised to adulthood and fin clipped in order to identify desirable frameshift mutations in founders.

Several F1s were identified exhibiting a range of mutations including large deletions of 169 bp and smaller deletions of 7 bp (Figure A2.1, C). Sequencing of the *shhb* target site revealed that 46% (21/46) of sequences from 6 F1 fish had *shhb* mutations. Only F1s carrying a frameshift mutation were kept.

Further studies are required to assess the phenotypic effects of disrupting the *shhb* coding region. Frameshift mutations may result in an alteration of the amino acid sequence leading to a non-functional protein. A more thorough Western blot protein analysis using an antibody specific to *D. rerio shhb* will confirm if the F1 zebrafish are null mutants relative to WT embryos and housekeeping gene controls. Differences in *shhb* expression between homozygote ($shhb^{-/-}$) and heterozygote *shhb* ($shhb^{+/-}$) mutants may also reveal subtle phenotypic effects in structures patterned by *shhb*, such as branchimotor neurons, and the zona limitans intrathalamica signaling

center in the brain (Chandrasekhar et al., 1998; Scholpp et al., 2006) . Moreover, out-crossing heterozygote and homozygote mutants to existing loss-of-function *shha* mutants such as $syu^{+/t4-}$ zebrafish may reveal as yet unknown contributions of each *shh* paralog to fin bud formation and development.

Materials and Methods

Preparation of Cas9 mRNA and *Shhb* sgRNA design and synthesis

Cas9 mRNA was synthesized from the pCS2+ Cas9 expression vector (Nakayama et al., 2013) by first digesting the plasmid with NotI enzyme. The digestion product was then purified using the NucleoSpin Gel and PCR Clean-up Kit (Macherey-Nagel). Cas9 RNA was synthesized using the mMESSAGE mMACHINE SP6 Transcription Kit according to the manufacturer's instructions (Ambion). A 20 basepair gene-specific target site in *D. rerio shhb* exon 1 was designed using the CHOPCHOP program (Montague et al., 2014) (Figure A2.1, A). This sequence was incorporated into an oligonucleotide containing the T7 (5'-TAATACGACTCACTATA-3') promoter sequence, the 20 bp *shhb* target site without the adjacent PAM cleavage site, and a region complementary to the tracrRNA and synthesized by Integrated DNA Technologies, Inc. (IDT). Next, the 60-bp oligonucleotide was annealed to a constant oligonucleotide encoding the reverse-complement of the tracrRNA tail (Gagnon et al., 2014) (Table A2.1). The ssDNA overhangs were then filled in with T4 DNA polymerase (NEB). The amplicon was then purified using the NucleoSpin Gel and PCR Clean-up Kit (Macherey-Nagel). *Shhb* sgRNA was then synthesized from the purified PCR product via *in vitro* transcription using the MEGAshortscript™ T7 kit (Ambion). The sgRNA was then purified via LiCl and ethanol precipitation.

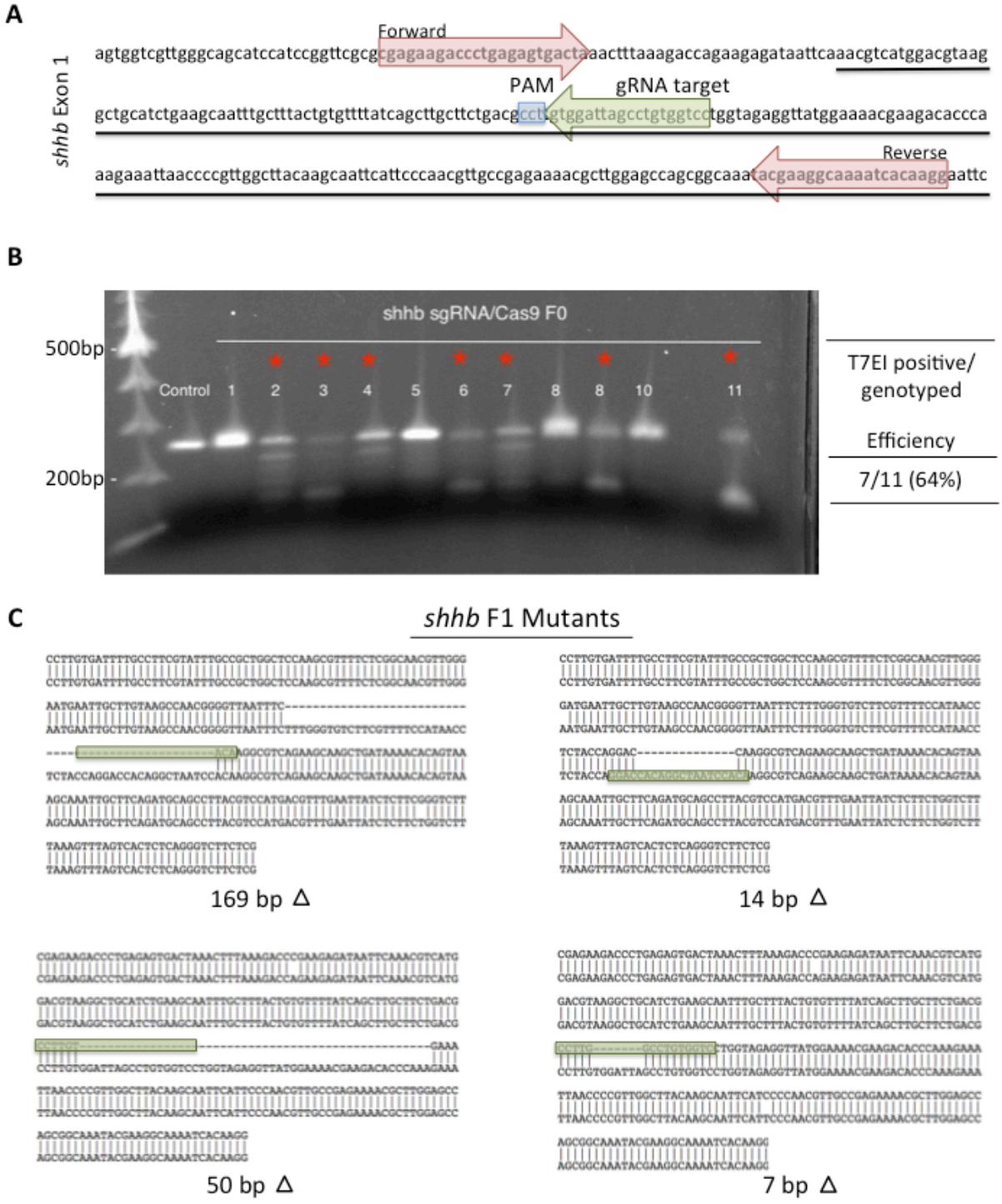

Figure A2.1 - Generating *Shhb* mutants using CRISPR/Cas9 technology. (A) Diagram illustrating target region with adjacent PAM site within the Exon 1 of *Shhb* (underlined portion). Primers used to amplify PCR product for T7E1 assay shown. **(B)** Results of T7E1 assay in F0 fish. Lanes marked with * indicate bp mismatch. **(C)** Sequencing results of *Shhb* target site in F1 embryos. Green box represents target site, size of deletion is marked below each result.

Shhb injection and genotyping

All experiments were performed in accordance with the University of Chicago ACUP protocol #72074. Zebrafish embryos (*AB strain) were collected from natural spawning and used for sgRNA and Cas9 mRNA co-injection. The cytoplasm of one- or two-celled embryos was injected with a ~2nl injection solution (from a total 5 ul solution containing 500 ng of *Shhb* sgRNA, 750ng Cas9, and phenol red, diluted in nuclease-free water). Embryos were grown to 24-28 hpf and genomic DNA was extracted from individual embryos (2 control and 11 injected) for PCR amplification of a 270bp region flanking the *shhb* target site (Figure A2.1 A, Table A2.1). PCR products were then assayed for mutations using the T7 endonuclease I (T7E1) assay to identify mismatches as previously reported (Jao et al., 2013). PCR fragments positive for mismatches were cloned into the pCRII-TOPO vector (Invitrogen) for further mutation analysis. Detailed analysis of basepair indels were performed by sequencing at the University of Chicago Sequencing Facility. The remaining embryos were raised to adulthood, and at approximately three months of age, individuals were genotyped using DNA from fin clips. Zebrafish were anesthetized using Tricaine (0.004%) and tips of the caudal fin (2-3mm^2) were removed and placed in a microcentrifuge tube. The fin tissue was lysed in standard lysis buffer (10 mM Tris pH 8.2, 10 mM EDTA, 200 mM NaCl, 0.5% SDS, 200 ug/mL proteinase K) in a 55°C water bath and DNA recovered by ethanol precipitation. Fin clip DNA was used as a PCR template to amplify a 270bp fragment and used for the T7E1 assay, cloning, and sequencing as with embryo mutant analysis as detailed earlier.

Establishment of *shhb* mutants

Identified adult mutant fish were out crossed to WT to select frameshift mutations from mosaic mutational patterns and generate heterozygous F1 progeny carrying germ-line *shhb*

mutations. At three months of age, F1s were fin-clipped and assessed for germ-line transmission via T7E1 and sequencing.

Genotyping Forward (5') Primer	**Genotyping Reverse (3') Primer**	***Shhb* Target Site**	***Shhb* gRNA oligonucleotide** (5'-T7 promoter-target site-tracr overlap region-3'
cgagaagaccctga gagtgacta	ccttgtgattttgc cttcgtat	ggaccacaggct aatccaca	taatacgactcactataggaccacaggctaatccaca gttttagagctagaaatagcaag
Product size:	270 bp		

Table A2.1 – List of oligos used in Appendix II. Primers used in T7 Endonuclease I assay and *Shhb* gRNA synthesis. Red text corresponds to gene-specific target site.

REFERENCES

Abe, G., Ide, H., and Tamura, K. 2007. Function of FGF signaling in the developmental process of the median fin fold in zebrafish. Dev. Biol. *304*, 355–366.

Abouheif, E., Akam, M., Dickinson, W.J., Holland, P.W., Meyer, A., Patel, N.H., Raff, R.A., Roth, V.L., and Wray, G.A. 1997. Homology and developmental genes. Trends Genet. *13*, 432–433.

Ahn, D., and Ho, R.K. 2008. Tri-phasic expression of posterior Hox genes during development of pectoral fins in zebrafish: implications for the evolution of vertebrate paired appendages. Dev. Biol. *322*, 220–233.

Akimenko, M. a, Ekker, M., Wegner, J., Lin, W., and Westerfield, M. 1994. Combinatorial expression of three zebrafish genes related to distal-less: part of a homeobox gene code for the head. J. Neurosci. *14*, 3475–3486.

Akimenko, M. a, Johnson, S.L., Westerfield, M., and Ekker, M. 1995. Differential induction of four msx homeobox genes during fin development and regeneration in zebrafish. Development *121*, 347–357.

Akimenko, M.A., and Ekker, M. 1995. Anterior duplication of the Sonic hedgehog expression pattern in the pectoral fin buds of zebrafish treated with retinoic acid. Dev. Biol. *170*, 243–247.

Akiyama, R., Kawakami, H., Wong, J., Oishi, I., Nishinakamura, R., and Kawakami, Y. 2015. Sall4-Gli3 system in early limb progenitors is essential for the development of limb skeletal elements. Proc. Natl. Acad. Sci. U. S. A. *112*, 5075–5080.

Amano, T., Sagai, T., Tanabe, H., Mizushina, Y., Nakazawa, H., and Shiroishi, T. 2009. Chromosomal dynamics at the Shh locus: limb bud-specific differential regulation of competence and active transcription. Dev. Cell *16*, 47–57.

Amemiya, C.T., Alföldi, J., Lee, A.P., Fan, S., Philippe, H., Maccallum, I., Braasch, I., Manousaki, T., Schneider, I., Rohner, N., et al. 2013. The African coelacanth genome provides insights into tetrapod evolution. Nature *496*, 311–316.

Amemiya, C.T., Powers, T.P., Prohaska, S.J., Grimwood, J., Schmutz, J., Dickson, M., Miyake, T., Schoenborn, M. a, Myers, R.M., Ruddle, F.H., et al. 2010. Complete HOX cluster characterization of the coelacanth provides further evidence for slow evolution of its genome. Proc. Natl. Acad. Sci. U. S. A. *107*, 3622–3627.

Amores, A., Catchen, J., Ferrara, A., Fontenot, Q., and Postlethwait, J.H. 2011. Genome evolution and meiotic maps by massively parallel DNA sequencing: Spotted gar, an outgroup for the teleost genome duplication. Genetics *188*, 799–808.

Andrews, S. 2010. FastQC: A quality control tool for high throughput sequence data.

Andrey, G., Montavon, T., Mascrez, B., Gonzalez, F., Noordermeer, D., Leleu, M., Trono, D., Spitz, F., and Duboule, D. 2013. A Switch Between Topological Domains Underlies HoxD Genes Collinearity in Mouse Limbs. Science. *340*, 1234167.

Archambeault, S., Taylor, J., and Crow, K.D. 2014. HoxA and HoxD expression in a variety of vertebrate body plan features reveals an ancient origin for the distal Hox program. Evodevo *5*, 44.

Arthur, W. 2002. The emerging conceptual framework of evolutionary developmental biology. Nature *415*, 757–764.

Avaron, F., Smith, A., and Akimenko, M.A. 2006. Sonic Hedgehog Signaling in the Developing and Regenerating Fins of Zebrafish. In Madame Curie Bioscience Database, C.E. Fisher, and S.E.M. Howie, eds. (Landes Bioscience and Springer Science & Business Media), pp. 93–106.

Balfour, M.F. 1881. On the Development of the Skeleton of the Paired Fins of Elasmobranchii, considered in Relation to its Bearings on the Nature of the Limbs of the Vertebrata. Proc Zool Soc London *43*, 656–671.

Ballard, W., and Needham, R. 1964. Normal embryonic stages of Polyodon spathula (Walbaum). J. Morphol. 465–477.

Bemis, W.E., and Grande, L. 1992. Early development of the actinopterygian head. I. External development and staging of the paddlefish Polyodon spathula. J. Morphol. *213*, 47–83.

Bemis, W.E., and Grande, L. 1999. Development of the median fins of the North American paddlefish (Polyodon spathula), and a reevaluation of the lateral fin-fold hypothesis. In Mesozoic Fishes 2 - Systematics and Fossil Record, G. Arratia, and H.-P. Schlutze, eds. pp. 41–68.

Bessa, J., Tena, J.J., de la Calle-Mustienes, E., Fernández-Miñán, A., Naranjo, S., Fernández, A., Montoliu, L., Akalin, A., Lenhard, B., Casares, F., et al. 2009. Zebrafish enhancer detection (ZED) vector: a new tool to facilitate transgenesis and the functional analysis of cis-regulatory regions in zebrafish. Dev. Dyn. *238*, 2409–2417.

Bird, N.C., and Mabee, P.M. 2003. Developmental Morphology of the Axial Skeleton of the Zebrafish, Danio rerio (Ostariophysi: Cyprinidae). Dev. Dyn. *228*, 337–357.

Birol, I., Jackman, S.D., Nielsen, C.B., Qian, J.Q., Varhol, R., Stazyk, G., Morin, R.D., Zhao, Y., Hirst, M., Schein, J.E., et al. 2009. De novo transcriptome assembly with ABySS. Bioinformatics *25*, 2872–2877.

Bolker, J.A. 2014. Model species in evo-devo: A philosophical perspective. Evol. Dev. *16*, 49–56.

Braasch, I., Gehrke, A.R., Smith, J.J., Kawasaki, K., Manousaki, T., Pasquier, J., Amores, A.,

Desvignes, T., Batzel, P., Catchen, J., et al. 2016. The spotted gar genome illuminates vertebrate evolution and facilitates human-teleost comparisons. Nat. Genet. *48*, 427–437.

Buenrostro, J.D., Giresi, P.G., Zaba, L.C., Chang, H.Y., and Greenleaf, W.J. 2013. Transposition of native chromatin for fast and sensitive epigenomic profiling of open chromatin, DNA-binding proteins and nucleosome position. Nat. Methods *10*, 1213–1218.

Burke, A.C., and Nowicki, J.L. 2003. A new view of patterning domains in the vertebrate mesoderm. Dev. Cell *4*, 159–165.

Butterfield, N.C., McGlinn, E., and Wicking, C. 2010. The molecular regulation of vertebrate limb patterning. Curr. Top. Dev. Biol. *90*, 319–341.

Camacho, C., Coulouris, G., Avagyan, V., Ma, N., Papadopoulos, J., Bealer, K., and Madden, T.L. 2009. BLAST+: Architecture and Applications. BMC Bioinformatics *10*, 421.

Capellini, T.D., Di Giacomo, G., Salsi, V., Brendolan, A., Ferretti, E., Srivastava, D., Zappavigna, V., and Selleri, L. 2006. Pbx1/Pbx2 requirement for distal limb patterning is mediated by the hierarchical control of Hox gene spatial distribution and Shh expression. Development *133*, 2263–2273.

Carroll, S.B. 2008. Evo-devo and an expanding evolutionary synthesis: a genetic theory of morphological evolution. Cell *134*, 25–36.

Chan, Y.F., Marks, M.E., Jones, F.C., Villarreal, G., Shapiro, M.D., Brady, S.D., Southwick, A.M., Absher, D.M., Grimwood, J., Schmutz, J., et al. 2010. Adaptive evolution of pelvic reduction in sticklebacks by recurrent deletion of a Pitx1 enhancer. Science *327*, 302–305.

Chandrasekhar, A., Warren, J.T., Takahashi, K., and Schauerte, H.E. 1998. Role of sonic hedgehog in branchiomotor neuron induction in zebrafish. Mech. Dev. *76*, 101–115.

Charité, J., McFadden, D.G., and Olson, E.N. 2000. The bHLH transcription factor dHAND controls Sonic hedgehog expression and establishment of the zone of polarizing activity during limb development. Development *127*, 2461–2470.

Chiang, C., Litingtung, Y., Lee, E., Young, K.E., Corden, J.L., Westphal, H., and Beachy, P. a 1996. Cyclopia and defective axial patterning in mice lacking Sonic hedgehog gene function. Nature *383*, 407–413.

Coates, M.I. 1994. The origin of vertebrate limbs. Dev. Suppl. *1994*, 169–180.

Coates, M.I. 2003. The Evolution of Paired Fins. Theory Biosci. *122*, 266–287.

Coates, M.I., and Cohn, M.J. 1998. Fins, limbs, and tails: Outgrowths and axial patterning in vertebrate evolution. BioEssays *20*, 371–381.

Cohn, M.J., Izpisúa-Belmonte, J.C., Abud, H., Heath, J.K., and Tickle, C. 1995. Fibroblast growth factors induce additional limb development from the flank of chick embryos. Cell *80*, 739–746.

Crow, K.D., Smith, C.D., Cheng, J.-F.F., Wagner, G.P., and Amemiya, C.T. 2012. An independent genome duplication inferred from Hox paralogs in the American paddlefish-A representative basal ray-finned fish and important comparative reference. Genome Biol. Evol. *4*, 937–953.

Dahn, R.D., Davis, M.C., Pappano, W.N., and Shubin, N.H. 2007. Sonic hedgehog function in chondrichthyan fins and the evolution of appendage patterning. Nature *445*, 311–314.

Davidson, E.H., and Erwin, D.H. 2006. Gene regulatory networks and the evolution of animal body plans. Science. *311*, 796–800.

Davis, M.C., Dahn, R.D., and Shubin, N.H. 2007. An autopodial-like pattern of Hox expression in the fins of a basal actinopterygian fish. Nature *447*, 473–476.

Davis, M.C., Shubin, N.H., and Force, A. 2004. Pectoral fin and girdle development in the basal actinopterygians Polyodon spathula and Acipenser transmontanus. J. Morphol. *262*, 608–628.

Du, S.J., and Dienhart, M. 2001. Zebrafish tiggy-winkle hedgehog promoter directs notochord and floor plate green fluorescence protein expression in transgenic zebrafish embryos. Dev. Dyn. *222*, 655–666.

Duboule, D., and Dollé, P. 1989. The structural and functional organization of the murine HOX gene family resembles that of Drosophila homeotic genes. EMBO J. *8*, 1497–1505.

van Eeden, F.J., Granato, M., Schach, U., Brand, M., Furutani-Seiki, M., Haffter, P., Hammerschmidt, M., Heisenberg, C.P., Jiang, Y.J., Kane, D. a, et al. 1996. Genetic analysis of fin formation in the zebrafish, Danio rerio. Development *123*, 255–262.

Ekker, S.C., Ungar, A.R., Greenstein, P., von Kessler, D.P., Porter, J.A., Moon, R.T., and Beachy, P.A. 1995. Patterning activities of vertebrate hedgehog proteins in the developing eye and brain. Curr. Biol. *5*, 944–955.

Favier, B., and Dollé, P. 1997. Developmental functions of mammalian Hox genes. Mol. Hum. Reprod. *3*, 115–131.

Fedtsova, N., Perris, R., and Turner, E.E. 2003. Sonic hedgehog regulates the position of the trigeminal ganglia. Dev. Biol. *261*, 456–469.

Fisher, S., Grice, E. a, Vinton, R.M., Bessling, S.L., Urasaki, A., Kawakami, K., and McCallion, A.S. 2006. Evaluating the biological relevance of putative enhancers using Tol2 transposon-mediated transgenesis in zebrafish. Nat. Protoc. *1*, 1297–1305.

Force, A., Lynch, M., Pickett, F.B., Amores, A., Yan, Y.-L., and Postlethwait, J. 1999. Preservation of duplicate genes by complementary, degenerative mutations. Genetics *151*, 1531–1545.

Force, A.G., Cresko, W.A., and Pickett, F.B. 2004. Informational accretion, gene duplication, and the mechanisms of genetic module parcellation. In Modularity in Development and Evolution, G. Schlosser, and G.P. Wagner, eds. (University of Chicago Press), pp. 315–337.

Frankel, N., Erezyilmaz, D.F., McGregor, A.P., Wang, S., Payre, F., and Stern, D.L. 2011. Morphological evolution caused by many subtle-effect substitutions in regulatory DNA. Nature *474*, 598–603.

Freitas, R., Gómez-Skarmeta, J.L., and Rodrigues, P.N. 2014. New frontiers in the evolution of fin development. J. Exp. Zool. B. Mol. Dev. Evol. *322*, 540–552.

Freitas, R., Zhang, G., and Cohn, M.J. 2006. Evidence that mechanisms of fin development evolved in the midline of early vertebrates. Nature *442*, 1033–1037.

Freitas, R., Zhang, G., and Cohn, M.J. 2007. Biphasic Hoxd gene expression in shark paired fins reveals an ancient origin of the distal limb domain. PLoS One *2*, e754.

Fromental-Ramain, C., Warot, X., Lakkaraju, S., Favier, B., Haack, H., Birling, C., Dierich, a, Doll e, P., and Chambon, P. 1996a. Specific and redundant functions of the paralogous Hoxa-9 and Hoxd-9 genes in forelimb and axial skeleton patterning. Development *122*, 461–472.

Fromental-Ramain, C., Warot, X., Messadecq, N., LeMeur, M., Dollé, P., and Chambon, P. 1996b. Hoxa-13 and Hoxd-13 play a crucial role in the patterning of the limb autopod. Development *122*, 2997–3011.

Gagnon, J. a, Valen, E., Thyme, S.B., Huang, P., Ahkmetova, L., Pauli, A., Montague, T.G., Zimmerman, S., Richter, C., and Schier, A.F. 2014. Efficient mutagenesis by Cas9 protein-mediated oligonucleotide insertion and large-scale assessment of single-guide RNAs. PLoS One *9*, e98186.

Galli, A., Robay, D., Osterwalder, M., Bao, X., Bénazet, J.-D., Tariq, M., Paro, R., Mackem, S., and Zeller, R. 2010. Distinct roles of Hand2 in initiating polarity and posterior Shh expression during the onset of mouse limb bud development. PLoS Genet. *6*, e1000901.

Gao, F., and Davidson, E.H. 2008. Transfer of a large gene regulatory apparatus to a new developmental address in echinoid evolution. Proc Natl Acad Sci U S A *105*, 6091–6096.

Garcia-Fernandez, J. 2005. The genesis and evolution of homeobox gene clusters. Nat Rev Genet *6*, 881–892.

Gegenbaur, C. 1878. Elements of Comparative Anatomy (London: MacMillan and Co).

Gehring, W.J. 2004. Historical perspective on the development and evolution of eyes and photoreceptors. Int. J. Dev. Biol. *48*, 707–717.

Gehrke, A., Schneider, I., de la Calle-Mustienes, E., Tena, J., Gomez-Marin, C Chandran, M., Nakamura, T., Braasch, I., Postlethwait, J., Gomez-Skarmeta, J., and Shubin, N. 2015. Deep conservation of wrist and digit enhancers in fish. Proc. Natl. Acad. Sci. U. S. A.

Gehrke, A.R., and Shubin, N.H. 2016. Cis-regulatory programs in the development and evolution of vertebrate paired appendages. Semin. Cell Dev. Biol. 1–9.

Germanguz, I., Lev, D., Waisman, T., Kim, C.H., and Gitelman, I. 2007. Four twist genes in zebrafish, four expression patterns. Dev. Dyn. *236*, 2615–2626.

Gillis, J.A., Dahn, R.D., and Shubin, N.H. 2009. Shared developmental mechanisms pattern the vertebrate gill arch and paired fin skeletons. Proc. Natl. Acad. Sci. U. S. A. *106*, 5720–5724.

Gillis, J.A., and Hall, B.K. 2016. A shared role for sonic hedgehog signalling in patterning chondrichthyan gill arch appendages and tetrapod limbs. Development *143*, 1313–1317.

Gompel, N., Prud'homme, B., Wittkopp, P.J., Kassner, V. a, and Carroll, S.B. 2005. Chance caught on the wing: cis-regulatory evolution and the origin of pigment patterns in Drosophila. Nature *433*, 481–487.

Gordon, K.L., and Ruvinsky, I. 2012. Tempo and mode in evolution of transcriptional regulation. PLoS Genet. *8*, e1002432.

Grandel, H., Lun, K., Rauch, G.-J., Rhinn, M., Piotrowski, T., Houart, C., Sordino, P., Küchler, A.M., Schulte-Merker, S., Geisler, R., et al. 2002. Retinoic acid signalling in the zebrafish embryo is necessary during pre-segmentation stages to pattern the anterior-posterior axis of the CNS and to induce a pectoral fin bud. Development *129*, 2851–2865.

Grandel, H., and Schulte-Merker, S. 1998. The development of the paired fins in the zebrafish (Danio rerio). Mech. Dev. *79*, 99–120.

Hadzhiev, Y., Lele, Z., Schindler, S., Wilson, S.W., Ahlberg, P., Strähle, U., and Müller, F. 2007. Hedgehog signaling patterns the outgrowth of unpaired skeletal appendages in zebrafish. BMC Dev. Biol. *7*, 75.

Hall, B.K. 1994. Homology: The Hierarchical Basis of Comparative Biology (Academic Press, Inc.).

Harfe, B.D., Scherz, P.J., Nissim, S., Tian, H., McMahon, A.P., and Tabin, C.J. 2004. Evidence for an expansion-based temporal Shh gradient in specifying vertebrate digit identities. Cell *118*, 517–528.

Hillis, D.M. 1994. Homology in Molecular Biology. In Homology: The Hierachical Basis of

Comparative Biology, B.K. Hall, ed. (Academic Press, Inc.), pp. 339–369.

Hoegg, S., Brinkmann, H., Taylor, J.S., and Meyer, A. 2004. Phylogenetic timing of the fish-specific genome duplication correlates with the diversification of teleost fish. J. Mol. Evol. *59*, 190–203.

Hoffman, L., Miles, J., Avaron, F., Laforest, L., and Akimenko, M.-A. 2002. Exogenous retinoic acid induces a stage-specific, transient and progressive extension of Sonic hedgehog expression across the pectoral fin bud of zebrafish. Int. J. Dev. Biol. *46*, 949–956.

Inoue, J.G., Miya, M., Tsukamoto, K., and Nishida, M. 2003. Basal actinopterygian relationships: A mitogenomic perspective on the phylogeny of the "ancient fish." Mol. Phylogenet. Evol. *26*, 110–120.

Irimia, M., Royo, J.L., Burguera, D., Maeso, I., Gómez-Skarmeta, J.L., and Garcia-Fernandez, J. 2012. Comparative genomics of the Hedgehog loci in chordates and the origins of Shh regulatory novelties. Sci. Rep. *2*, 433.

Iwamatsu, T. 2013. Growth of the Medaka (II)- Formation of Fins and Fin Appendages. Bull. Aichi Univ. Educ. *62*, 53–60.

Janvier, P. 1996. Early Vertebrates (Oxford University Press).

Janvier, P. 2007. Homologies and evolutionary transitions in early vertebrate history. In Major Transitions in Vertebrate Evolution, J.S. Anderson, and H.-D. Sues, eds. (Indiana: Indiana University Press), pp. 57–121.

Jao, L.-E., Wente, S.R., and Chen, W. 2013. Efficient multiplex biallelic zebrafish genome editing using a CRISPR nuclease system. Proc. Natl. Acad. Sci. U. S. A. *110*, 13904–13909.

Jenner, R.A., and Wills, M.A. 2007. The choice of model organisms in evo-devo. Nat. Rev. Genet. *8*, 311–319.

Jeong, Y., El-Jaick, K., Roessler, E., Muenke, M., and Epstein, D.J. 2006. A functional screen for sonic hedgehog regulatory elements across a 1 Mb interval identifies long-range ventral forebrain enhancers. Development *133*, 761–772.

Jinek, M., Chylinski, K., Fonfara, I., Hauer, M., Doudna, J.A., and Charpentier, E. 2012. A programmable dual-RNA-guided DNA endonuclease in adaptive bacterial immunity. Science *337*, 816–821.

Johanson, Z. 2010. Evolution of paired fins and the lateral somitic frontier. J. Exp. Zool. Part B Mol. Dev. Evol. *314 B*, 347–352.

Johanson, Z.A., Joss, J., Boisvert, C.A., Ericsson, R., Sutija, M., and Ahlberg, P.E. 2007. Fish Fingers: Digit Homologues in Sarcopterygian Fish Fins. J. Exp. Zool. B. Mol. Dev. Evol.

308B, 757–768.

Joshi, N.A., and Fass, J.N. 2011. Sickle: A sliding-window, adaptive, quality-based trimming tool for FastQ files.

Jowett, T., and Lettice, L.A. 1994. Whole-mount in situ hybridizations on zebrafish embryos using a mixture of digoxigenin and fluorescein-labelled probes. Trends Genet. *10*, 73–74.

Kano, S., Xiao, J.-H., Osório, J., Ekker, M., Hadzhiev, Y., Müller, F., Casane, D., Magdelenat, G., and Rétaux, S. 2010. Two lamprey Hedgehog genes share non-coding regulatory sequences and expression patterns with gnathostome Hedgehogs. PLoS One *5*, e13332.

Kawakami, K., Takeda, H., Kawakami, N., Kobayashi, M., Matsuda, N., and Mishina, M. 2004. A Transposon-Mediated Gene Trap Technique Approach Identifies DevelopmentallyRegulated Genes in Zebrafish. *7*, 1–12.

Kellogg, E.A., and Shaffer, H.B. 1993. Model Organisms in Evolutionary Studies. Syst. Biol. *42*, 409–414.

Keys, D.N., Lewis, D.L., Selegue, J.E., Pearson, B.J., Goodrich, L. V, Johnson, R.L., Gates, J., Scott, M.P., and Carroll, S.B. 1999. Recruitment of a hedgehog Regulatory Circuit in Butterfly Eyespot Evolution. Science. *283*, 532–534.

Kimmel, C.B., Ballard, W.W., Kimmel, S.R., Ullmann, B., and Schilling, T.F. 1995. Stages of embryonic development of the zebrafish. Dev. Dyn. *203*, 253–310.

Klomp, J., Athy, D., Kwan, C.W., Bloch, N.I., Sandmann, T., Lemke, S., and Schmidt-Ott, U. 2015. Embryo development. A cysteine-clamp gene drives embryo polarity in the midge Chironomus. Science. *348*, 1040–1042.

Kmita, M., Tarchini, B., Zàkàny, J., Logan, M., Tabin, C.J., and Duboule, D. 2005. Early developmental arrest of mammalian limbs lacking HoxA/HoxD gene function. Nature *435*, 1113–1116.

Kopinke, D., Sasine, J., Swift, J., Stephens, W.Z., and Piotrowski, T. 2006. Retinoic acid is required for endodermal pouch morphogenesis and not for pharyngeal endoderm specification. Dev. Dyn. *235*, 2695–2709.

Koudijs, M.J., den Broeder, M.J., Keijser, A., Wienholds, E., Houwing, S., van Rooijen, E.M.H.C., Geisler, R., and van Eeden, F.J.M. 2005. The zebrafish mutants dre, uki, and lep encode negative regulators of the hedgehog signaling pathway. PLoS Genet. *1*, e19.

Kozhemyakina, E., Ionescu, A., and Lassar, A.B. 2014. GATA6 Is a Crucial Regulator of Shh in the Limb Bud. PLoS Genet. *10*,.

Krauss, S., Concordet, J.P., and Ingham, P.W. 1993. A functionally conserved homolog of the Drosophila segment polarity gene hh is expressed in tissues with polarizing activity in

zebrafish embryos. Cell *75*, 1431–1444.

Krumlauf, R. 1994. Hox genes in vertebrate development. Cell *78*, 191–201.

Kuraku, S., and Meyer, A. 2009. The evolution and maintenance of Hox gene clusters in vertebrates and the teleost-specific genome duplication. Int. J. Dev. Biol. *53*, 765–773.

Kurosawa, G., Takamatsu, N., Takahashi, M., Sumitomo, M., Sanaka, E., Yamada, K., Nishii, K., Matsuda, M., Asakawa, S., Ishiguro, H., et al. 2006. Organization and structure of hox gene loci in medaka genome and comparison with those of pufferfish and zebrafish genomes. Gene *370*, 75–82.

de la Calle-Mustienes, E., Feijóo, C.G., Manzanares, M., Tena, J.J., Rodríguez-Seguel, E., Letizia, A., Allende, M.L., and Gómez-Skarmeta, J.L. 2005. A functional survey of the enhancer activity of conserved non-coding sequences from vertebrate Iroquois cluster gene deserts. Genome Res. *15*, 1061–1072.

Larouche, O., Cloutier, R., and Zelditch, M.L. 2015. Head, body, and fins, patterns of morphological integration and modularity in fishes. Evol. Biol. *42*, 296–311.

LeClair, E.E., Bonfiglio, L., and Tuan, R.S. 1999. Expression of the Paired-Box Genes Pax-1 and Pax-9. Dev. Dyn. *115*, 101–115.

Lettice, L.A., Heaney, S.J.H., Purdle, L.A., Li, L., de Beer, P., Oostra, B.A., Goode, D., Elgar, G., Hill, R.E., and de Graaff, E. 2003. A long-range Shh enhancer regulates expression in the developing limb and fin and is associated with preaxial polydactyly. Hum. Mol. Genet. *12*, 1725–1735.

Lettice, L.A., Hill, A.E., Devenney, P.S., and Hill, R.E. 2008. Point mutations in a distant sonic hedgehog cis-regulator generate a variable regulatory output responsible for preaxial polydactyly. Hum. Mol. Genet. *17*, 978–985.

Lettice, L.A., Horikoshi, T., Heaney, S.J.H., van Baren, M.J., van der Linde, H.C., Breedveld, G.J., Joosse, M., Akarsu, N., Oostra, B. a, Endo, N., et al. 2002. Disruption of a long-range cis-acting regulator for Shh causes preaxial polydactyly. Proc. Natl. Acad. Sci. U. S. A. *99*, 7548–7553.

Lettice, L.A., Williamson, I., Devenney, P.S., Kilanowski, F., Dorin, J., and Hill, R.E. 2014. Development of five digits is controlled by a bipartite long-range cis-regulator. Development *141*, 1715–1725.

Lettice, L.A., Williamson, I., Wiltshire, J.H., Peluso, S., Devenney, P.S., Hill, A.E., Essafi, A., Hagman, J., Mort, R., Grimes, G., et al. 2012. Opposing functions of the ETS factor family define Shh spatial expression in limb buds and underlie polydactyly. Dev. Cell *22*, 459–467.

Li, H., Handsaker, B., Wysoker, A., Fennell, T., Ruan, J., Homer, N., Marth, G., Abecasis, G.,

and Durbin, R. 2009. The Sequence Alignment/Map format and SAMtools. Bioinformatics *25*, 2078–2079.

Liebeskind, B.J., Hillis, D.M., Zakon, H.H., and Hofmann, H.A. 2016. Complex Homology and the Evolution of Nervous Systems. Trends Ecol. Evol. *31*, 127–135.

Litingtung, Y., Dahn, R.D., Li, Y., and Fallon, J.F. 2002. Shh and Gli3 are dispensable for limb skeleton formation but regulate digit number and identity. 979–983.

Livak, K.J., and Schmittgen, T.D. 2001. Analysis of relative gene expression data using real-time quantitative PCR and the 2^(-ΔΔCT) method. Methods *25*, 402–408.

Maas, S. a, Suzuki, T., and Fallon, J.F. 2011. Identification of spontaneous mutations within the long-range limb-specific Sonic hedgehog enhancer (ZRS) that alter Sonic hedgehog expression in the chicken limb mutants oligozeugodactyly and silkie breed. Dev. Dyn. *240*, 1212–1222.

Mabee, P.M., Crotwell, P.L., Bird, N.C., and Burke, A.C. 2002. Evolution of median fin modules in the axial skeleton of fishes. J. Exp. Zool. *294*, 77–90.

Magoč, T., and Salzberg, S.L. 2011. FLASH:Ffast length adjustment of short reads to improve genome assemblies. Bioinformatics *27*, 2957–2963.

Manceau, M., Domingues, V.S., Linnen, C.R., Rosenblum, E.B., and Hoekstra, H.E. 2010. Convergence in pigmentation at multiple levels: mutations, genes and function. Philos. Trans. R. Soc. Lond. B. Biol. Sci. *365*, 2439–2450.

Mao, J., McGlinn, E., Huang, P., Tabin, C.J., and McMahon, A.P. 2009. Fgf-Dependent Etv4/5 Activity Is Required for Posterior Restriction of Sonic hedgehog and Promoting Outgrowth of the Vertebrate Limb. Dev. Cell *16*, 600–606.

Marigo, V., Scott, M.P., Johnson, R.L., Goodrich, L. V, and Tabin, C.J. 1996. Conservation in hedgehog signaling: Induction of a chicken patched homolog by Sonic hedgehog in the developing limb. Development *122*, 1225–1233.

Martin, M. 2011. Cutadapt removes adapter sequences from high-throughput sequencing reads. Embnet.Journal *17*, 10–12.

Maxwell, E.E., Fröbisch, N.B., and Heppleston, A.C. 2008. Variability and conservation in late chondrichthyan development: ontogeny of the winter skate (Leucoraja ocellata). Anat. Rec. (Hoboken). *291*, 1079–1087.

McCune, A.R., and Schimenti, J.C. 2012. Using Genetic Networks and Homology to Understand the Evolution of Phenotypic Traits. Curr. Genomics *13*, 74–84.

Mehta, T.K., Ravi, V., Yamasaki, S., Lee, A.P., Lian, M.M., Tay, B.-H., Tohari, S., Yanai, S., Brenner, S., and Venktatesh, B. 2013. Evidence for at least six Hox clusters in the

Japanese lamprey (Lethenteron japonicum). Proc. Natl. Acad. Sci. U. S. A. *110*, 16044–16049.

Mercader, N. 2007. Early steps of paired fin development in zebrafish compared with tetrapod limb development. Dev. Growth Differ. *49*, 421–437.

Metscher, B.D., Takahashi, K., Crow, K., Amemiya, C., Nonaka, D.F., and Wagner, G.P. 2005. Expression of Hoxa-11 and Hoxa-13 in the pectoral fin of a basal ray-finned fish, Polyodon spathula: Implications for the origin of tetrapod limbs. Evol. Dev. *7*, 186–195.

Mivart, S.G. 1879. Notes on the Fins of Elasmobranchs, with Considerations on the Nature and Homologues of Vertebrate Limbs. Trans Zool Soc London *10*, 439–484.

Moczek, A.P., and Rose, D.J. 2009. Differential recruitment of limb patterning genes during development and diversification of beetle horns. Proc. Natl. Acad. Sci. U. S. A. *106*, 8992–8997.

Modrell, M.S., Buckley, D., and Baker, C.V.H. 2011. Molecular analysis of neurogenic placode development in a basal ray-finned fish. Genesis *49*, 278–294.

Montague, T.G., Cruz, J.M., Gagnon, J.A., Church, G.M., and Valen, E. 2014. CHOPCHOP: A CRISPR/Cas9 and TALEN web tool for genome editing. Nucleic Acids Res. *42*, 401–407.

Montavon, T., Soshnikova, N., and Mascrez, B. 2011. A Regulatory Archipelago Controls Hox Genes Transcription in Digits. Cell *147*, 1132–1145.

Moore-Scott, B.A., and Manley, N.R. 2005. Differential expression of Sonic hedgehog along the anterior-posterior axis regulates patterning of pharyngeal pouch endoderm and pharyngeal endoderm-derived organs. Dev. Biol. *278*, 323–335.

Moriyama, Y., and Takeda, H. 2013. Evolution and development of the homocercal caudal fin in teleosts. Dev. Growth Differ. *55*, 687–698.

Muller, G.B. 2003. Homology: The Evolution of Morphological Organization. In Origination of Organismal Form: Beyond the Gene in Developmental and Evolutionary Biology, G.B. Muller, and S.A. Newman, eds. (MIT Press), pp. 51–69.

Mungpakdee, S., Seo, H.C., Angotzi, A.R., Dong, X., Akalin, A., and Chourrout, D. 2008. Differential evolution of the 13 Atlantic salmon hox clusters. Mol. Biol. Evol. *25*, 1333–1343.

Nakamura, T., Klomp, J., Pieretti, J., Schneider, I., Gehrke, A.R., and Shubin, N.H. 2015. Molecular mechanisms underlying the exceptional adaptations of batoid fins. Proc. Natl. Acad. Sci. *112*, 15940–15945.

Nakayama, T., Fish, M.B., Fisher, M., Oomen-Hajagos, J., Thomsen, G.H., and Grainger, R.M.

2013. Simple and efficient CRISPR/Cas9-mediated targeted mutagenesis in Xenopus tropicalis. Genesis *51*, 835–843.

Nasevicius, A., and Ekker, S.C. 2000. Effective targeted gene “knockdown” in zebrafish. Nat. Genet. *26*, 216–220.

Nelson, A.C., and Wardle, F.C. 2013. Conserved non-coding elements and cis regulation: actions speak louder than words. Development *140*, 1385–1395.

Neumann, C.J., Grandel, H., Gaffield, W., Schulte-Merker, S., and Nüsslein-Volhard, C. 1999. Transient establishment of anteroposterior polarity in the zebrafish pectoral fin bud in the absence of sonic hedgehog activity. Development *126*, 4817–4826.

Niederreither, K., McCaffery, P., Dräger, U.C., Chambon, P., and Dollé, P. 1997. Restricted expression and retinoic acid-induced downregulation of the retinaldehyde dehydrogenase type 2 (RALDH-2) gene during mouse development. Mech. Dev. *62*, 67–78.

O’Neill, P., McCole, R.B., and Baker, C.V.H. 2007. A molecular analysis of neurogenic placode and cranial sensory ganglion development in the shark, Scyliorhinus canicula. Dev. Biol. *304*, 156–181.

Ohuchi, H., Nakagawa, T., Yamamoto, A., Araga, A., Ohata, T., Ishimaru, Y., Yoshioka, H., Kuwana, T., Nohno, T., Yamasaki, M., et al. 1997. The mesenchymal factor, FGF10, initiates and maintains the outgrowth of the chick limb bud through interaction with FGF8, an apical ectodermal factor. Development *124*, 2235–2244.

Olson, E.N. 2006. Gene regulatory networks in the evolution and development of the heart. Science *313*, 1922–1927.

Onimaru, K., Marcon, L., Musy, M., Tanaka, M., and Sharpe, J. 2016. The fin-to-limb transition as the re-organization of a Turing pattern. Nat. Commun. *7*, 11582.

Organ, C.L., Cooper, L.N., and Hieronymus, T.L. 2015. Macroevolutionary developmental biology: Embryos, fossils, and phylogenies. Dev. Dyn. *244*, 1184–1192.

Osterwalder, M., Speziale, D., Shoukry, M., Mohan, R., Ivanek, R., Kohler, M., Beisel, C., Wen, X., Scales, S.J., Christoffels, V.M., et al. 2014. HAND2 Targets Define a Network of Transcriptional Regulators that Compartmentalize the Early Limb Bud Mesenchyme. Dev. Cell *31*, 345–357.

Owen, R. 1848. On the Archetype and Homologies of the Vertebrate Skeleton (London).

Owen, R. 1849. On the Nature of Limbs. A Discourse. (London: John van Voorst).

Pages, H., Gentleman, R., Aboyoun, P., and DebRoy, S. 2009. Biostrings: String objects representing biological sequences, and matching algorithms.

Panganiban, G., Irvine, S.M., Lowe, C., Roehl, H., Corley, L.S., Sherbon, B., Grenier, J.K., Fallon, J.F., Kimble, J., Walker, M., et al. 1997. The origin and evolution of animal appendages. Proc. Natl. Acad. Sci. U. S. A. *94*, 5162–5166.

Panganiban, G., and Rubenstein, J.L.R. 2002. Developmental functions of the Distal-less/Dlx homeobox genes. Development *129*, 4371–4386.

Parker, H.J., Bronner, M.E., and Krumlauf, R. 2014a. A Hox regulatory network of hindbrain segmentation is conserved to the base of vertebrates. Nature *514*, 493–493.

Parker, H.J., Sauka-Spengler, T., Bronner, M., and Elgar, G. 2014b. A reporter assay in lamprey embryos reveals both functional conservation and elaboration of vertebrate enhancers. PLoS One *9*, e85492.

Peter, I.S., and Davidson, E.H. 2011. A gene regulatory network controlling the embryonic specification of endoderm. Nature *474*, 635–639.

Pieretti, J., Gehrke, A.R., Schneider, I., Adachi, N., Nakamura, T., and Shubin, N.H. 2015. Organogenesis in deep time: A problem in genomics, development, and paleontology. Proc. Natl. Acad. Sci. U. S. A. *112*, 4871–4876.

Piotrowski, T., and Nüsslein-Volhard, C. 2000. The endoderm plays an important role in patterning the segmented pharyngeal region in zebrafish (Danio rerio). Dev. Biol. *225*, 339–356.

Pöpperl, H., Rikhof, H., Chang, H., Haffter, P., Kimmel, C.B., and Moens, C.B. 2000. Lazarus Is a Novel Pbx Gene That Globally Mediates Hox Gene Function in Zebrafish. Mol. Cell *6*, 255–267.

Pradel, A., Maisey, J.G., Tafforeau, P., Mapes, R.H., and Mallatt, J. 2014. A Palaeozoic shark with osteichthyan-like branchial arches. Nature *509*, 608–611.

Qu, Q., Haitina, T., Zhu, M., and Ahlberg, P.E. 2015. New genomic and fossil data illuminate the origin of enamel. Nature *526*, 108–111.

Raff, R.A. 1996. The shape of life: genes, development, and the evolution of animal shape (Chicago, IL: University of Chicago Press).

Raff, R.A. 2000. Evo-devo: the evolution of a new discipline. Nat. Rev. Genet. *1*, 74–79.

Reichenbach, B., Delalande, J.M., Kolmogorova, E., Prier, A., Nguyen, T., Smith, C.M., Holzschuh, J., and Shepherd, I.T. 2008. Endoderm-derived Sonic hedgehog and mesoderm Hand2 expression are required for enteric nervous system development in zebrafish. Dev. Biol. *318*, 52–64.

Riddle, R.D., Johnson, R.L., Laufer, E., and Tabin, C. 1993. Sonic hedgehog mediates the polarizing activity of the ZPA. Cell *75*, 1401–1416.

Romero, I., Ruvinsky, I., and Gilad, Y. 2012. Comparative studies of gene expression and the evolution of gene regulation. Nat. Rev. Genet. *13*, 505–516.

Roselló-Díez, A., Arques, C.G., Delgado, I., Giovinazzo, G., and Torres, M. 2014. Diffusible signals and epigenetic timing cooperate in late proximo-distal limb patterning. Development *141*, 1534–1543.

Rotem, A., Ram, O., Shoresh, N., Sperling, R.A., Goren, A., Weitz, D.A., and Bernstein, B.E. 2015. Single-cell ChIP-seq reveals cell subpopulations defined by chromatin state. Nat. Biotechnol. *33*, 1165–1172.

Ruvinsky, I., and Gibson-Brown, J.J. 2000. Genetic and developmental bases of serial homology in vertebrate limb evolution. Development *127*, 5233–5244.

Sagai, T., Amano, T., Tamura, M., Mizushina, Y., Sumiyama, K., and Shiroishi, T. 2009. A cluster of three long-range enhancers directs regional Shh expression in the epithelial linings. Development *136*, 1665–1674.

Sagai, T., Hosoya, M., Mizushina, Y., Tamura, M., and Shiroishi, T. 2005. Elimination of a long-range cis-regulatory module causes complete loss of limb-specific Shh expression and truncation of the mouse limb. Development *132*, 797–803.

Sagai, T., Masuya, H., Tamura, M., Shimizu, K., Yada, Y., Wakana, S., Gondo, Y., Noda, T., and Shiroishi, T. 2004. Phylogenetic conservation of a limb-specific, cis-acting regulator of Sonic hedgehog (Shh). Mamm. Genome *15*, 23–34.

Sakamoto, K., Onimaru, K., Munakata, K., Suda, N., Tamura, M., Ochi, H., and Tanaka, M. 2009. Heterochronic shift in Hox-mediated activation of sonic hedgehog leads to morphological changes during fin development. PLoS One *4*, e5121.

Sansom, R.S. 2010. Taphonomy and affinity of an enigmatic Silurian vertebrate, Jamoytius kerwoodi White. Palaeontology *53*, 1393–1409.

Schauerte, H.E., van Eeden, F.J., Fricke, C., Odenthal, J., Strähle, U., and Haffter, P. 1998. Sonic hedgehog is not required for the induction of medial floor plate cells in the zebrafish. Development *125*, 2983–2993.

Scherz, P.J., McGlinn, E., Nissim, S., and Tabin, C.J. 2007. Extended exposure to Sonic hedgehog is required for patterning the posterior digits of the vertebrate limb. Dev. Biol. *308*, 343–354.

Schlosser, G. 2004. The Role of Modules in Development & Evolution. In Modularity in Development and Evolution, G. Schlosser, and G.P. Wagner, eds. (The University of Chicago Press), pp. 519–582.

Schneider, I., Aneas, I., Gehrke, A.R., Dahn, R.D., Nobrega, M. a, and Shubin, N.H. 2011. Appendage expression driven by the Hoxd Global Control Region is an ancient

gnathostome feature. Proc. Natl. Acad. Sci. U. S. A. *108*, 12782–12786.

Schneider, I., and Shubin, N.H. 2013. The origin of the tetrapod limb: from expeditions to enhancers. Trends Genet. *29*, 419–426.

Scholpp, S., Wolf, O., Brand, M., and Lumsden, A. 2006. Hedgehog signalling from the zona limitans intrathalamica orchestrates patterning of the zebrafish diencephalon. Development *133*, 855–864.

Shearman, R.M., and Burke, A.C. 2009. The lateral somitic frontier in ontogeny and phylogeny. J. Exp. Zool. Part B Mol. Dev. Evol. *312*, 603–612.

Sheth, R., Grégoire, D., Dumouchel, A., Scotti, M., Pham, J.M.T., Nemec, S., Bastida, M.F., Ros, M. a, and Kmita, M. 2013. Decoupling the function of Hox and Shh in developing limb reveals multiple inputs of Hox genes on limb growth. Development *140*, 2130–2138.

Shimeld, S.M., and Donoghue, P.C.J. 2012. Evolutionary crossroads in developmental biology: cyclostomes (lamprey and hagfish). Development *139*, 2091–2099.

Shubin, N., Tabin, C., and Carroll, S. 1997. Fossils, genes and the evolution of animal limbs. Nature *388*, 639–648.

Shubin, N., Tabin, C., and Carroll, S. 2009. Deep homology and the origins of evolutionary novelty. Nature *457*, 818–823.

Simpson, J.T., Wong, K., Jackman, S.D., Schein, J.E., and Jones, S.J.M. 2009. ABySS : A parallel assembler for short read sequence data. 1117–1123.

Sordino, P., van der Hoeven, F., and Duboule, D. 1995. Hox gene expression in teleost fins and the origin of vertebrate digits. Nature *375*, 678–681.

Spitz, F., Gonzalez, F., and Duboule, D. 2003. A global control region defines a chromosomal regulatory landscape containing the HoxD cluster. Cell *113*, 405–417.

Stern, D.L. 2000. Perspective: Evolutionary Developmental Biology and the Problem of Variation. Evolution (N. Y). *54*, 1079.

Stewart, T.A., Smith, W.L., and Coates, M.I. 2014. The origins of adipose fins: an analysis of homoplasy and the serial homology of vertebrate appendages. Proc. Biol. Sci. *281*, 20133120.

Suster, M.L., Abe, G., Schouw, A., and Kawakami, K. 2011. Transposon-mediated BAC transgenesis in zebrafish. Nat. Protoc. *6*, 1998–2021.

Suzuki, T. 2013. How is digit identity determined during limb development? Dev. Growth Differ. *55*, 130–138.

Takahashi, M., Tamura, K., Büscher, D., Masuya, H., Yonei-Tamura, S., Matsumoto, K., Naitoh-Matsuo, M., Takeuchi, J., Ogura, K., Shiroishi, T., et al. 1998. The role of Alx-4 in the establishment of anteroposterior polarity during vertebrate limb development. Development *125*, 4417–4425.

Tanaka, M. 2013. Molecular and evolutionary basis of limb field specification and limb initiation. Dev. Growth Differ. *55*, 149–163.

Tanaka, M. 2016. Fins into limbs: Autopod acquisition and anterior elements reduction by modifying gene networks involving 5'Hox, Gli3, and Shh. Dev. Biol. *413*, 1–7.

Tanaka, M., Münsterberg, A., Anderson, W.G., Prescott, A.R., Hazon, N., Tickle, C., Munsterberg, A., Anderson, W.G., Prescott, A.R., Hazon, N., et al. 2002. Fin development in a cartilaginous fish and the origin of vertebrate limbs. Nature *416*, 527–531.

Tanaka, M., and Tickle, C. 2007. The Development of Fins and Limbs. In Fins into Limbs: Evolution, Development, and Transformation, B.K. Hall, ed. (University of Chicago Press), p. 344.

Tarchini, B., and Duboule, D. 2006. Control of Hoxd genes' collinearity during early limb development. Dev. Cell *10*, 93–103.

Tarchini, B., Duboule, D., and Kmita, M. 2006. Regulatory constraints in the evolution of the tetrapod limb anterior-posterior polarity. Nature *443*, 985–988.

Taylor, J.S., Braasch, I., Frickey, T., Meyer, A., and Van de Peer, Y. 2003. Genome duplication, a trait shared by 22 000 species of ray-finned fish. Genome Res. 382–390.

Tena, J.J., Alonso, M.E., de la Calle-Mustienes, E., Splinter, E., de Laat, W., Manzanares, M., and Gómez-Skarmeta, J.L. 2011. An evolutionarily conserved three-dimensional structure in the vertebrate Irx clusters facilitates enhancer sharing and coregulation. Nat. Commun. *2*, 310.

Teraoka, H., Dong, W., Okuhara, Y., Iwasa, H., Shindo, A., Hill, A.J., Kawakami, A., and Hiraga, T. 2006. Impairment of lower jaw growth in developing zebrafish exposed to 2,3,7,8-tetrachlorodibenzo-p-dioxin and reduced hedgehog expression. Aquat. Toxicol. *78*, 103–113.

Thacher, J. 1877. Median and paired fins, a contribution to the history of the vertebrate limbs. Trans. Connect. Acad. Arts Sci. *3*, 281–310.

Tickle, C. 1981. The number of polarizing region cells required to specify additional digits in the developing chick wing. Nature *289*, 295–298.

True, J.R., and Haag, E.S. 2001. Developmental system drift and flexibility in evolutionary trajectories. Evol. Dev. *3*, 109–119.

Tulenko, F.J., Augustus, G., J., M., L., J., Sims, S.E., Mazan, S., and Davis, M.C. 2016. HoxD expression in the fin-fold compartment of basal gnathostomes and implications for paired appendage evolution. Nat. Publ. Gr. 1–10.

VanderMeer, J.E., Smith, R.P., Jones, S.L., and Ahituv, N. 2014. Genome-wide identification of signaling center enhancers in the developing limb. Development 4194–4198.

Wagner, G. 1989. The Biological Homology Concept. Annu. Rev. Ecol. Syst. *20*, 51–69.

Wagner, G.P. 2007. The Developmental Genetics of Homology. Nat. Rev. Genet. *8*, 473–479.

Wagner, G.P. 2014. Homology, Genes, and Evolutionary Innovation (Princeton: Princeton University Press).

Wagner, G.P., and Altenberg, L. 1996. Complex Adaptations and the Evolution of Evolvability. Evolution (N. Y). *50*, 967–976.

Wagner, G.P., and Chiu, C.H. 2001. The tetrapod limb: a hypothesis on its origin. J. Exp. Zool. *291*, 226–240.

Wagner, G.P., and Mezey, J.G. 2004. The Role of Genetic Architecture Constraints in the Origin of Variational Modularity. In Modularity in Development and Evolution, G. Schlosser, and G.P. Wagner, eds. (Chicago, IL: University of Chicago Press), p. 338.

Wagner, G.P., Pavlicev, M., and Cheverud, J.M. 2007. The road to modularity. Nat. Rev. Genet. *8*, 921–931.

Wallace, K.N., and Pack, M. 2003. Unique and conserved aspects of gut development in zebrafish. Dev. Biol. *255*, 12–29.

Wang, B., Fallon, J.F., and Beachy, P.A. 2000. Hedgehog-Regulated Processing of Gli3 Produces an Anterior/Posterior Repressor Gradient in the Developing Vertebrate Limb. Cell *100*, 423–434.

Wang, Z., Gerstein, M., and Snyder, M. 2009. RNA-Seq: a revolutionary tool for transcriptomics. Nat. Rev. Genet. *10*, 57–63.

Wang, Z., Pascual-Anaya, J., Zadissa, A., Li, W., Niimura, Y., Huang, Z., Li, C., White, S., Xiong, Z., Fang, D., et al. 2013. The draft genomes of soft-shell turtle and green sea turtle yield insights into the development and evolution of the turtle-specific body plan. Nat. Genet. *45*, 701–706.

te Welscher, P., Zuniga, A., Kujiper, S., Drenth, T., Goedemans, H.J., Meijlink, F., and Zeller, R. 2002. Progression of Vertebrate Limb Development Through SHH-Mediated Counteraction of GLI3. Science. *298*, 827–830.

Woltering, J.M., Noordermeer, D., Leleu, M., and Duboule, D. 2014. Conservation and

divergence of regulatory strategies at Hox Loci and the origin of tetrapod digits. PLoS Biol. *12*, e1001773.

Wyffels, J., King, B.L., Vincent, J., Chen, C., Wu, C.H., and Polson, S.W. 2014. SkateBase, an elasmobranch genome project and collection of molecular resources for chondrichthyan fishes. F1000Research *3*, 191.

Xiaoni, G., Zhuo, C., Xuzhen, W., Dengqiang, W., and Xinwen, C. 2012. Molecular cloning and characterization of interferon regulatory factor 1 (IRF-1), IRF-2 and IRF-5 in the chondrostean paddlefish Polyodon spathula and their phylogenetic importance in the Osteichthyes. Dev. Comp. Immunol. *36*, 74–84.

Yano, T., Abe, G., Yokoyama, H., Kawakami, K., and Tamura, K. 2012. Mechanism of pectoral fin outgrowth in zebrafish development. Development *139*, 2916–2925.

Yano, T., and Tamura, K. 2013. The making of differences between fins and limbs. J. Anat. *222*, 100–113.

Yelon, D., Ticho, B., Halpern, M.E., Ruvinsky, I., Ho, R.K., Silver, L.M., and Stainier, D.Y. 2000. The bHLH transcription factor hand2 plays parallel roles in zebrafish heart and pectoral fin development. Development *127*, 2573–2582.

Yeo, G.H., Cheah, F.S.H., Winkler, C., Jabs, E.W., Venkatesh, B., and Chong, S.S. 2009. Phylogenetic and evolutionary relationships and developmental expression patterns of the zebrafish twist gene family. Dev. Genes Evol. *219*, 289–300.

Yonei-Tamura, S., Abe, G., Tanaka, Y., Anno, H., Noro, M., Ide, H., Aono, H., Kuraishi, R., Osumi, N., Kuratani, S., et al. 2008. Competent stripes for diverse positions of limbs/fins in gnathostome embryos. Evol. Dev. *10*, 737–745.

Zakany, J., and Duboule, D. 2007. The role of Hox genes during vertebrate limb development. Curr. Opin. Genet. Dev. *17*, 359–366.

Zhang, J., Wagh, P., Guay, D., Sanchez-Pulido, L., Padhi, B.K., Korzh, V., Andrade-Navarro, M. a, and Akimenko, M.-A. 2010a. Loss of fish actinotrichia proteins and the fin-to-limb transition. Nature *466*, 234–237.

Zhang, Z., Sui, P., Dong, A., Hassell, J., Cserjesi, P., Chen, Y.-T., Behringer, R.R., and Sun, X. 2010b. Preaxial polydactyly: interactions among ETV, TWIST1 and HAND2 control anterior-posterior patterning of the limb. Development *137*, 3417–3426.

Zhao, X., Sirbu, I.O., Mic, F.A., Molotkova, N., Molotkov, A., Kumar, S., and Duester, G. 2009. Retinoic Acid Promotes Limb Induction through Effects on Body Axis Extension but Is Unnecessary for Limb Patterning. Curr. Biol. *19*, 1050–1057.

Zhu, J., Zhang, Y.-T., Alber, M.S., and Newman, S. a 2010. Bare bones pattern formation: a core regulatory network in varying geometries reproduces major features of vertebrate limb

development and evolution. PLoS One *5*, e10892.

Zuniga, A. 2015. Next generation limb development and evolution: old questions, new perspectives. Development *142*, 3810–3820.